Uniwersytet Jagielloński
Collegium Medicum

Tasnim Mohaissen, MPharm

Nowe mechanizmy dysfunkcji śródbłonka naczyń obwodowych w niewydolności mięśnia sercowego u myszy Tgαq*44

Novel mechanisms of peripheral vascular endothelial dysfunction in heart failure in Tgαq*44 mice

Praca doktorska
PhD thesis

Supervisor: Prof. Stefan Chlopicki, M.D., Ph.D.
Auxiliary supervisor: Magdalena Sternak, PhD

Jagiellonian Centre for Experimental Therapeutics (JCET)
JCET Director: Prof. Stefan Chlopicki, M.D., Ph.D.

Kraków, 2023

My most profound appreciation goes to ***Professor Stefan Chłopicki, M.D****. my Ph.D. advisor and mentor, for his time, effort, and understanding in helping me succeed in my studies. His vast wisdom and wealth of experience have inspired me throughout my studies.*

I'd like to thank my supportive ***parents****,* ***brothers*** *and* ***sister****. It would have been impossible to finish my studies without their unwavering support over the past few years.*

Also, I want to thank all my friends and colleagues at Jagiellonian Centre for Experimental Therapeutics for making my work more enjoyable and feasible.

The work was funded under the project:

National Science Centre, Poland PRELUDIUM 15 grant (UMO 2018/29/N/NZ4/02915
to **Tasnim Mohaissen**)

and partial by:

Team Tech–Core Facility program of the FNP (Foundation for Polish Science) co-financed by the European Union under the European Regional Development Fund (project No. POIR.04.04.00-00-5CAC/17–00
to **Prof. Stefan Chłopicki**)

The National Science Centre, Poland, through a MAESTRO 13 (UMO 2021/42/A/NZ4/00273
to **Prof. Stefan Chłopicki**)

Table of contents

1. Summary

Red blood cells (RBC) alterations and excessive activation of angiotensin (Ang)-(1–12)/II pathway contribute to cardiovascular pathology, but their involvement in the development of peripheral endothelial dysfunction in heart failure (HF) remains unknown. Therefore, the aim of this PhD thesis was the following:

1) To describe the relationship between the development of peripheral endothelial dysfunction and RBCs alterations in HF

2) To define the effect of exogenous Ang-(1–12) and its conversion to Ang II on endothelial function in HF, focusing particularly on chymase and vascular-derived thromboxane A_2 (TXA_2) involvement.

In this study, a unique mouse model of chronic heart failure (HF) driven by cardiomyocyte-specific overexpression of activated Gαq protein was used (Tgαq*44 mice).

In 8-month-old Tgαq*44 mice, systemic endothelial dysfunction was detected as evidenced by a decreased acetylcholine-induced vasodilation in the aorta *in vivo,* which was associated with impaired nitric oxide (NO) production, increased superoxide anion (O^{2-}) and increased eicosanoid production. Moreover, 8-month-old Tgαq*44 mice showed significant structural RBC alterations, as well as increased RBC stiffness. Erythropathy in 12-month-old Tgαq*44 mice involved significantly altered RBC shape and increased elasticity, increased red cell distribution width (RDW), poor RBC deformability and elevated oxidative stress (gluthatione (GSH)/glutathione disulfide (GSSG) ratio). Inhibition of arginase reversed endothelial dysfunction induced by RBCs isolated from Tgαq*44 mice, *ex vivo* model of RBCs-endothelial interaction in the isolated aorta.

Ang-(1–12) induced endothelial dysfunction in 4- and 12- month-old Tgαq*44 mice, was associated with increased Ang II generation, which was not inhibited by chymostatin, a chymase inhibitor. Moreover, TXA_2 generation was upregulated in response to Ang-(1-12) or

Ang II in aortic rings isolated from 12-month-old Tgαq*44 mice, but not from 4-month-old Tgαq*44 mice. Furthermore, the adverse effects of Ang-(1–12) and Ang II on endothelium-dependent vasodilation in the aorta were inhibited by TXA_2 receptor antagonist (SQ 29548) or Ang receptor type I antagonist (losartan) in 12-month-old-Tgαq*44 mice, but these antagonists remained without effects in 4-month-old- Tgαq*44 mice.

Altogether in this Ph.D. thesis it was demonstrated that in the Tgαq*44 murine model of HF, erythropathy involving structural and biochemical alterations, upregulated arginase as well as overactivity of intravascular Ang-(1–12)/Ang II/TXA_2 pathway may contribute to the development endothelial dysfunction in the aorta. Accordingly, RBC arginase and intravascular Ang-(1–12)/Ang II/TXA_2 pathways may represent a novel therapeutic target for systemic endothelial dysfunction in HF.

2. *Streszczenie*

Do patologii układu sercowo-naczyniowego przyczyniają się zarówno zmiany w erytrocytach, jak i nadmierna aktywacja szlaku angiotensyny (Ang)-(1–12) /Ang II. Udział tych mechanizmów w rozwoju dysfunkcji śródbłonka obwodowego w niewydolności serca (HF) pozostaje jednak nieznany.

Celem niniejszej rozprawy doktorskiej było:

1) opisanie związku pomiędzy rozwojem dysfunkcji śródbłonka naczyniowego, a zmianami zachodzącymi w erytrocytach w trakcie progresji niewydolności serca (HF).
2) określenie wpływu egzogennej Ang-(1–12) i jej konwersji do Ang II na funkcjonowanie śródbłonka obwodowego w HF, ze szczególnym uwzględnieniem roli chymazy i tromboksanu A_2 pochodzenia naczyniowego (TXA_2) w tym procesie.

Aby osiągnąć założone cele, wykorzystano unikatowy mysi model przewlekłej niewydolności serca (HF), wywoływanej przez specyficzną dla kardiomiocytów nadekspresję aktywowanego białka Gαq (myszy Tgαq*44).

W toku przeprowadzonych badań wykazano, że u 8-miesięcznych myszy Tgαq*44 występuje dysfunkcja śródbłonka obwodowego, objawiająca się poprzez zmniejszony rozkurcz aorty *in vivo* po podaniu acetylocholiny. Dysfunkcja śródbłonka występująca u 8-miesięcznych myszy Tgαq*44 była także związana z upośledzoną produkcją tlenku azotu (NO), zwiększoną produkcją anionów ponadtlenkowych i eikozanoidów. Co więcej, u 8-miesięcznych myszy Tgαq*44 zaobserwowano również znaczące zmiany w budowie erytrocytów oraz ich zwiększoną sztywność. Zahamowanie arginazy odwracało dysfunkcję śródbłonka wywołaną przez erytrocyty wyizolowanych od myszy Tgαq*44, w modelu interakcji erytrocytów z aortą (*ex vivo*).

U 12-miesięcznych myszy Tgαq*44 zmiany strukturalne erytrocytów obejmowały: zmianę kształtu i zwiększoną elastyczność, zwiększoną szerokość rozkładu krwinek czerwonych

(RDW), słabą odkształcalność i podwyższony poziom stresu oksydacyjnego (stosunek glutationu (GSH)/dwusiarczku glutationu (GSSG)).

Ang-(1–12) wywołała dysfunkcję śródbłonka zarówno u 4- jak i u 12-miesięcznych myszy Tgαq*44, co było związane ze zwiększoną produkcją Ang II. Efekt ten nie był hamowany przez chymostatynę (inhibitor chymazy). Wytwarzanie TXA_2 w odpowiedzi na Ang-(1-12) i Ang II w aortach piersiowych izolowanych od 12-miesięcznych myszy Tgαq*44, ale nie od myszy 4-miesięcznych było zwiększone. Co więcej, niekorzystne działanie Ang-(1–12) i Ang II na zależny od śródbłonka rozkurcz aorty, było hamowane przez antagonistę receptora TXA_2 (SQ 29548) lub antagonistę receptora Ang typu I (losartan) u 12-miesięcznych, ale nie u 4-miesięcznych myszy Tgαq*44.

Przedstawiona przeze mnie praca doktorska dowodzi, że obserwowane w mysim modelu niewydolności serca (Tgαq*44) patologiczne zmiany w budowie czynności erytrocytów, up- regulacja arginazy oraz nadmierna aktywność wewnątrznaczyniowego szlaku Ang-(1–12)/Ang II/TXA_2 mogą przyczyniać się do rozwoju dysfunkcji śródbłonka w niewydolności serca. Arginaza i wewnątrznaczyniowe szlaki Ang-(1–12) / Ang II / TXA_2 mogą więc stanowić nowy cel terapeutyczny w leczeniu dysfunkcji śródbłonka naczyniowego w przebiegu niewydolności serca.

3. Introduction

3.1. The role of endothelium in cardiovascular homeostasis

Endothelium is the inner layer of all capillaries and blood vessels, forming a lining of blood vessels and the interface with flowing blood or lymph (Gevaert et al., 2017). Endothelial cells primarily maintain the integrity of physiological functioning by balancing the production of vasodilators and vasoconstrictions which regulate vascular tone (Rajendran *et al.*, 2013). Predominate mediator of vasodilation is nitric oxide (NO), but other factors such as derived hyperpolarizing factor (EDHF), prostacyclin, and bradykinin also play an important role as endothelial-derived vasodilators *(Figure 1)* (Pearson, 2000; Khazaei, Moien-afshari and Laher, 2008; Daiber and Chlopicki, 2020). In the case of vasoconstriction, the endothelial-derived vasoconstrictors are catecholamine, endothelin-1 (ET-1), and thromboxane (TXA_2) (Daiber *et al.*, 2017; Alem, 2019). Importantly, the endothelium is involved in many vascular hemostasis processes: thrombosis, inflammation, immune modulation, platelet activation, and aggregation as well as vascular permeability and vascular smooth muscle cell proliferation (Daiber and Chlopicki, 2020). Important function o endothelium is to regulate flow by the mechanism of endothelium-dependent vasodilation (Khazaei, Moien-afshari and Laher, 2008). Additionally, endothelium shows phenotypic heterogeneity, and the type of vasodilator-mediator depends on the region. In larger vessels, the primary vasodilator is NO, whereas it is more heterogeneous in the smaller vessels involving EDHF, prostacyclin (PGI_2), or others (Pearson, 2000; Khazaei, Moien-afshari and Laher, 2008; Rajendran *et al.*, 2013).

Endothelium-derived relaxing factors:

Nitric oxide (NO) is the dominant mediator of vasodilation by activation of guanylyl cyclase and thereby generation of cyclic guanosine monophosphate (cGMP) (Daiber *et al.*, 2017). NO is released from the endothelium and relaxes the smooth muscle which can be triggered by vasoactive mediators (Ach, histamine, thrombin, serotonin, bradykinin, substance

P) and stimulated by a shear stress induced by blood flow (Bauersachs *et al.*, 1999; Daiber and Chlopicki, 2020). NO has antithrombic (increasing cGMP in platelets), anti-inflammatory (inhibiting leukocyte adhesion and infiltration), and antioxidant (scavenging free radicals) effects (Rajendran *et al.*, 2013).

Endothelial-dependent hyperpolarizing factor (EDHF) hyperpolarizes vascular smooth muscle and dilates arteries by activating calcium-activated potassium channels (Gaubert *et al.*, 2007; Oyama and Node, 2013). EDHF relaxes blood vessels, by activating Ca^{2+} activated K channels (Gaubert *et al.*, 2007; Garland, Hiley and Dora, 2011; Oyama and Node, 2013). EDHF is also induced by shear stress, and its synthesis and release are stimulated by an increase of intracellular calcium in the endothelium by calcium-independent endothelial cell hyperpolarization (Teerlink *et al.*, 1993; Alem, 2019). EDHF is a more prominent vasodilator in smaller vessels and may be a compensatory pathway that is typically blocked by NO and it is increased in acquired disease states with reduced NO-mediated vasodilation (Chlopicki *et al.*, 2005; Liu *et al.*, 2011; Beyer and Gutterman, 2012).

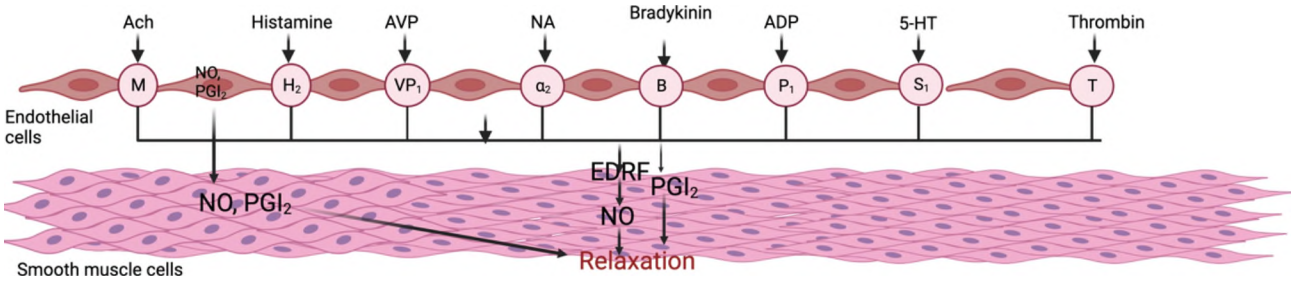

Figure 1. Vasoactive factors in endothelium. Nitric oxide (NO) and other relaxing factors may be released by a variety of substances when certain endothelial cell receptors on the cells are activated. This results in the relaxation of arterial vessels. Acetylcholine (Ach), Muscarinic receptors (M), Histaminergic receptors (H2), Vasopressin (AVP), Vasopressinergic receptors (VP), Purinergic receptors (Pt), Noradrenaline (NA), a2-adrenergic receptor (a2), adenosine diphosphate (ADP) 5-hydroxytryptamine (5-HT), serotonergic receptors (S) and thrombin receptors (T). Figure based on (Vanhoutte, 1989)

Prostacyclin (PGI_2) is produced by metabolism of arachidonic acid *via* cyclooxygenase (COX), which is a coronary vasodilator when it is administered exogenously. COX-2 is the primary isoform involved in the synthesis of vascular prostacyclin but COX-1 is also of

importance (Toniolo *et al.*, 2013). The synthesis of prostacyclin in the endothelium is a calcium-dependent process (Ricciotti and Fitzgerald, 2011). Prostacyclin stimulates the IP receptor, which promotes smooth muscle relaxation by activating adenylate cyclase and increasing intracellular levels of cyclic AMP (Daiber *et al.*, 2017; Daiber and Chlopicki, 2020; Wang *et al.*, 2021). Although some data suggest that prostacyclin can lead to tonic coronary vasodilation, COX-inhibitors do not change flow during distal ischemia or reduce oxygen consumption in response to metabolic increases (Leung and Vanhoutte, 2017; Suryavanshi and Kulkarni, 2017).

Endothelial dysfunction which is characterized by an imbalance that occurs between nitric oxide (NO) and superoxide anions production (O^{2-}) in the vascular bed is associated with alterations in the production of prostanoids (PGI_2/TXA_2) as well as increased production of endothelin-1, and angiotensin II *(Figure 2)* (Daiber *et al.*, 2017; Daiber and Chlopicki, 2020). Decreased endothelium-dependent vasodilatation is a hallmark of endothelial dysfunction and plays an important role in the development and progression of various diseases including atherosclerosis, hypertension, diabetes, viral myocarditis, and many others diseases (Leung and Vanhoutte, 2017; Suryavanshi and Kulkarni, 2017).

Decreased endothelial-dependent vasodilation and decreased NO-dependent function are linked with numerous alterations involving dysregulated production of vasoactive mediators pro-inflammatory and pro-thrombotic changes in endothelial phenotypes as well alterations in the endothelial permeability and glycocalyx disruption (Pearson, 2000; Khazaei, Moien-afshari and Laher, 2008; Rajendran *et al.*, 2013; Bar *et al.*, 2019).

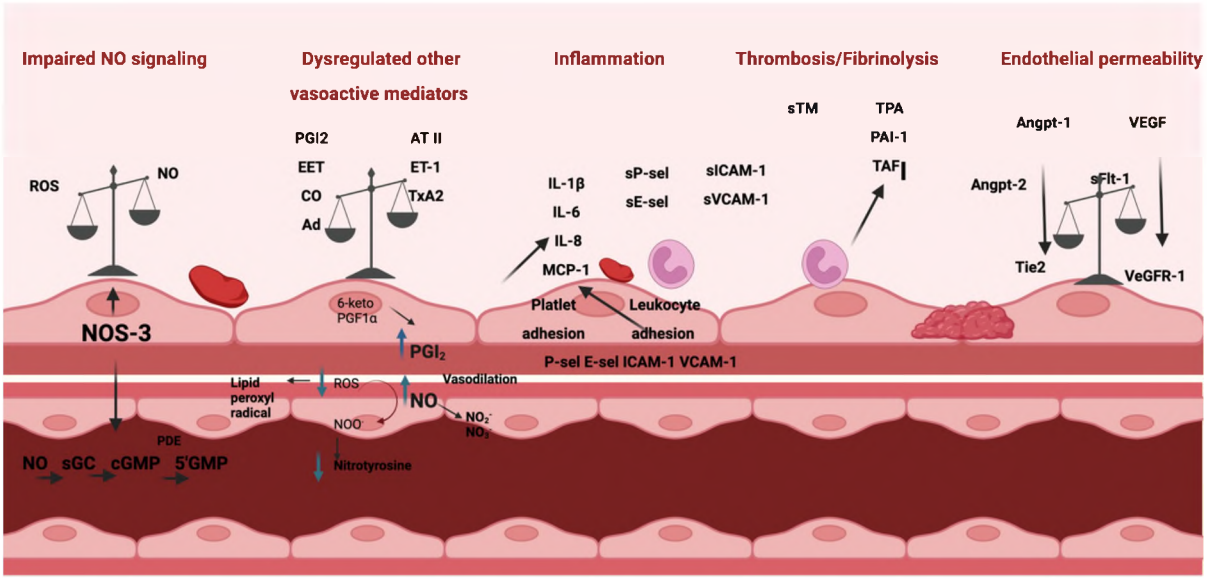

Figure 2. Phenotype of endothelial dysfunction. ROS, oxygen species; EET, Epoxyeicosatrienoic Acid; CO, Carbon monoxide; Ang II, angiotensin II; VEGF, vascular endothelial growth factor; TXA_2; Thromboxane A_2, sE-selectin, soluble form of E-selectin; sP-selectin, soluble form of P-selectin; IL-6/8, interleukin 6/8; MCP-1, monocyte chemoattractant protein 1; sVCAM-1, soluble form of vascular cell adhesion molecule 1; sICAM-1, soluble form of intercellular adhesion molecule 1 1; TPA, tissue plasminogen activator; Angpt-1, Angiopoietin 1; VEGF, Vascular Endothelial Growth Factor NO, nitric oxide; NOS3, nitric oxide synthase 3. Based on (Daiber and Chlopicki, 2020)

3.2. Measurement of endothelial function

Endothelial function can be assessed based on functional assays and biochemical biomarkers *(Table 1)*. As regards endothelial function can be assessed using both **invasive** and **non-invasive** techniques (Tousoulis, Antoniades and Stefanadis, 2005). Due to the risks associated with artery catheterization, **invasive** techniques are not widely used as a screening procedure for large asymptomatic populations. Nowadays, **non-invasive methods** are most often used to assess endothelial function in humans (Tousoulis, Antoniades and Stefanadis, 2005). The most common methods used to measure endothelium-dependent changes in the vessel are Doppler ultrasonography (Dupouy *et al.*, 1993), plethysmography (Wilkinson *et al.*, 2002), angiography(Ludmer *et al.*, 1986), dynamic retinal vessel analysis (Streese *et al.*, 2019) and the **gold standard method: flow-mediated dilation** (FMD) (Dobbie *et al.*, 2020).

Peripheral arterial **tonometry technology** is based on the principle of reactive hyperemia, which refers to an increase in blood flow to an organ or tissue following an ischemia period (lack of blood flow) (Malheiro *et al.*, 2021).

Venous occlusion strain-gauge **plethysmography** is a technique used to monitor forearm muscle blood flow following intra-arterial infusion of muscarinic receptor agonists such as acetycholine or hyperemia (Benjamin *et al.*, 1995; Higashi *et al.*, 2001; Wilkinson *et al.*, 2002).

The **flow mediated skin fluorescence (FMSF)** is a method, based on the observation of the fluorescence of NADH (nicotinamide adenine dinucleotide) coenzyme from skin tissue (Marcinek *et al.*, 2023).

Interestingly, JCET team has developed a technique that allows assessing endothelial function in animal models based on endothelial-dependent vasodilation induced by acetylcholine or flow (Ach or FMD) using magnetic resonance imaging (MRI) (Bar *et al.*, 2015, 2020; Marcinek *et al.*, 2023). This approach provides a good tool for assessment of endothelial function in animal models *in vivo*.

Tabela 1. Selective methods of assessing endothelial function based on functional or biochemical tests. Based on (Dobbie* et al., *2020; Malheiro* et al., *2021; Marcinek* et al., *2023)

Peripheral circulation	Circulating biomarkers
Non-invasive peripheral artery tonometry (RH-PAT)	ADMA-asymmetric dimethylarginine NO-nitric oxide ET-endothelin-1 vWF-von Willebrand factor, PAI-1-plasminogen activator inhibitor 1 sICAM-intercellular adhesion molecule sVCAM-vascular cell adhesion molecule EP cells-endothelial progenitor cell EMP-endothelial-derived microparticle
Ultrasonography-flow-mediated dilation (FMD)	
Plethysmography-forearm blood flow (FMD) Flow Mediated Skin Fluorescence (FMSF)	

3.3. The role of endothelial dysfunction in heart failure

Endothelial dysfunction is one of the earliest clinically detected stages in *atherothrombosis* and other cardiovascular diseases (Daiber *et al.*, 2017; Daiber and Chlopicki, 2020). In particular, endothelial dysfunction is considered to have a significant prognostic value for mortality and hospitalization due to **heart failure** (HF) regardless of its etiology (Schächinger, Britten and Zeiher, 2000; Neglia *et al.*, 2002; Fischer *et al.*, 2005; Durand and Gutterman, 2013; Alem, 2019) *(Figure 3)* HF is a complex syndrome that represents a main cause of morbidity worldwide (Shah *et al.*, 2010; Savarese and Lund, 2017). HF is an outcome of various primary and secondary incidents, that in the advanced stage result not only in impaired cardiac function but also in the development of endothelial dysfunction in the peripheral circulation (Alem, 2019; Mohaissen *et al.*, 2022). Moreover, peripheral and coronary artery endothelial dysfunction have been described in individuals with symptomatic and asymptomatic left ventricular dysfunction, respectively (Shah et al. 2010).

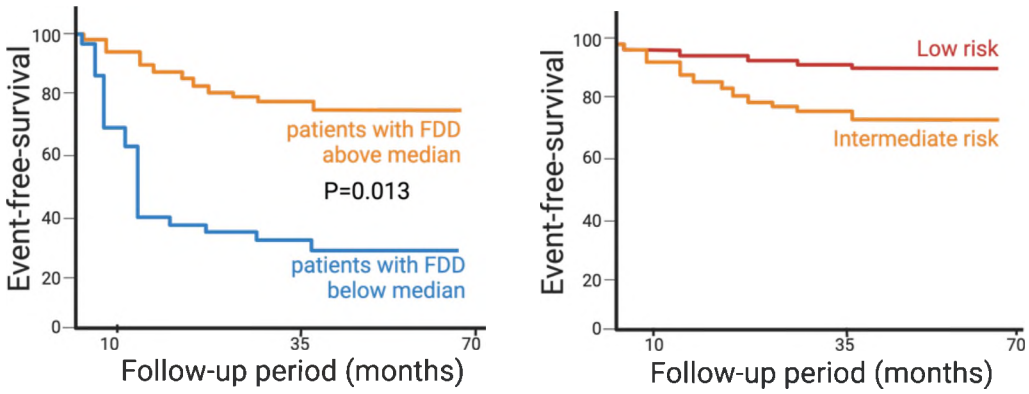

Figure 3. Prognostic value of peripheral and coronary endothelial dysfunction in HF. A) Peripheral endothelial dysfunction predicts progression of HF independently whether ischemic or non-ischemic origin. Fisher et al. study suggested that endothelial dysfunction in patients with HF was independently associated with an increased in cardiovascular events which thought to reflect progression of HF (Fischer* et al., *2005). The study population was categorized as follows: those with FDD more than the median (6.2%), and those with FDD less than the median B) Free survival plots for patients separated into groups based on resting depressed myocardial blood flow shown that coronary endothelial dysfunction has a prognostic value in patients with non-ischemic HF. Based on (Neglia* et al., *2002)

Recent clinical studies have shown that patients with chronic cardiac failure have a reduced endothelium-dependent relaxation of peripheral resistance and conduct arteries, associated with **decreased NO availability** (Alem, 2019; Giannitsi *et al.*, 2019). Patients with HF who have impaired endothelial function may have decreased tissue perfusion increased vascular resistance, therefore exercise intolerance was present in HF (Giannitsi *et al.*, 2019). Exercise intolerance present in HF patients have been demonstrated to be improved by treatments that enhance endothelial function (Hambrecht *et al.*, 1998).

Several studies have proven that ischemic HF has attenuated endothelium-mediated dilatation to bigger extend as compared to **non-ischemic HF** (Giannitsi et al., 2019), although other data indicate that endothelial dysfunction only occurred in patients with **ischemic HF** (Alem, 2019). The etiology of ischemic HF is mostly caused by coronary atherosclerosis associated with endothelial dysfunction (Shah *et al.*, 2010), whereas, in nonischemic HF disease the pathogenic processes are mainly limited to the heart injury (Błyszczuk & Szekanecz, 2020; Shah et al., 2010). Nevertheless, endothelial dysfunction in non-ischemic HF can contribute to unmatched vascular needs related to the failing heart. Coronary endothelial dysfunction in non-ischemic HF patients suggests an early involvement of the endothelium in HF progression (Alem, 2019). Altogether, coronary and peripheral endothelial dysfunction is a hallmark of HF, but better understanding of mechanisms of endothelial dysfunction in non-ischemic HF is needed.

3.4. Mechanisms of development of endothelial dysfunction in heart failure

Best known **mechanism** responsible for the development of endothelial dysfunction in HF is an increased vascular **oxidative stress** that can be linked to the rapid inactivation of NO and oxidation of tetrahydrobiopterin (BH4, cofactor of endothelial NOS). O^{2-} by scavenging NO within the vascular wall, provides also peroxynitrite, which leads to nitration of prostacyclin synthase and other enzymes (Bendall et al., 2014). Decreased bioavailability of NO can results

from reduced expression of eNOS, increased generation of ROS, or both, combined with weakened antioxidant defenses that normally eliminate these radicals, are likely to cause increased oxidative stress in HF patients (Buys and Sips, 2014; Konior *et al.*, 2014; Montfort, Wales and Weichsel, 2017). Moreover, hypertrophy of HF in coarctation-induced hypertension is associated with increased oxidative stress and could be prevented by treatment with the antioxidant vitamin E, thus indicating a pathophysiological role for oxidative stress in the pathogenesis of HF (Mak and Newton, 2001; Nasri, Baradaran and Rafieian-Kopaei, 2014). Of note, vitamin C given to patients with HF improved NO-mediated vasodilation (Konior et al., 2014).

Hemodynamic factors contribute to endothelial dysfunction in HF (Davies, 2009). Shear stress is known as the force exerted by blood flow on the endothelial cells as it moves through the blood vessels (Davies, 2009). In healthy people, shear stress causes the release of NO and other vasodilators which helps to maintain vascular tone and prevent blood clots from forming (Chiu and Chien, 2011). However, in HF patiens shear stress on endothelial cells is frequently altered due to increased reduced cardiac output and impaired vascular function (Davies, 2009; Natarajan *et al.*, 2016). Decrease shear stress can result in decreased NO production and increased ROS production which can cause oxidative stress and endothelial dysfunction (Higashi, 2022). SOD is essential for superoxide neutralization, preventing oxidative damage, and maintaining endothelial function (Ighodaro and Akinloye, 2018). Several studies showed that SOD may be a possible therapeutic target in HF (Romuk *et al.*, 2019). Recent study has shown that overexpression of SOD-1 in HF mice, improved left ventricular function and reduced oxidative stress (Chen *et al.*, 2021). Moreover, another study showed that using a SOD mimetic reduced oxidative stress and improved endothelial function in HF patients (Nasri, Baradaran and Rafieian-Kopaei, 2014).

Endothelial dysfunction may be also driven by imbalance in **neurohormonal activation** as renin-angiotensin-aldosterone and autonomic nervous system (RAAS). RAAS activation causes angiotensin II (Ang II) production, which promotes vasoconstriction, inflammation, and oxidative stress (Buys and Sips, 2014; Montfort, Wales and Weichsel, 2017). In turn, increased in Ang II leads to endothelial dysfunction not only by increasing NAD(P)H-oxidases activation that contributes to the increase of O^{2-} production but also results in the release of a variety of cytokines, growth factors in the vascular wall as well as in the smooth muscle (Konior *et al.*, 2014). Current pharmacotherapy of HF such as angiotensin-converting enzyme (ACE) inhibitors or angiotensin receptor blockers (ARBs) could improve endothelial function (Ruilope, Redón and Schmieder, 2007; Fortini *et al.*, 2021). There is no doubt that the RAAS pathway plays a very important role in the progression of HF and the overactivation of this system may contribute to the development of peripheral endothelial dysfunction (Ames, Atkins and Pitt, 2019).

Inflammatory changes were also proposed to contribute to endothelial dysfunction in HF. It is well known that during HF, endothelium release inflammatory molecules (cytokines, chemokines), which could lead to an imbalance between vasoconstrictive versus vasodilatory molecules (Félétou, Huang and Vanhoutte, 2011; Ricciotti and Fitzgerald, 2011; Sun *et al.*, 2020). The high concentration of cytokines (TNF, IL-6) in plasma observed in HF patients may represent a mechanism contributing to endothelial dysfunction by inhibiting the release of NO from the endothelium, by impairing the stability of eNOS mRNA (Reina-Couto *et al.*, 2021). The inflammatory process can also contribute to HF through fibrosis and remodeling of blood vessels and tissues, further impairing endothelial function (Sun *et al.*, 2020).

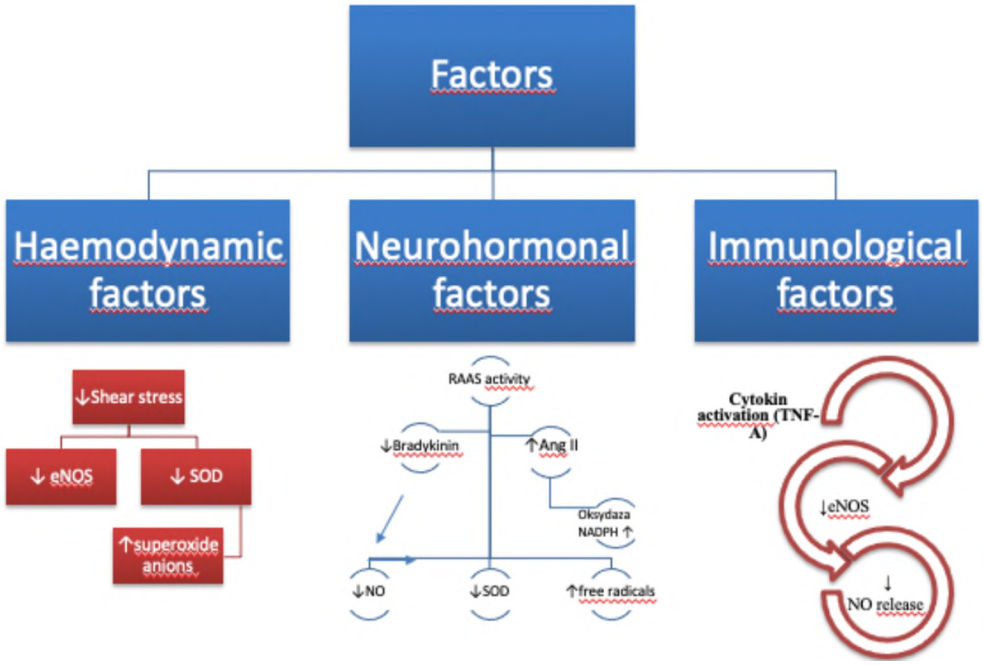

Figure 4. Proposed mechanism of endothelial dysfunction in heart failure. Figure based on (Villar et al.*, 2006; Durand and Gutterman, 2013; Leung and Vanhoutte, 2017)*

Taken together, so far, this free major mechanism of peripheral endothelial dysfunction in HF were proposed involving hemodynamic, neurohormonal, or inflammatory factors, while oxidative stress is a hallmark of dysfunctional endothelial phenotype in HF, likewise in many other diseases *(Figure 4)*. However, they are another possible mechanism that could also play a role and are therefore investigated in this Ph.D. thesis, such as alterations in red blood cells (RBCs) and overactivation of vascular Ang (1-12)/TXA_2 pathway.

3.5. Erytropathy in cardiovascular diseases

Red blood cells (RBCs) play important role in vascular function through oxygen and NO delivery (Helms, Gladwin and Kim-Shapiro, 2018). Under pathophysiological conditions, RBCs increase the formation of reactive oxygen species, the adhesion to vascular wall, and change the amount of protein (Gwozdzinski, Pieniazek and Gwozdzinski, 2021).

Changes in RBCs parameters have been proposed to be a better predictor of cardiovascular disease than changes in other blood components such as white blood cells (WBC) or platelets (PLT) (Lassale *et al.*, 2018). Many cardiovascular diseases are associated with mean

corpuscular volume (MCV), RBC distribution width (RDW) (Franczuk et al. 2015), and hematocrit (Danesh *et al.*, 2000; Franczuk *et al.*, 2015). RDW reflects RBCs size variability is a commonly used parameter and useful in anemia, that has been recently considered to be an additional predictor of acute and chronic HF outcomes (Danesh *et al.*, 2000; Arbel *et al.*, 2013; Lippi *et al.*, 2018).

A recent study has shown that RBCs express arginase, which competes with eNOS for the common substrate L-arginine (Yang *et al.*, 2013). Arginase is found in two distinct isoforms, arginase I and II (Pernow *et al.*, 2019; Mahdi, Kövamees and Pernow, 2020). Despite the fact that both isoforms are present throughout the body, arginase I is primarily a cytosolic enzyme found in the liver, and arginase II is a mitochondrial enzyme expressed in the kidney, prostate, and vasculature (Pernow and Jung, 2013; Mahdi, Kövamees and Pernow, 2020). Arginase I and II contribute to vascular homeostasis by controlling NO generation in endothelial cells (Mahdi, Kövamees, et al. 2020; Pernow et al. 2019). Increased arginase is induced by hypoxia, proinflammatory cytokines, hypoxia, and reactive oxygen species *(Figure 5)*, whereas arginase inhibitor improves endothelial-dependent vasodilation in diabetes (Pernow and Jung, 2013; Yang *et al.*, 2013; Zhou, Yang and Pernow, 2018; Pernow *et al.*, 2019; Mahdi, Kövamees and Pernow, 2020; Mahdi *et al.*, 2021).

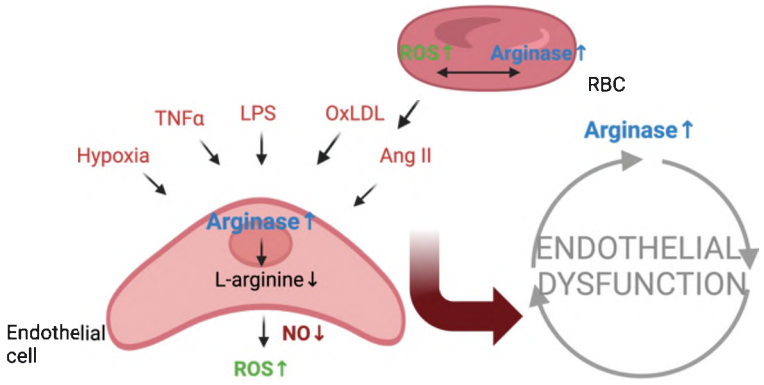

Figure 5. Factors regulating arginase activity in endothelium. Endothelial dysfunction is induced by upregulated arginase via NO reduction and ROS production. Ang II, angiotensin II; LPS; lipopolysaccharide; OxLDL; oxidized low density lipoprotein; NO, nitric oxide, ROS; reactive oxygen species. Based on (Mahdi, Kövamees, et al. 2020)

Moreover, a recent study showed that dysfunction of RBCs and excessive activity of arginase are involved in the progression of cardiovascular diseases in diabetes, preeclampsia, and dyslipidemia (Kontidou *et al.*, 2023). In diabetes arginase expressed in RBC, which competes with eNOS for L-arginine, is a critical regulator of NO-bioactivity. That causes a decrease in NO production and an increase in oxidative stress, which in turn results in endothelial dysfunction (Mahdi, Collado, et al., 2021a, 2021b; Mahdi, Wernly, et al., 2021; Zhou et al., 2018). Moreover, Pernow team showed that RBCs isolated from patients with hypercholesterolemia cause peripheral endothelial dysfunction in healthy rats via ROS imbalance in RBCs and increased vascular arginase activity (Kontidou *et al.*, 2023). However, still little is known about RBCs dysfunction along with the progression of HF.

3.6. Non-ACE pathway-induced angiotensin II production in cardiovascular diseases

The systemic renin-angiotensin system is a major controller of fluid balance, blood pressure and electrolytic homeostasis (Fountain and Lappin, 2018). It is well known that angiotensinogen is angiotensin I (Ang I) formatting substrates processed by renin, then, Ang I is easily activated to Ang II by ACE, which is expressed on the surface of endothelial cells. (Tyrankiewicz *et al.*, 2019). However, recently studies demonstrated the co-existence of alternative Ang II production pathway in tissues as evidence by the fact that tissue Ang II level was not decreased after long term therapy with ACE inhibitors (Varagic *et al.*, 2013; Ferrario *et al.*, 2019, 2021; Li *et al.*, 2020). Most of the published works focus on the role of alternative sources of Ang II in the heart (Ahmad *et al.*, 2010, 2013; Ahmad and Ferrario, 2018), while only few of them describe alternative mechanisms of Ang II formation in the vessels (Ahmad *et al.*, 2014).

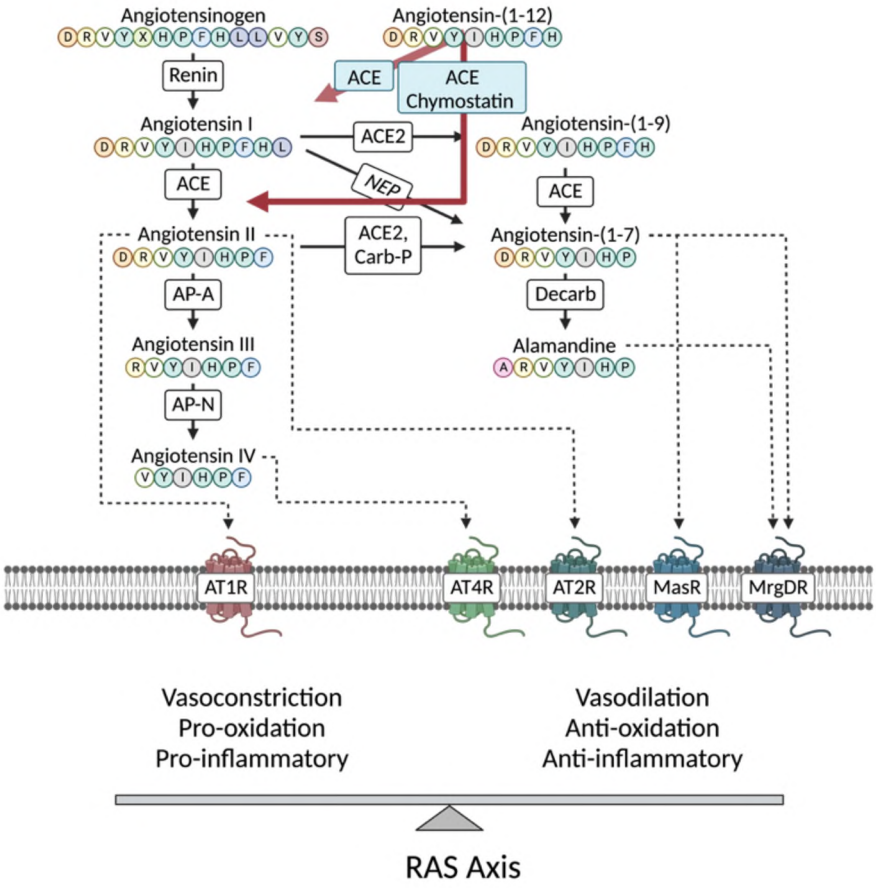

Figure 6. Diagram of the main angiotensin pathways, illustrating the relevant enzymes and receptors. ACE, angiotensin-converting enzyme; ACE2, angiotensin-converting enzyme 2; NEP, neutral endopeptidase; AT1R, angiotensin receptor type 1; AT2R, angiotensin receptor type 2. Based on (Tyrankiewicz et al.*, 2013; Fountain and Lappin, 2018)*

Chymase as an ACE-independent angiotensin II-forming enzyme is present in two forms: α and β and this enzyme seems to contribute, more than ACE, to the generation of Ang II in the tissue (Okunishi *et al.*, 1993). Interestingly, it was shown that chymase can convert Ang-(1-12) and Ang-(1-25) to Ang II in humans and in animal models (Takai and Jin, 2016). Interestingly, Wand et al demonstrated that chymase affinity for Ang (1-12) is nearly 25-fold higher than ACE in human atrial tissue, while chymase-mediated Ang II generation from Ang-(1-12) substrate was approximately 1000-fold higher than ACE. Moreover, Doggrell and Wanstall (Doggrell and Wanstall, 2004) demonstrated that chymase inhibitors (chymostatin) had the capacity to reduce Ang II generation. It was also demonstrated that increased expression of chymase in the aorta of mice with atherosclerosis was responsible for the significant increase of Ang II activity (Dell'italia, Collawn and Ferrario, 2018) while Takai et al., reported that

chymase inhibition improved vascular function in mice with hypertension (Takai and Jin, 2016). Additionally, alternative Ang II production mechanisms may contribute to HF. Moreover, Ang II levels were elevated in parts of tissues following ACE-I therapy, suggesting that other enzymes contributed to Ang II production (Ola *et al.*, 2017).

The discovery of Ang-(1-12) and Ang-(1-25) as the two alternative substrates for Ang II formation based on non-renin-dependent mechanism has revealed new paradigms regarding the biochemical mechanisms necessary for angiotensin's action (Ahmad & Ferrario, 2018). This alternative pathways take place primarily in tissues rather than in the circulation (Ferrario, 2006). Interestingly, Alnord et al., indicated that Ang-(1–12) conversion into Ang II was mediated by ACE, while Prosser et al. (Prosser *et al.*, 2010), demonstrated that chymase and neprilysine contributed to metabolism of Ang-(1-12) (Ferrario, 2006; Arnold *et al.*, 2010; Prosser *et al.*, 2010; Varagic *et al.*, 2013).

Taken together, evidence accumulated that **erytropathy** contributes to endothelial dysfunction in diabetes, hypertension, hypercholesterolemia, and preeclampsia. However, no data existed on whether erythropaty could contribute to endothelial dysfunction in heart failure. Overwhelming evidence support that **Ang (1-12)/Ang II pathway** plays important role in cardiac remodeling, yet still little data existed about the vascular function of Ang (1-12)/Ang II and nothing was known about its role in HF. That is why, in the current Ph.D. thesis a possible role erythopathy and of vascular Ang-(1–12)/ Ang II in endothelial dysfunction was studied using a unique model of HF (Tgαq*44 mice).

4. Aim of the study

It is well known, that endothelial dysfunction has a predictive value in HF, however mechanisms involved are not clear. The role of hemodynamic factors neurohormonal overactivation or inflammation were previously proposed. The aim of this PhD thesis was to characterized a possible role of novel mechanisms involving alterations in RBCs function and vascular Ang-(1-12) pathway that may be responsible for endothelial dysfunction in HF.

Specifically, the goal of PhD thesis was:

1) To describe the relationship between the development of peripheral endothelial dysfunction and RBCs alterations in HF.

2) To define the effect of exogenous Ang-(1–12) and its vascular conversion to Ang II on endothelial function in HF, focusing particularly on chymase and vascular-derived thromboxane A_2 (TXA_2) involvement.

The doctoral dissertation results where partly published in:

- Mohaissen T, Proniewski B, Targosz-Korecka M, Bar A, Kij A, Bulat K, Wajda A, Blat A, Matyjaszczyk-Gwarda K, Grosicki M, Tworzydlo A, Sternak M, Wojnar-Lason K, Rodrigues-Diez R, Kubisiak A, Briones A, Marzec KM, Chlopicki S. "*Temporal relationship between systemic endothelial dysfunction and alterations in erythrocyte function in a murine model of chronic heart failure*". Cardiovasc Res. 2022 Sep 20;118(12):2610-2624. doi: 10.1093/cvr/cvab306.

and also contains unpublished results.

5. Methodology

5.1. Animal model

Tgαq*44 mice represent a murine model of Heart Failure (HF) with cardiomyocytes specific over-expression of Gαq protein that imitates neurohormonal activation *(Figure 7)*. Female Tgαq*44 mice, initially developed by Mende et al. (U Mende *et al.*, 2001; U. Mende *et al.*, 2001) and FVB (control) mice, were bred in the Animal Laboratory of the Medical Research Centre of the Polish Academy of Sciences (Warsaw, Poland). All animal procedures were in accordance the Guide for the Care and Use of Laboratory Animals published by the US National Institutes of Health (NIH Publication No. 85-23, revised 1985) as well as with the local Ethical Committee on Animal Experiments in Cracow. Mice were fed a standard chow diet and kept in 12:12 light-dark conditions**.** The size of a given experimental groups is reported in the legends of the corresponding graphs.

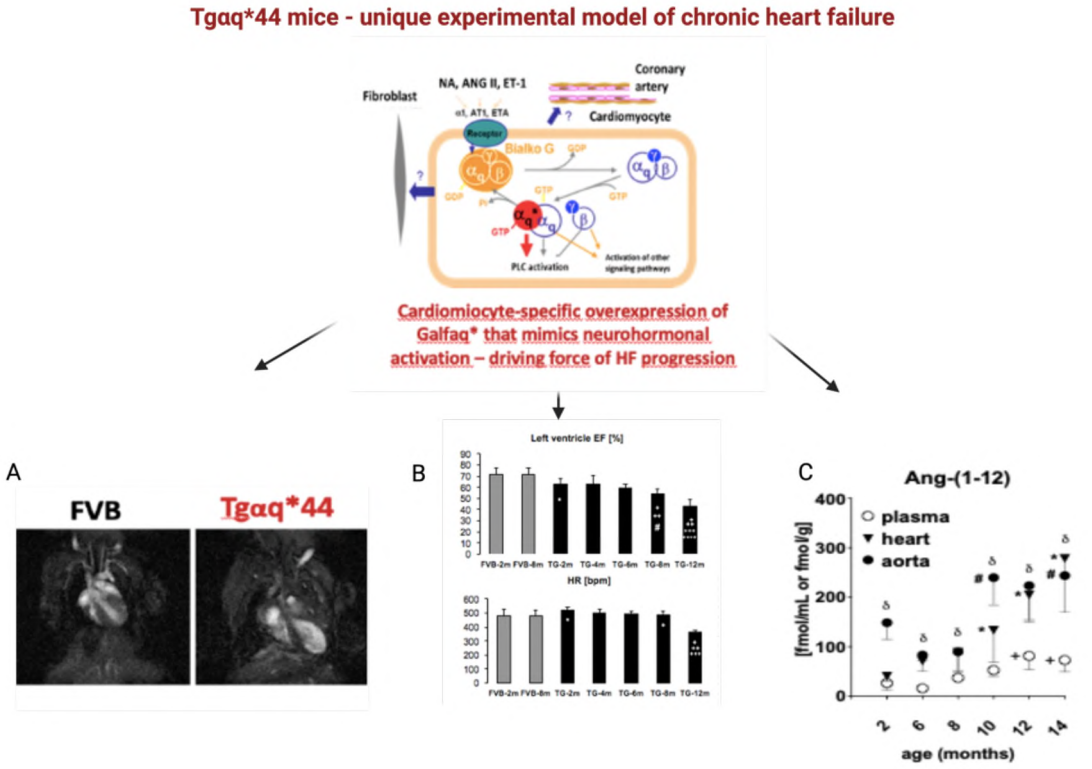

*Figure 7. Tgαq*44 mice as slowly progressing model of chronic HF. A) Tgαq *44 vs FVB mouse heart images taken* in vivo *by MRI. (T.Skorka et al., IFJ PAN B) progressive cardiac dysfunction in Tgαq *44 mice as compared to FVB mice. C) Ang-(1-12) profile in plasma, heart, and aortic in Tgαq*44 mice. Based on (Tyrankiewicz et al., 2018)*

5.2. Assessment of endothelium-dependent vasodilation in vivo using MRI (Magnetic Resonance Imaging)

Endothelium-dependent vasodilation *in vivo* were measured by endothelium-dependent response to acetylcholine (Ach) in abdominal aorta (AA) and flow-mediated dilatation (FMD) in response to reactive hyperemia in femoral artery (FA) (Bar *et al.*, 2015, 2020; Sternak *et al.*, 2018; Mohaissen *et al.*, 2022)

Endothelium-dependent vasodilation was determined by measuring the response to acetylcholine (Sigma-Aldrich, Poznan, Poland:16.6 mg/kg, i.p.) administration in the abdominal aorta (AA), whereas flow-mediated dilatation (FMD) was measured in response to reactive hyperemia (after 5 min vessel occlusion) in the femoral artery (FA) (Bar *et al.*, 2015, 2020; Mohaissen *et al.*, 2022).

Comparing two time-resolved 3D pictures of the vasculature before and 25 minutes after intraperitoneal Ach injection (Sigma-Aldrich, Poznań Poland: 50 µl, 16.6 mg/kg, i.p.) in the abdominal aorta to investigate vasomotor responses (AA) or following a short-term (5 min) blockage of the femoral artery (FA), as described in (Bar *et al.*, 2015; Sternak *et al.*, 2018), caused by a homemade vascular occlude. Images were captured with the IntraGateTM FLASH 3D sequence and reconstructed with the IntraGate 1.2.b.2 macro (Bruker). Endothelial function changes were expressed as changes in vessel volume [%]. The following imaging parameters were used to assess endothelial function: Field of view (FOV) - 30x30x14 mm3 for the AA and 30x30x5 mm3 for the FA, matrix size - 256x256x35 for the AA and 256x256x30 for the FA, flip angle (FA) - 30°, and number of accumulations (NA) - 15, reconstructed to 7 (AA) or 3 (FA) cardiac frames. The total scan time was approximately 10-12 minutes (Bar *et al.*, 2015, 2020; Sternak *et al.*, 2018; Mohaissen *et al.*, 2022).

5.3. Aorta isolation

Mice were euthanized intraperitoneally with a mixture of ketamine and xylazine at the doses of 100 and 10 mg/kg of body weight, respectively (Sternak *et al.*, 2018; Mohaissen *et al.*, 2022). The aorta was then removed and placed in a cold Krebs-Henseleit solution (KB) bubbled with a 95% O2/5% CO2 mixture (pH = 7.4) (Mohaissen *et al.*, 2022). Next, aortic segments were immediately placed in Minimum Essential Medium (MEM Vitamin Solution, 1% antibiotics, 1% amino acids, 0.5 FBS) or KB and subjected to the incubation for assessment of endothelium-dependent and -independent vasodilation (wire myograph), angiotensin conversion, eicosanoids production. After isolation and cleaning, a for functional and biochemical analysis aorta samples were immediately frozen and stored at 80°C or placed in fresh KB (Mohaissen *et al.*, 2022).

5.3.1. Assessment of endothelium-dependent and -independent vasodilation ex vivo using wire and culture myograph system

The aorta was cut into about 2 mm rings and mounted between two stainless steel wires filled with 5000 µl Krebs-Solution in Mulvany myograph system (620 M, Danish Myo Technology, Denmark). Once mounted, unstretched aortic rings were allowed to equilibrate for 30 min by warmed to 37°C and bubbled with 5% CO_2 and 95% O_2. Following, tension of the rings was increased stepwise to reach 10 mN and incubated in KB for 20 min before further study. After the normalization process the vessels were examined by contractile responses to potassium chloride (KCl 30 mM, 60 mM) and Phe ($3*10^{-6}$ M) to achieve the maximum concentration of the vessel. After the stimulation procedure, the vessels were rinsed two-three times with KB. Endothelial-dependent response was assessed by adding cumulatively increasing concentrations of ACh (10^{-9} to 10^{-5} mol/L) while endothelium-independent vasodilator SNP was added (10^{-9} to 10^{-6} mol/L) in the presence of an unchanged concentration of Phe. Vasodilator response were expressed as percentage of the previous tone induced by phenylephrine in each case. All solutions were prepared before the experiment. ACh, Phe and

SNP were purchased from Sigma (Poland). All reagents were prepared and diluted in distilled water.

To assess if RBCs isolated from Tgαq*44 mice at the late stage of HF could impair endothelial function, RBCs from 12-month Tgαq*44 mice were incubated with aortic rings isolated from FVB mice (control) in MEM at 37°C with 5% CO_2 for 18 hrs in the absence or presence of ROS scavenger FeTPPs, (Fe(III)5,10,15,20-tetrakis(4-sulfonatophenyl) porphyrinato chloride) peroxynitrite scavenger and NAC (N-acetyl-L-cysteine).

To assess the effect of angiotensins on endothelial function, aortic rings isolated from 4- and 12-month-old Tgαq*44 and FVB mice were placed in MEM at 37°C with 5% $CO_2$for 18 hrs in the absence or presence of Ang I (100nM), Ang II (100nM) and Ang-(1-12) (100nM).

To verify weather TXA_2-dependent pathway is involved in endothelial dysfunction induced by Ang I, Ang II or Ang-(1-12), antagonist of TP receptor (SQ 29,548; 300 µM) was used.To test the involvement of AT1 receptor in endothelial dysfunction induced by Ang I, Ang II or Ang-(1-12), an AT_1 receptor antagonist (losartan; 10 nM) was used. After incubations, aortic rings were mounted in a Mulvany myograph system (620 M, Danish Myo Technology, Denmark), followed by assessment of the endothelium-dependent and independent vasodilation *ex vivo*, carried out as previously described (Mohaissen *et al.*, 2022).

FMD and acetylcholine-induced endothelium-dependent vasodilation was assessed in mesenteric resistance artery segment by using culture myograph system (Danish Myo Technology, Denmark). The mesentery artery was removed and placed in cold and oxygenated Krebs buffer. A 2-3 mm segment of the first mesenteric artery was isolated and mounted on an culture myograph. Mesenteric artery was pre-constricted with 10^{-5} M phenylephrine before assessing vasodilation response to stepwise increases in intraluminal flow (3, 6, 10, 15, 20, 25, 50, 75, and 100 L/min) (Hamzaoui et al. 2021).

5.3.2. Assessment of NO production in aorta by Electron Paramagnetic Resonance (EPR) spectroscopy

As previously described (Dikalov, Griendling and Harrison, 2007; Frolow *et al.*, 2015; Przyborowski *et al.*, 2018; Mohaissen *et al.*, 2022), nitric oxide production in isolated aorta was measured using EPR (electron paramagnetic resonance) with the cell-permeable NO spin trapping agent diethyldithiocarbamate (DETC). Tissue samples were placed in 100 L Krebs-HEPES buffer in a plate and preincubated at 37°C for 30 minutes. After that, a 1,5-hour incubation with a 285 µM colloidal spin trap of Fe-$(DETC)_2$ and a 1µM calcium ionophore stimulation of A23187 began. Then, the tissues were dried on a Kimwipe, their weight was recorded, and they were placed in liquid nitrogen and kept at -80°C until being measured with an EMX Plus spectrometer that had a rectangular resonator cavity H102 (Bruker, Germany). The total amplitude of the NO-Fe-$(DETC)_2$ after baseline correction was used to quantify signals. Results were expressed in AU/mg of tissue and normalized to the weight of the aorta (Proniewski, Miszalski-Jamka and Jaźwiec, 2014; Proniewski *et al.*, 2018, 2019; Przyborowski *et al.*, 2018; Mohaissen *et al.*, 2022).

5.3.3. Assessment of O^{2-} production in aorta by Electron Paramagnetic Resonance (EPR) spectroscopy

EPR detection of oxidation of the cell permeable cyclic hydroxylamine spin probe 1-hydroxy-3-methoxycarbonyl-2,2,5,5-tetramethypyrrolidine (CMH), as described in(Dikalov, Griendling and Harrison, 2007; Mohaissen *et al.*, 2022), was used to detect intracellular superoxide radical production in isolated aortic rings. Briefly, six 2-mm aortic rings from the thoracic aorta were incubated in Krebs-HEPES buffer preincubated on ice for 3 hours with or without polyethylene glycol-SOD (100 U/mL). The rings were then placed in 100 L of 1 mM CMH dissolved in Krebs/HEPES buffer containing 0.1 mM DTPA, and the mixture was incubated for 30 minutes at 37°C.Next, the segments were frozen in liquid nitrogen and EPR spectra were captured using a Bruker EMX Plus spectrometer with the scan settings of 120 G

for field sweep, 9.44 GHz for microwave frequency, 2 mW for microwave power, and 5 G for modulation amplitude (Przyborowski *et al.*, 2018; Mohaissen *et al.*, 2022).

5.3.4. Assessment of angiotensin production by aortic ring using ultra-pressure liquid chromatography coupled to mass spectrometry (UPLC–MS/MS)

To evaluate the angiotensin conversion by vascular wall, the concentration of angiotensin peptides including Ang-(1-12), Ang I, Ang II, Ang A, Ang III, Ang-(1-7) and Ang IV was determined in MEM collected after aorta incubation by ultra-pressure liquid chromatography-tandem mass spectrometry (UPLC-MS/MS)–based method as described previously (Mohaissen *et al.*, 2022). First, the cleaned aorta rings were incubated in MEM with Ang I, Ang II or Ang-(1-12) at the final concentration of 100 nM, with and without inhibitors of chymase (chymostatin; 10 µM), ACE-1 (perindopril; 10 µM) and ACE-2 (MLN-4760; 30 µM). After 24hrs of incubation, the medium was collected and stored at -80°C for further measurements. The quantification of angiotensin peptides in MEM samples was performed using a UFLC Nexera liquid chromatograph system (Shimadzu, Kyoto, Japan) coupled to a QTrap 5500 triple quadrupole mass spectrometer (Sciex, Framingham, MA, USA). At the beginning, samples were spiked with the internal standard [Asn1, Val5] – Ang II) and subsequently subjected to purification process by solid-phase extraction (SPE) using Oasis HLB 96-well µ-elution plates (Waters, Milford, MA, USA). Plate sorbent was equilibrated using MiliQ water and MeOH, and in the next steps the samples were loaded, washed with MiliQ water and eluted with MeOH. Collected fractions were lyophilized and the dry residues were resuspended in MiliQ water. The samples were injected onto an Acquity UPLC BEH C8 (Waters, Milford, MA, USA) analytical column, and angiotensin peptides were separated under gradient elution mode. The MS detection of analytes and their internal standard were carried out in positive ion electrospray ionization applying the multiple reaction monitoring mode. The quantification of studied angiotensin peptides was performed based on the calibration curves plotted for each analyte as

the relationship between the peak area ratios of analyte/IS to the nominal concentration of the analyte.

5.3.5. Assessment of eicosanoids production by vascular wall using ultra-pressure liquid chromatography coupled to mass spectrometry (UPLC–MS/MS)

To analyzed eicosanoids generation by vascular wall, the aortic rings were placed into a 24-well plate containing KB alone or with the addition of Ang I, Ang II or Ang-(1-12) and the plate was placed into a BIO-V gas treatment chamber under CO_2 flow at 37°C (Noxygen Science, Elzach, Germany). After pre-incubation (15 min), the aortic rings were placed into 500 µL of fresh KB, and 100 µL samples of the incubation buffer were taken after 45 min of incubation. The concentrations of thromboxane B_2 (TXB_2), prostaglandin E_2 (PGE_2), prostaglandin D_2 (PGD_2) and prostaglandin $F_{2\alpha}$ ($PGF_{2\alpha}$) in the aorta effluents, were examined by a liquid chromatograph UFLC Nexera (Shimadzu, Kyoto, Japan) coupled to a triple quadrupole mass spectrometer QTrap 5500 (SCIEX, Framingham, MA, USA) following the methodology previously described (Kij *et al.*, 2020). The biosynthesis of thromboxane A_2 (TXA_2) were assessed based on the concentration of its stable metabolite thromboxane B_2 (TXB_2) (Mohaissen *et al.*, 2022). Results are presented as the concentration measured after 24h incubation (Kij *et al.*, 2020; Mohaissen *et al.*, 2022).

5.3.6. Assessment of COX-2 and eNOS protein expression by Western Blot

Aorta from Tgαq*44 and FVB mice were homogenized in a buffer composed of 10 mM Tris-HCl, pH 7.4, 10% SDS and 8 M urea. Homogenates containing 10 µg protein were electrophoretically separated on a 7.5% SDS and transferred to polyvinyl difluoridine membranes overnight containing (25 mM Tris-HCl, 10% SDS, pH 7.4). Immunoblots were blocked with 5% non-fat milk in TBS containing 0.01% Tween-20 (TBST) and probed with indicated antibodies COX-2 and eNOS (1:2500 dilution) for 1 hour at 24 °C. After washing in TBST five times, blots were incubated with HRP-conjugated secondary antibodies for 2 h at

room temperature and developed with Luminate Forte detected system (Millipore) in Gel DOC™ EZ Imager (Bio-Rad). The same membrane was used to determine α-actin expression.

5.3.7. Assessment of IL- 1β, TNFα, renin, angiotensinogen, ACE-1, ACE-2, AT_1 and AT_2 gene receptor expression by quantitative reverse transcriptase real-time PCR (qRT-PCR)

To assess vascular gene expression of RAS components and cytokines, total RNA was extracted from the isolated aorta of Tgαq*44 mice and FVB mice with TRI Reagent (Sigma-Aldrich, St. Louis, MO, USA) following the manufacturer's procedures as described previously (Avendaño *et al.*, 2018). The primer/probe sets for, *IL- 1β* (Mm.PT.58.975676), *TNFα* (Mm. PT. 58.9672672), renin (Mm.PT.58.9797336), angiotensinogen (Mm. PT. 58.9672092), ACE-1 (Mm.PT.58.43658045), ACE-2 (Mm. PT.58.8312550), AT_1 (Mm.PT.58.41990121) and AT_2 (Mm.PT.58.33432129) receptors, and GAPDH (Mm.PT.39a.1) were purchased from IDT (Foster City, CA) (Briones *et al.*, 2009; Avendaño *et al.*, 2018; Mohaissen *et al.*, 2022).

5.3.8. Histological analysis

Aortic rings were fixed in a 4%bufffered formalin (for at least 48 h). After macroscopic analysis aortic rings were processed using standard paraffin procedures. The paraffin samples were serially sectioned into 5-micrometer-thick slides on an Accu-Cut® SRM™ 200 Rotary Microtome. Paraffin tissue sections were stained with hematoxylin and eosin (H&E) for general histology. Light microscopic examination and photographic documentation were performed using Olympus BX51 microscope with equipped with a digital camera. Pictures were taken under the magnification 400× and qualitatively assessed them for morphological changes (Buczek *et al.*, 2018).

5.4. Blood sampling and biochemical analysis

Blood samples were collected from the right heart ventricle using a syringe containing additional anticoagulant (heparin). Blood count was analyzed using an automatic hematology analyzer ABC Vet (Horiba, Germany) and whole blood was used for RBCs deformability and

flow cytometric analysis. Up to 1 hour after collection, whole blood was subjected to centrifugation (acceleration: 1000 x *g*, run time: 10 min,4°C). Separated plasma was used for measuring NO metabolites with ENO-20 (Eicom Corp, Kyoto, Japan). Remaining packed RBCs were used for GSH and GSSG concentration measurement, as well as nitrosylhemoglobin (HbNO) detection with EPR spectroscopy (Frolow et al., 2015).

5.4.1. Assessment of RBCs deformability

Erythrocyte deformability was measured using the microfluidic RheoScan AnD 300 (RheoMeditech, Seoul, Korea) according to the manufacturer's protocol. In brief, a 5 µl whole blood sample was suspended in 500 µl of polyvinylpyrrolidone solution (PVP, Rheomeditech) and pre-warmed (37°C) for 15 minutes on a thermoblock (Liebisch Labortechnik). Following, the solution was loaded onto a microfluidic chip. Ektacytometry created mechanisms that allowed RBCs to flow through micro-channels during the measurements. The software analyzed the image data automatically by calculating (A-B)/(A+B), where A is the light and B is the width of the deformed cell at the diffraction pattern. RBC deformation was measured in terms of Maximum Elongation Index at maximal shear stress 20 Pa (Dybas *et al.*, 2020, 2022; Mohaissen *et al.*, 2022)

5.4.2. NO metabolites determination

The ENO-20 NOx Analyzer (Eicom, Kyoto, Japan) was used to measure nitrate (NO_3^-) and nitrite (NO_2^-) concentrations via liquid chromatography with post-column derivatization using Griess reagent. Nitrite and nitrate were specifically separated in a matrix on NO-PAK columns. Using a cadmium-cooper column, nitrate was converted to nitrite. Next, nitrite was mixed with the Griess reagent to form a purple azo dye in a reaction coil placed in a column oven at 35 °C, and the absorbance of the derivatives product was measured at 540 nm. The mobile phase flow rate was 0.33 ml/min. The Griess reagent was pumped at a rate of 0.11 ml/min (Przyborowski *et al.*, 2018).

5.4.3. GSH and GSSG concentrations in RBCs were measured

As previously described (Hempe and Ory-Ascani, 2014; Mohaissen *et al.*, 2022), GSH and GSSG concentrations were determined using an AP/ACE MDQ capillary electrophoresis system (Beckman Coulter, Fullerton, CA, USA) and Karat software (ver. 8.0). Hemolysate was made by combining 50 l of RBCs with 200 l of hemolyzing reagent (10 mmol/L KCN and 5 mmol/L EDTA in double distilled H_2O). After that, 100 l of 5% metaphosphoric acid was added to 100 l of hemolysate to deproteinize the samples. Following that, the samples were centrifuged again, and the supernatants were diluted 1:4 with dd H_2O before being utilized for CE analysis. The apparatus was outfitted with a PDA detector tuned at 200 nm.

Biochemical analysis of plasma

5.4.4. Detection of catecholamines

According to the manufacturer's instructions, plasma concentrations of adrenaline, noradrenaline, and dopamine were measured using an ELISA immunoassay with a TriCAT TM ELISA Kit (IBL International-TECAN Group, Hamburg, Germany). OD measurements were made at 405/620 nm. Sensitivity (S) and assay range (AR): dopamine (S = 4 pg/mL, AR = 6-11,470 ng/mL), noradrenaline (S = 20 pg/mL), and adrenaline (S = 8 pg/mL, respectively). The ELISA immunoassay was conducted using a plate reader.

5.4.5. Cytokine measurement

Luminex technology-based BioPlex ProTM mouse Cytokine 8-plex Assay (BioRad, Berkeley, CA, USA) and the BioPlex® MAGPIXTM Multiplex Reader were used to measure the concentrations of specific cytokines and chemokines (BioRad). To remove cell debris, media were centrifuged for 15 min. at 2000 g before being processed in accordance with the manufacturer's instructions. The following interleukins' concentrations were determined using the Bio-Plex Manager MP and Bio-Plex Manager 6.1 software: Tumor Necrosis Factor-alpha

(TNF-a), Interleukin-1 (IL-1), IL-2, IL-3, IL-4, IL-5, IL-9, and Interferon gamma (IFN) (BioRad).

5.5. Statistical analysis

Statistical analyses were performed using GraphPad Prism 8.4 (GraphPad Software) software. Normality of the distribution and homogeneity of variance were tested using the Shapiro-Wilk and F- tests, respectively. When these assumptions were violated, the nonparametric tests were performed (Mann-Whitney U-test for independent groups or Kruskal-Wallis ANOVA).

6. Results:

PART I

ENDOTHELIAL FUNCTION IN PERIPHERAL CIRCULATION IN TGαQ*44 MICE

*6.1. Peripheral endothelial function in the aorta, femoral artery and mesenteric artery isolated from Tgαq*44 mice in vivo and ex vivo measurements.*

Endothelial function in Tgαq*44 mice was assessed ex vivo using a myograph setup and in vivo by MRI approach, respectively and the results are presented in chapter 6.1.1-6.1.2 and chapter 6.1.3 respectively.

*6.1.1. Endothelial function in the aorta isolated from Tgαq*44 mice in ex vivo measurements*

In *ex vivo* measurements of endothelial function wire myograph systems were used to assess endothelium-dependent and -independent vasodilatation in the **aorta**. Ach-induced endothelium-dependent vasodilation in the aorta was preserved in 6- and 8-month-old Tgαq*44 but decreased in 10- and 12-month-old Tgαq*44 mice compared with the age-matched FVB mice (*Figure 8 A, C, E, G*). However, in all experimental groups of Tgαq*44 mice, endothelium-independent vasodilation induced by sodium nitroprusside (SNP) in the aorta was fully preserved as compared with the age-matched FVB (control) mice (*Figure 8 B, D, F, G, H*).

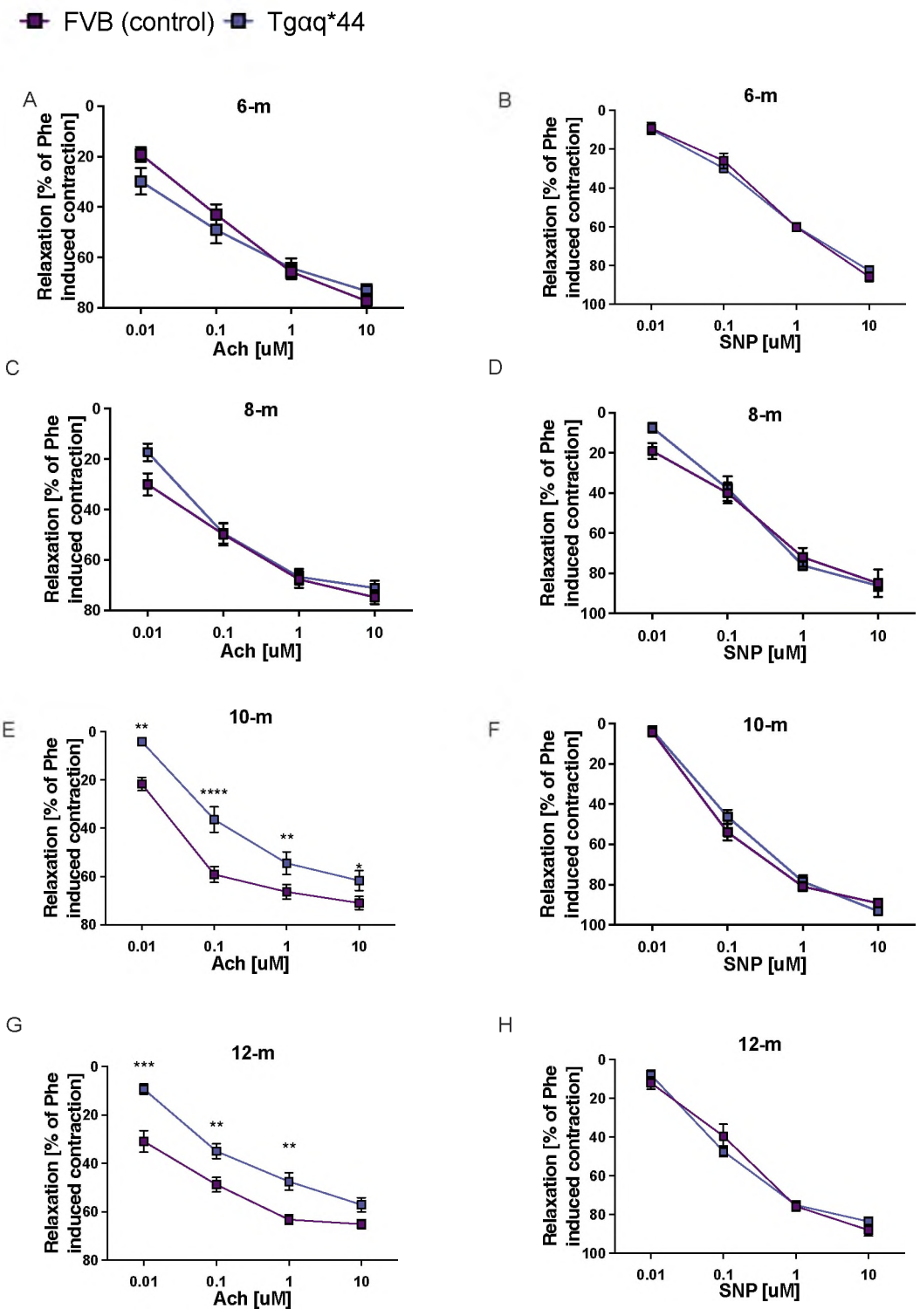

*Figure 8. Vascular endothelial function measured in wire myograph ex vivo along the progression of HF in Tgαq*44 mice as compared with age-matched FVB mice (control). Aortic ring relaxation in response to increasing concentration of Ach (A, C, E, G) and SNP (B, D, F, H) in 6-, 8-, 10-, and 12-month-old Tgαq*44 mice versus age-matched FVB mice (control) are presented. Normality was assessed using a Shapiro–Wilk test. Results are presented as mean ± SEM (D–K). *p < 0.05, **p < 0.01, ***p < 0.001 ****p < 0.0001, Tgαq*44 mice and age matched FVB control mice compared using Two-way Anova with Post Hoc Sidak test, n = 5-6. Ach, acetylocholine; SNP, sodium nitroprusside; m-months. Figure based on T. Mohaissen et al., 2021; modified.*

*6.1.2. Endothelial function in the mesenteric artery isolated from Tgαq*44 mice in ex vivo measurements*

To understand endothelial heterogeneity along the progression of HF, endothelial function in **mesenteric artery (MA)** was assessed using culture myograph system ex vivo.

Angiotensin

Flow-mediated vasodilation (FMD) and Ach-induced endothelium-dependent vasodilation in **MA** was maintained at the same level even in 12-month-old Tgαq*44 mice as in age-matched FVB mice (*Figure 9*).

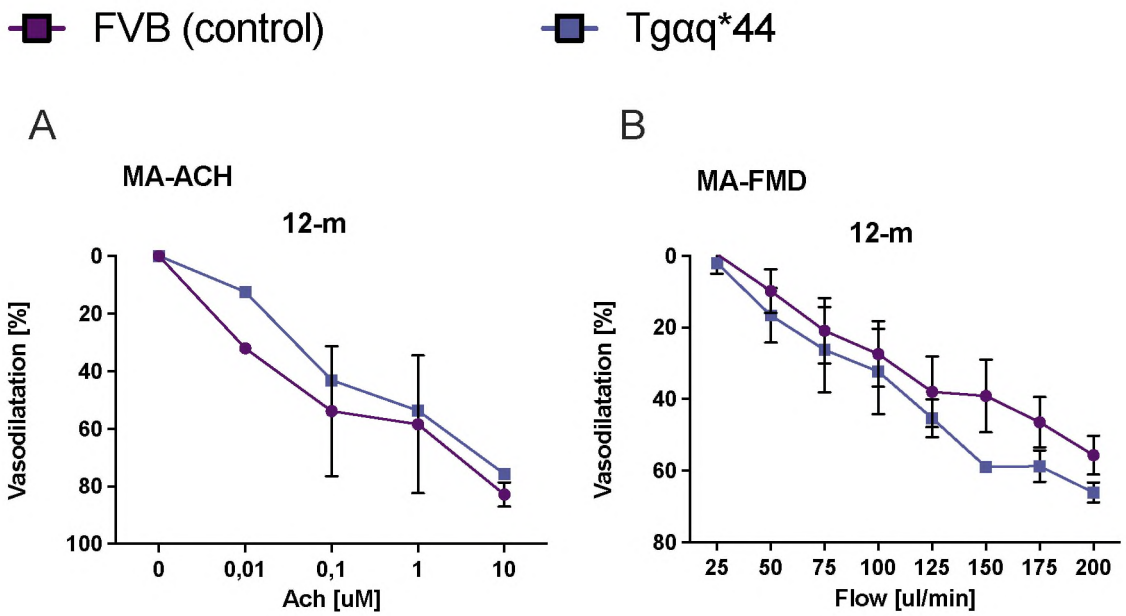

*Figure 9. Vascular endothelial function measured in the mesenteric artery in culture myograph system ex vivo along the progression of HF (Tgαq*44 mice) compared with age matched FVB mice (control). Mesenteric artery relaxation in response to increasing concentration of Ach (A) and FMD (B) in 12-month-old Tgαq*44 mice versus age-matched FVB mice (control) are presented. Normality was assessed using a Shapiro–Wilk test. Results are presented as mean ± SEM Tgαq*44 mice and age matched FVB control mice compared using Two-way Anova with Post Hoc Sidak test, n = 5-6. Ach-acetylocholine; FMD, flow-mediated vasodilation; m-months.*

*6.1.3. Endothelial function in aorta and femoral artery isolated from Tgαq*44 mice in in vivo measurements*

Endothelial function *in vivo* was measured by MRI in **abdominal aorta (AA) and in the femoral artery (FA)**.

Assessment of endothelium-dependent response *in vivo* using MRI showed that Ach-induced vasodilation in the **AA** was impaired in 8-month-old Tgαq*44 mice, whereas in 10- to 12-month-old Tgq*44 mice, Ach-induced vasodilation was lost and changed to vasoconstriction (*Figure 10A*).

Flow-mediated vasodilation (FMD) in FA (*in vivo*) (*Figure 10B*) was maintained at the same level until 12-month-old Tgαq*44 mice and comparable as in age-matched FVB mice. Although 12-month-old Tgαq*44 mice had a slightly lower FMD in FA, the difference was not significant compared with the age-matched FVB mice.

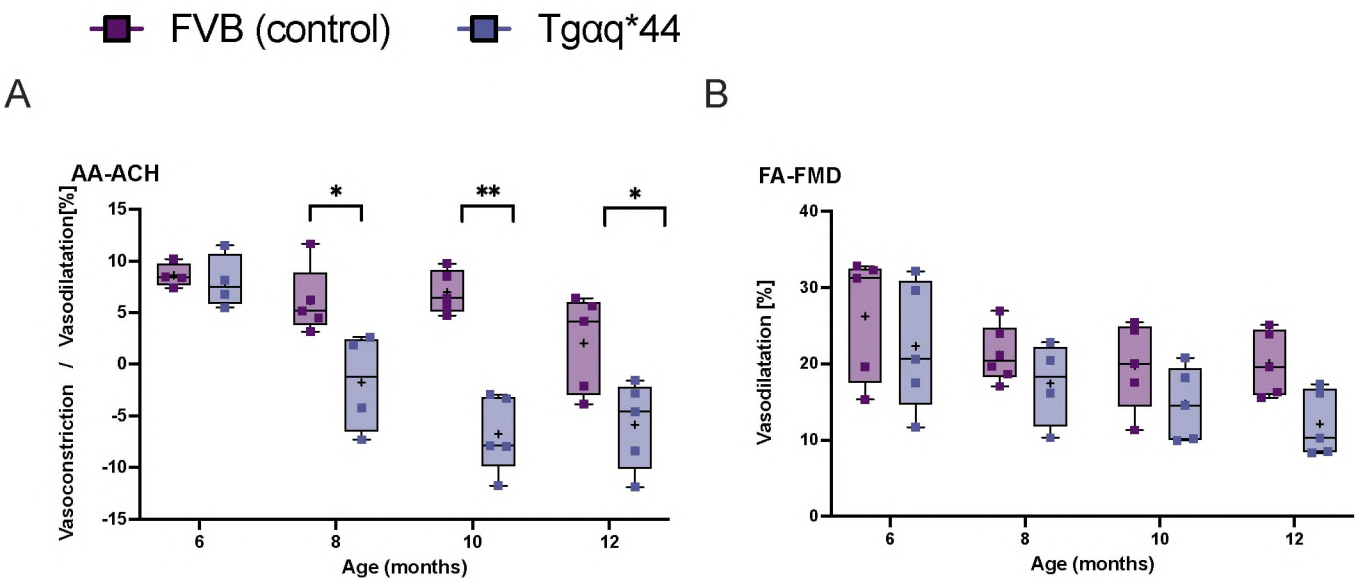

*Figure 10. Vascular endothelial function measured by MRI in aorta and femoral artery in vivo along the progression of HF (Tgαq*44 mice) compared with age matched FVB mice (control). Changes in the end-diastolic volume of the abdominal aorta after Ach administration (after 25 min) (A) and Flow-mediated vasodilation induced femoral artery volume changes (FA-FMD) after 5-minute vascular closure (B are presented. Results are presented as box plots (median, Q1, Q3, whiskers indicate minimum/maximum), Q1 and Q3 indicate the 25th and 75th percentile, *p < 0.05, **p < 0.01, ***p < 0.001 ****p < 0.0001, Tgαq*44 mice and age matched FVB control mice compared using Two-way Anova with Post Hoc Sidak test, n = 5-6. Ach, acetylcholine; AA, abdominal aorta; FMD, flow-mediated vasodilation. (MRI measurements made in cooperation with dr. A. Bar JCET, Kraków). (Figure based on T.Mohaissen et al., 2021; modified).*

*6.2. Bioavailability of Nitric Oxide (NO) and superoxide (O^{2-}) production in the aorta isolated from Tgαq*44 mice*

To confirm that endothelial dysfunction was linked to biochemical changes in the balance of NO/ROS levels as HF progressed, NO and O^{2-} production were measured in the aorta using EPR and HPLC, respectively.

There were no changes in NO and O^{2-} production in the aorta isolated from 6-10- month-old Tgαq*44 mice as compared with age-matched control FVB mice. However, the impairment of endothelial function in the aorta was accompanied with decrease NO production (*Figure 11A*) and increased O^{2-} production (*Figure 11B*) in 12-month-old Tgαq*44 mice compared with age-matched control FVB.

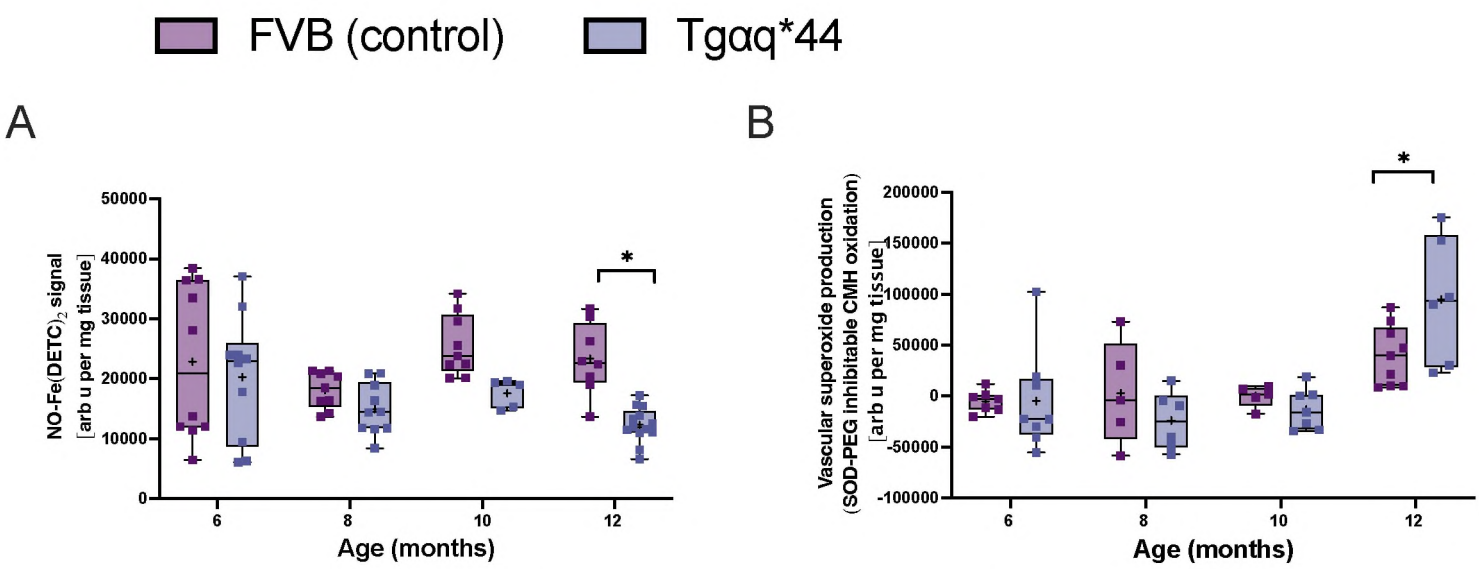

*Figure 11. Alterations in NO/ O^{2-} balance in the aorta along the progression of HF in Tgαq*44 mice compared with age-matched FVB mice. NO production in the isolated aorta (n = 5–13) (A), O^{2-} production in aortic rings (n = 5–13) (B). Results are presented as box plots (median, Q1, Q3, whiskers indicate minimum/maximum), Q1 and Q3 indicate the 25th and 75th percentiles, respectively, *p < 0.05, **p < 0.01, ***p < 0.001 ****p < 0.0001, Tgαq*44 mice and age matched FVB control mice compared using Two-way Anova with Post Hoc Sidak test, n = 5–6. (EPR measurements made in cooperation with dr. Bartosz Proniewski, JCET, Krakow). Figure based on T. Mohaissen et al., 2021; Modified)*

*6.3. Eicosanoid production in the aorta isolated from Tgαq*44 mice*

To determine whether a decrease in NO production and an increase in O^{2-} production in endothelial dysfunction in the aorta are associated with eicosanoid production, the production of 6-keto prostaglandin F1α (6-keto $PGF_{1\alpha}$), prostaglandin E_2 (PGE_2,) prostaglandin D_2 (PGD_2) prostaglandin $F_{1\alpha}$ ($PGF_{1\alpha}$), 12- and 15-hydroxyeicosatetraenoic acid (15-HETE, 12-HETE) were assessed.

The profile of eicosanoids production released in Tgαq*44 mice aorta isolated from 4- and 10-month-old Tgaq*44 mice did not differ as compared with age-matched FVB mice. However, the concentration of prostanoids: 6-keto-PGF1a (*Figure 12A*), PGE_2, (*Figure 12B*), PGD_2 (*Figure 12C*), $PGF_{1\alpha}$ (*Figure 12D*), 12-HETE (*Figure 12E*) and 15-HETE (*Figure12*) was increased in aortic effluent in 12-month-old Tgαq*44 mice as compared with age-matched FVB mice.

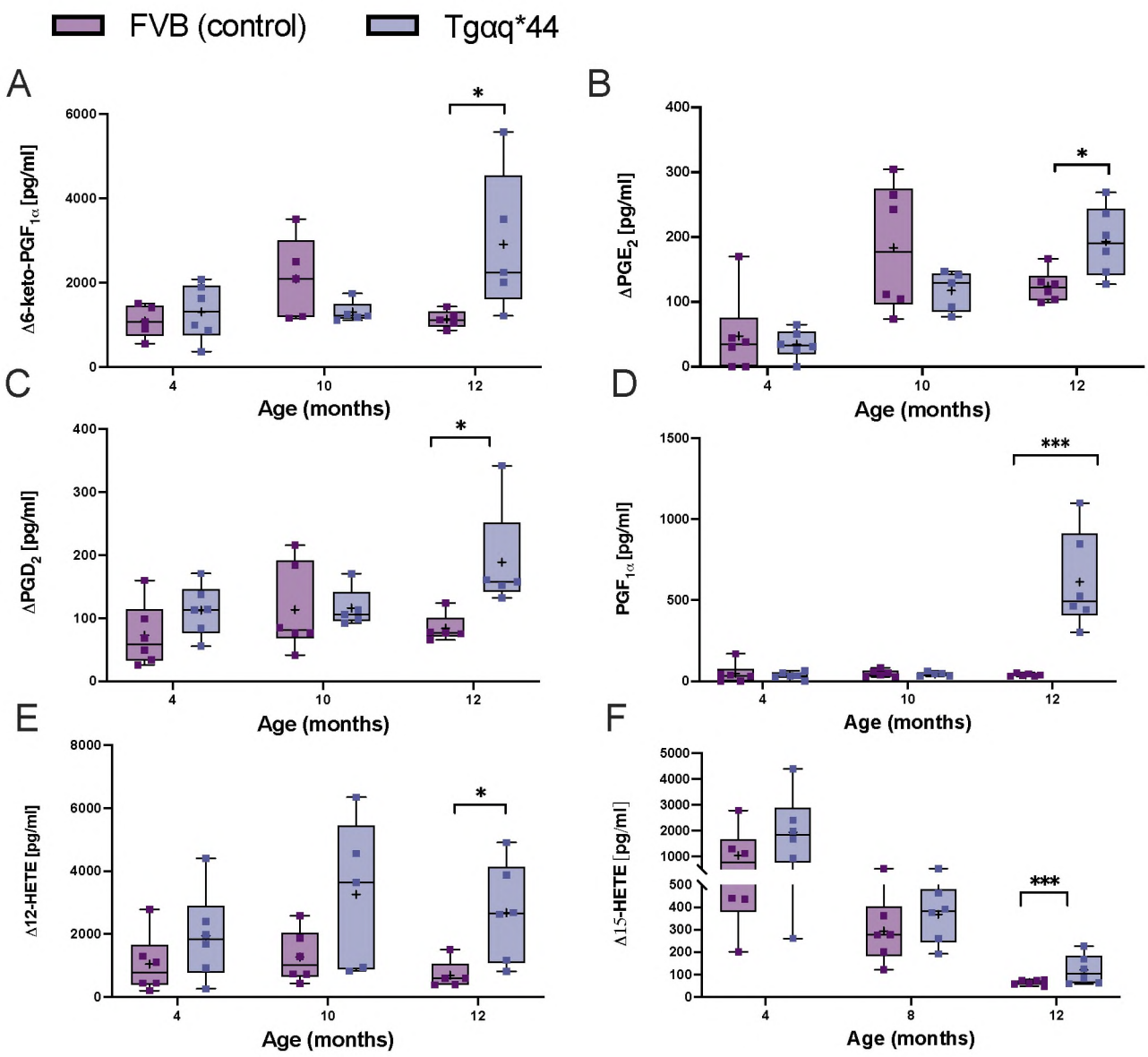

*Figure 12. Alterations in eicosanoid production in the aorta along the progression of HF in Tgαq*44 mice compared with age-matched FVB mice. Basal production of eicosanoid 6-keto PGF_{1a} (A), PGE_2 (B), PGD_2 (C), PGF_{1a} (D), 12-HETE (E) and 15-HETE (F) detected in the effluent after 45 min of incubation of isolated aortic rings are presented. Results are presented as box plots (median, Q1, Q3, whiskers indicate minimum/maximum), Q1 and Q3 indicate the 25th and 75th percentiles, respectively, *p < 0.05, **p < 0.01, ***p < 0.001 ****p < 0.0001, Tgαq*44 mice and age matched FVB control mice compared using Two-way Anova with Post Hoc Sidak test, n = 5–6. (HPLC measurements made in cooperation with dr Agnieszka Kij JCET, Krakow). (Figure based on T. Mohaissen et al., 2021; Modified).*

*6.4. Gene and protein expression in the aorta isolated from Tgαq*44 mice*

The qRT-PCR and western blot methods were used to determine whether endothelial dysfunction in the **aorta** was associated with protein and gene expression changes of NOS and selected pro-inflammatory cytokines in **the aorta**.

IL-1β (*Figure 13A*) and TNFα (*Figure 13B*) mRNA gene level expression did not differ in the **aorta** isolated from 12-month-old Tgαq*44 mice as compared with age-matched FVB mice. However, an increase of COX-2 protein expression levels was observed in the aorta isolated from 12-month-old Tgαq*44 mice as compared with age-matched FVB mice.

Moreover, an increased eNOS protein level was noticed in the aorta isolated from 4-month-old Tgαq*44 mice as compared with age-matched FVB mice.

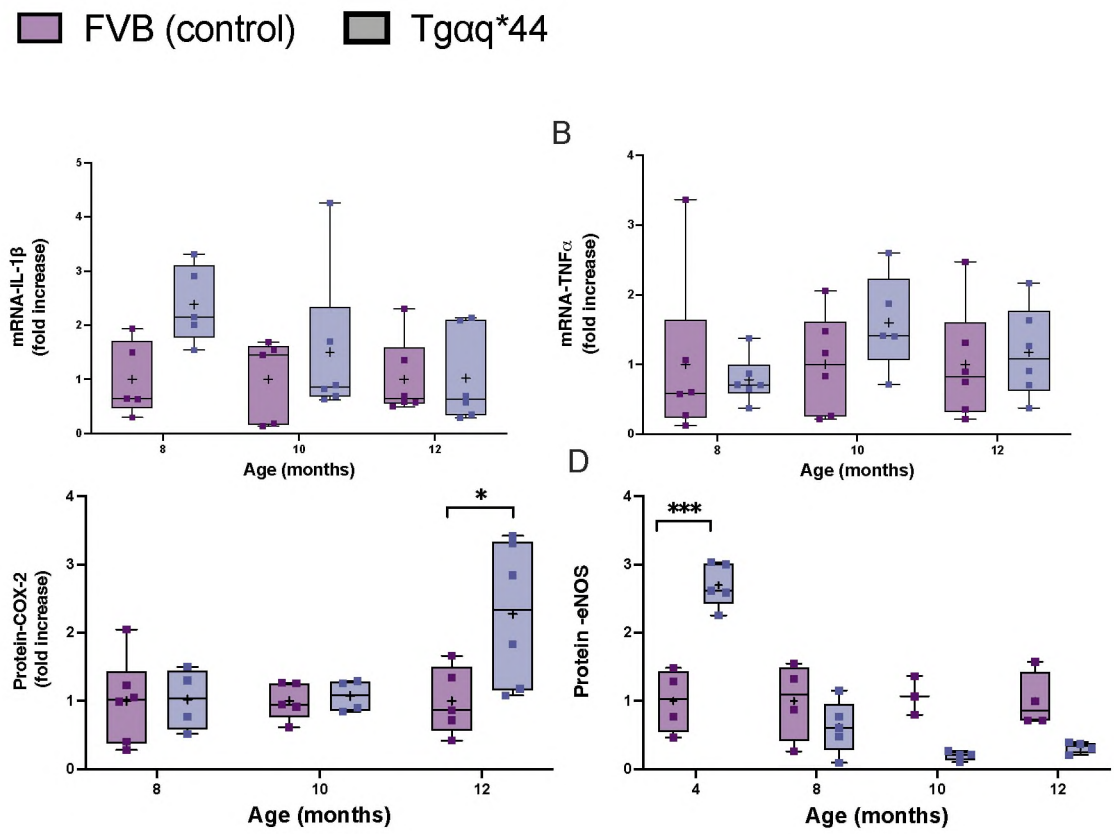

*Figure 13. Alterations in the expression of selected genes and proteins in the aorta along the progression of HF in Tgαq*44 mice compared with age-matched FVB mice. IL-1β (A) and TNF (B) gene expression (n = 5–6) COX-2 (C) and eNOS (D) protein expression levels in the aorta in 4-, 8-, 10-, and 12-month-old Tgαq*44 mice vs. FVB controls are presented. Results are presented as box plots (median, Q1, Q3, whiskers indicate minimum/maximum), Q1 and Q3 indicate the 25th and 75th percentiles, respectively, *p < 0.05, **p < 0.01, ***p < 0.001 ****p < 0.0001, Tgαq*44 mice and age matched FVB control mice compared using Two-way Anova with Post Hoc Sidak test, n = 5–6. (Figure based on T. Mohaissen et al., 2021; Modified).*

*6.5. Plasma cytokine concentration in Tgαq*44 mice*

To assess if in 12-month-old Tgαq*44 mice model is characterized by systemic inflammation BioPlex 2200 automated analyzer were used. Obtained results showed no differences in the plasma concentration of Tumor Necrosis Factor-alpha (TNF-a) (*Figure 14A*), Interleukin-1β (IL-1β) (*Figure 14B*), IL-2 (*Figure 14C*), IL-3 (*Figure 14D*), IL-4 (*Figure 14E*), IL-5 (*Figure 14F*), IL-9 (*Figure 14G*), Interferon gamma (IFNγ) (*Figure 14H*) in 12-month-old Tgαq*44 mice Tgαq*44 mice as compared to age-matched FVB mice.

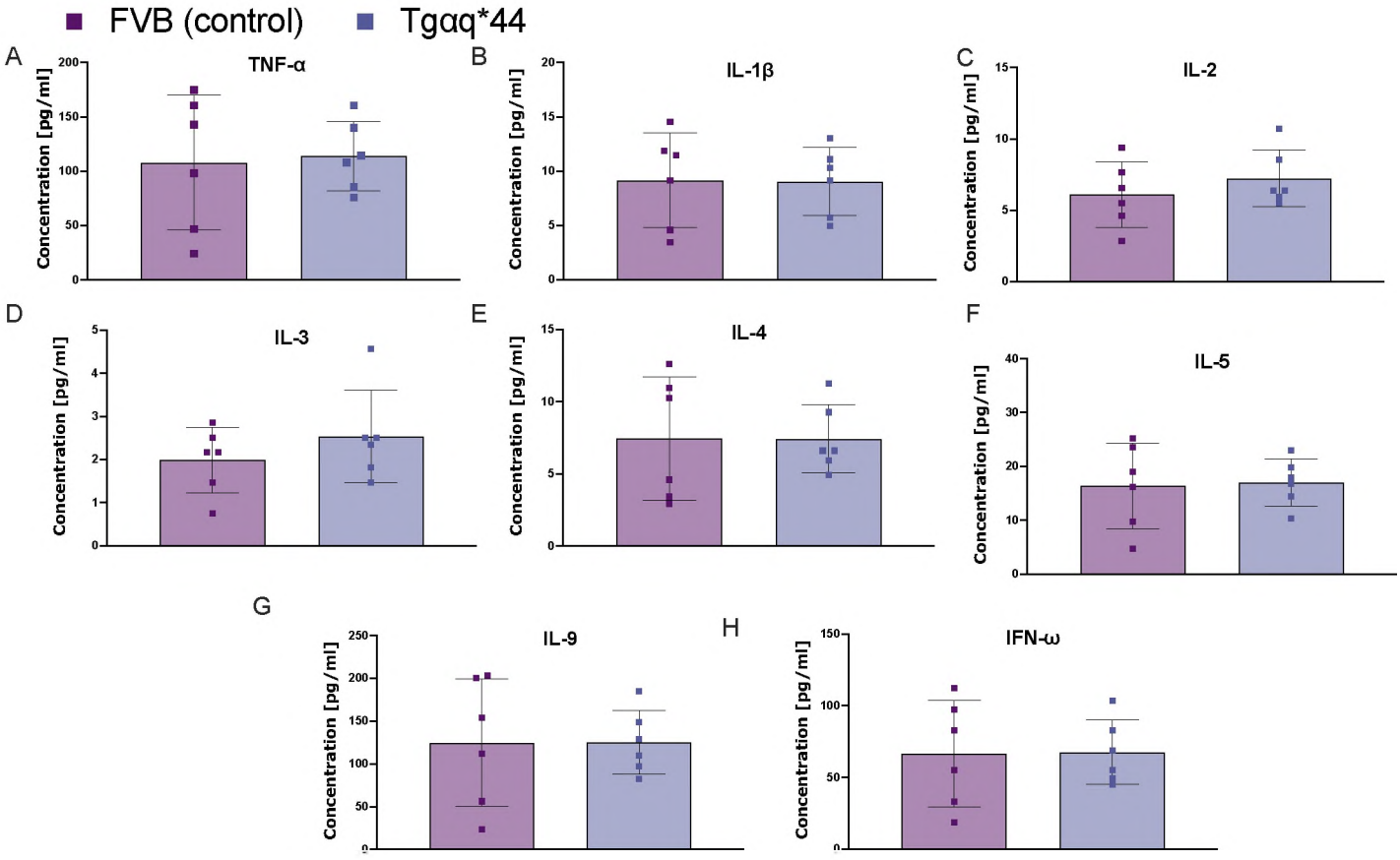

*Figure 14. Plasma concentration of proinflammatory cytokines in HF in 12-month-old Tgαq*44 mice compared with age-matched FVB mice. Tumor Necrosis Factor-alpha (TNFα) (A), Interleukin-1 (IL- 1β) (B), Interleukin-2 (IL-2) (C), Interleukin-3 (IL-3) (D), Interleukin-4 (IL-4) (E), Interleukin-5 (IL-5) (F), Interleukin-9 (IL-9) (G), Interferon gamma (IFNγ) (H) of 12-m Tgαq*44 mice vs FVB are presented. Normality was assessed using Shapiro-Wilk test. Results are presented as mean ± SEM, n=5-6.*

*6.6. Plasma catecholamines concentration levels in Tgαq*44 mice*

To determine the association of neurohormonal activation with endothelial dysfunction plasma concentration of noradrenalin, adrenalin and dopamine were assessed in Tgαq*44 mice.

It was found that 12-month-old Tgαq*44 mice were characterized by higher plasma concentrations of noradrenaline *(Figure 15A)* and adrenaline *(Figure 15B)*, while plasma concentration of dopamine *(Figure 15C)* tended to decrease in 12-month-old Tgαq*44 mice as compared to age-matched FVB mice. Additionally, the plasma concentration of noradrenaline, adrenaline, and dopamine were impaired in 4-month-old Tgαq*44 mice as compared to age-matched FVB mice (*Figure 15*).

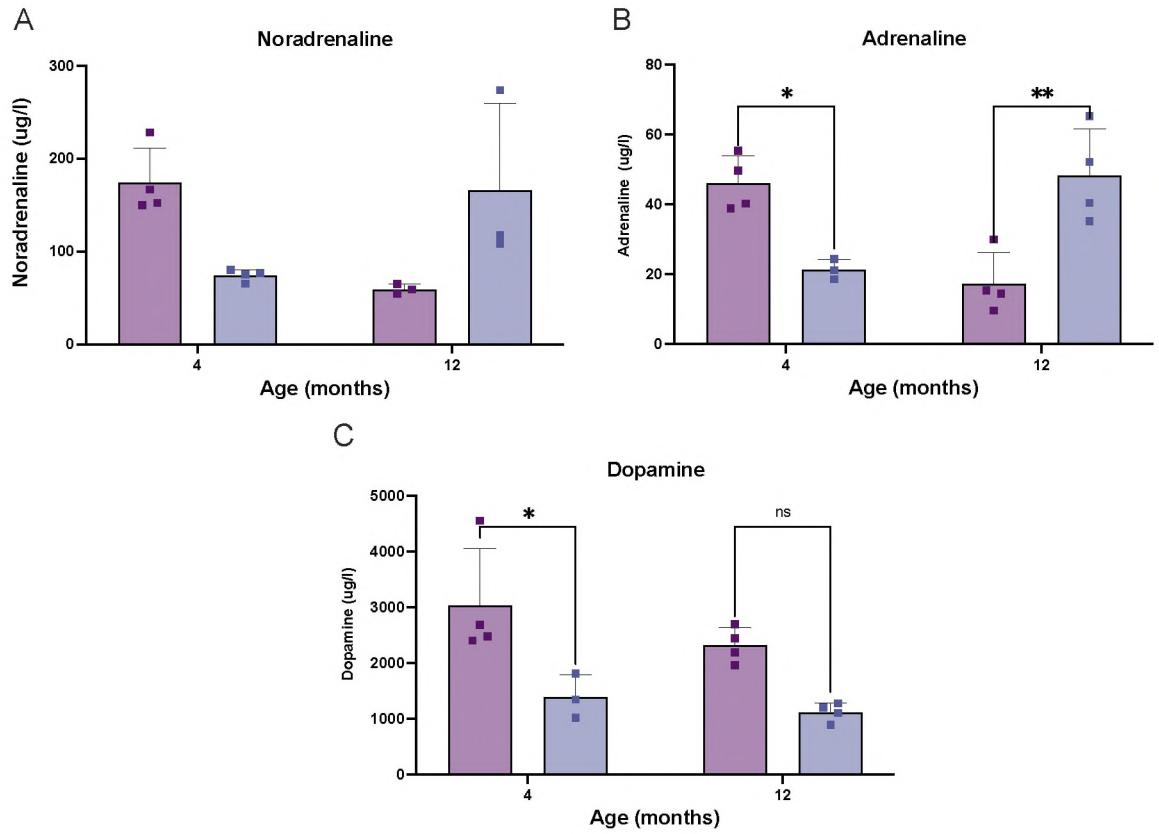

*Figure 15. Plasma concentration of noradrenaline (A) adrenaline (B) and dopamine (C) in plasma in Tgαq*44 mice compared with age-matched FVB mice are presented. Normality was assessed using a Shapiro-Wilk test. Results are given as mean ± SD *p<0.05, **p<0,05, n=5-6.*

*6.7 Nitrite, nitrate plasma concentration and nitrosylhaemoglobin (HBNO) content in RBCs in Tgαq*44 mice*

Systemic endothelial dysfunction in Tgαq*44 mice was not associated with a decrease in NO_2^- *(Figure 16A)* concentration in plasma, however NO_3^- (*Figure 16B*), plasma concentration was lower in 10-and 12-month-old Tgαq*44 mice as compared to age-matched FVB mice.

Interestingly, HbNO RBC content was lower in plasma in 12- month-old Tgαq*44 mice as compared to age-matched FVB mice confirming impaired NO bioavailability in 12-month-old Tgαq*44 mice (*Figure 16C*).

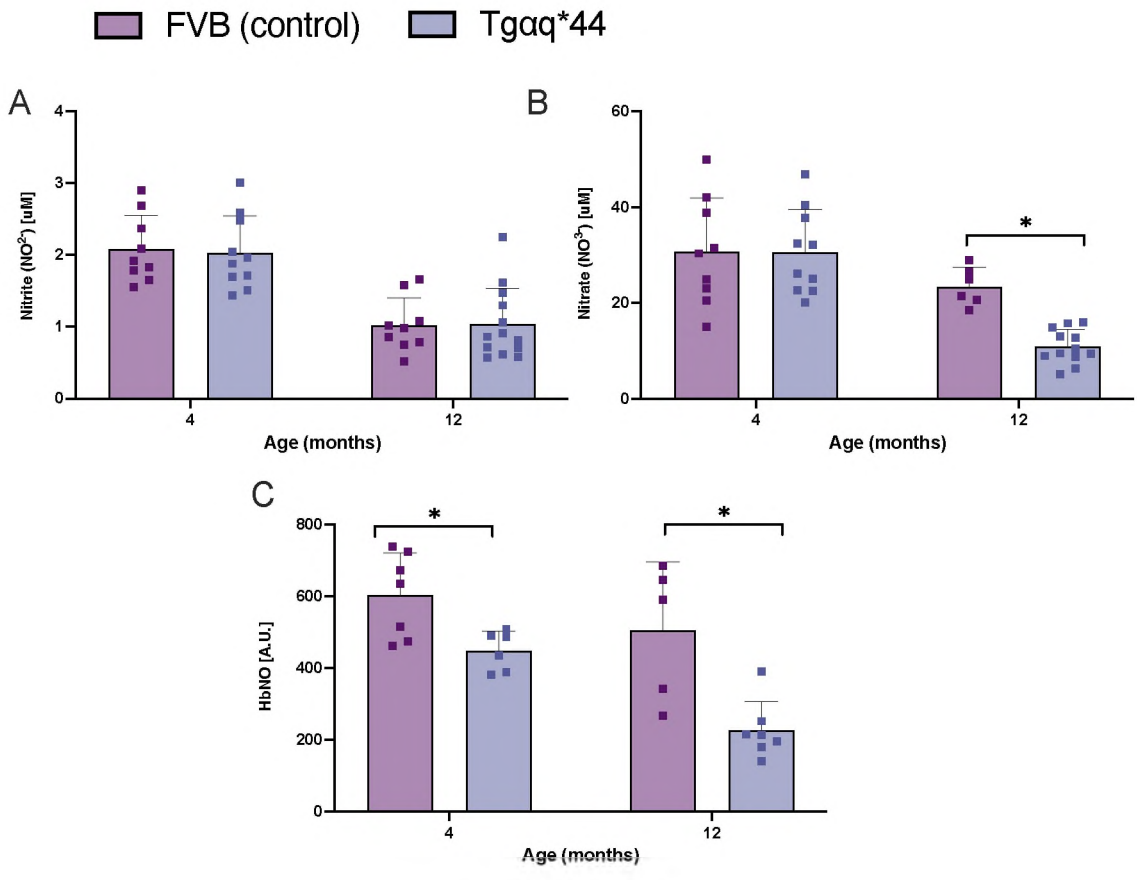

*Figure 16. Nitrite, nitrate plasma concentration and nitrosylhaemoglobin (HbNO) content in RBC in Tgαq*44 mice compared with age-matched FVB mice are presented. Nitrite (NO^{2-}), (A) Nitrate (NO^{3-}) (B; HbNO content, (C) Normality was assessed using a Shapiro-Wilk test. Results are given as mean ± SEM *p<0.05, **p<0,05, n=5-13.*

*6.8 Histology of aorta of Tgαq*44 mice*

In histological sections of aorta endothelial cells in 8-month-old Tgαq*44 mice showed slight change in the shape as they become thicker that was accompanied with loss of adhesion and detachment from the elastic lamina. At a large part of the surface of the vessel the endothelial cells remain in contact with the medium only pointwise.

In 12-month-old Tgαq*44 mice, the process of endothelial damage intensified leading locally to the loss of endothelial contact with the subendothelial layers (*Figure 17C-D*).

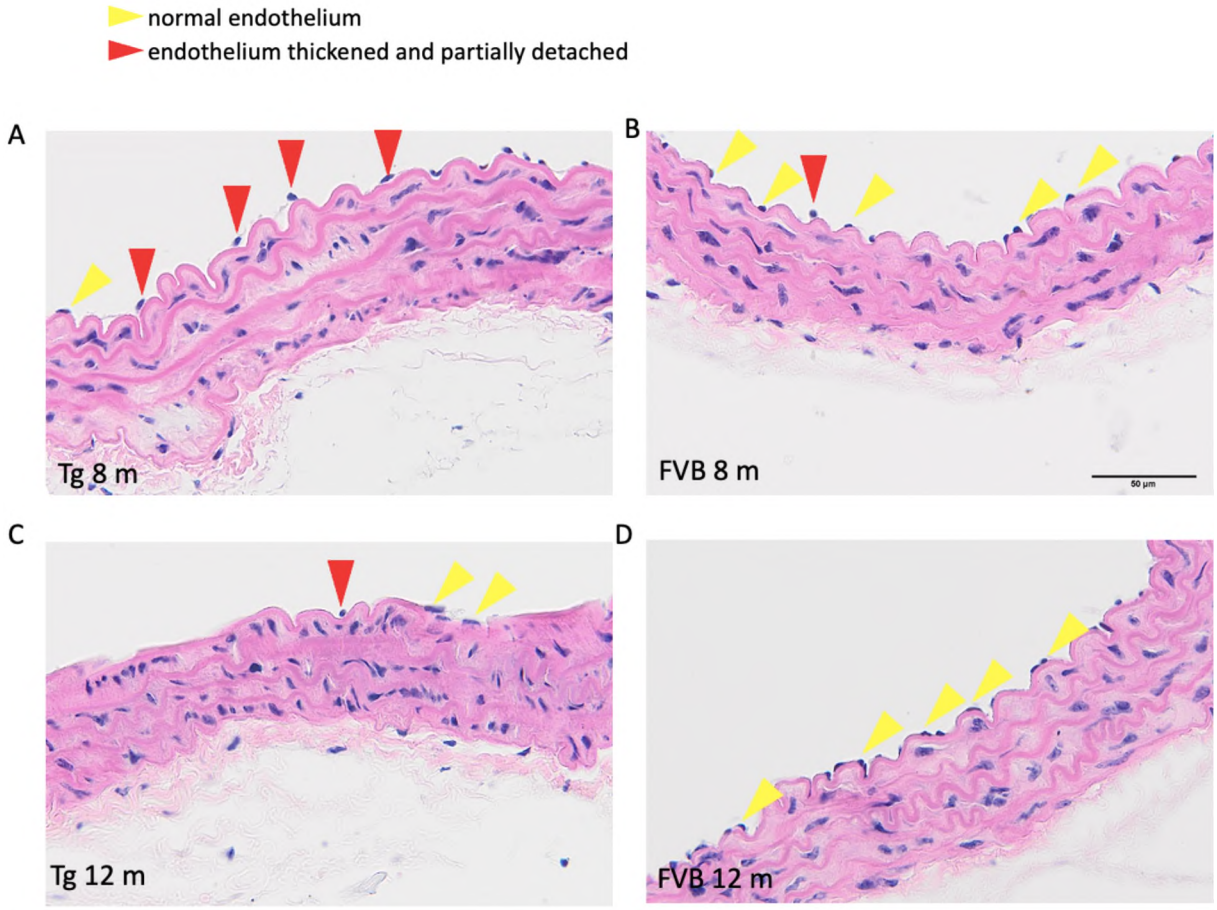

Figure 17. Images of cross-section of aorta isolated from 8- and 12-month-old Tgαq*44 mice compared with age-matched FVB mice are presented.

PART II

ERYTHROCYTE ALTERATIONS IN TGαQ*44 MICE

6.9. Erythrocyte Alterations along the progression of HF

*6.9.1. Effects of RBCs isolated from Tgαq*44 and FVB mice on endothelium-dependent vasodilation*

To test if RBCs isolated from Tgαq*44 mice at the stage of HF could impair endothelial function, RBCs from 12-month Tgαq*44 mice were incubated with aortic rings isolated from FVB mice (control).

Endothelium-dependent relaxation was impaired in aortic segments when incubated with RBCs isolated from **12-month-old Tgαq*44** mice (*Figure 18A*). In contrast, RBCs isolated from **12-month-old FVB mice did** not induce the impairment of endothelial-dependent vasodilation in similar experimental conditions. However, in all experimental groups of Tgαq*44 mice, endothelium-independent vasodilation induced by sodium nitroprusside (SNP) was fully preserved compared with the age-matched FVB (control) mice

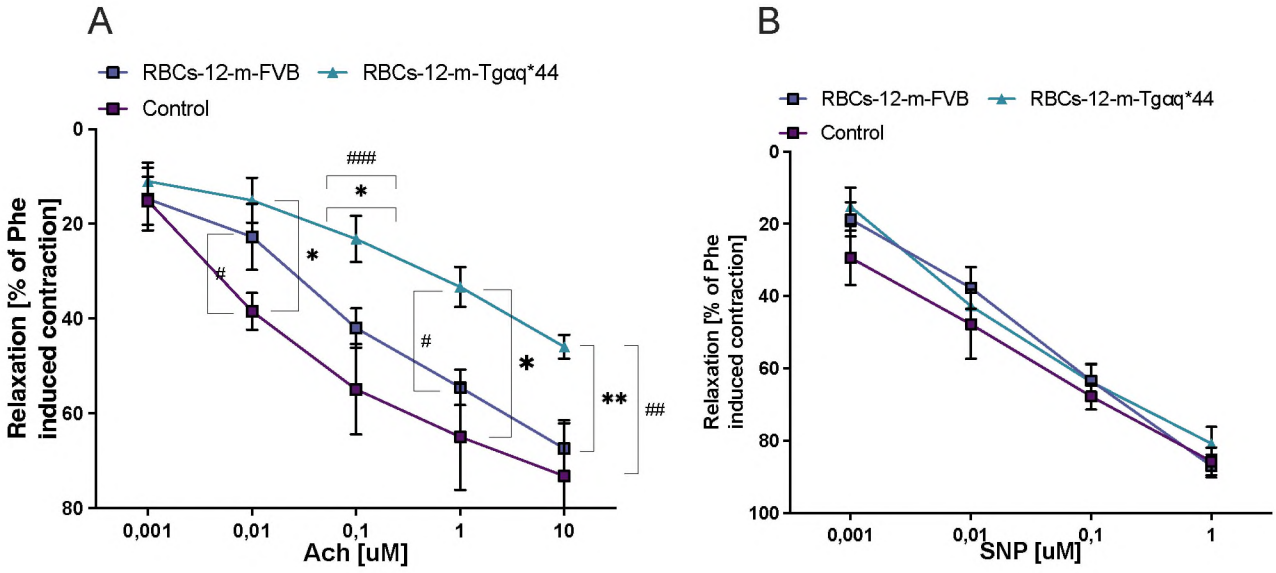

*Figure 18. Effects of RBCs isolated from 12-month-old Tgαq*44 and FVB mice on endothelium-dependent relaxation induced by Ach (A) and endothelium-independent vasodilation induced by SNP (B) in aorta isolated from 4-month-old FVB mice. Controls were incubated with medium for 18h. *p<0.05, **p<0.01, ***p<0.001 ****p<0.0001, 2-way ANOVA, 12-mFVB vs 12-m-Tgαq*44, Control vs. 12-m-Tgαq*44. Results presented as mean ± SEM, n=6. RBCs-12-m-FVB; aorta isolated from 4-m-FVB incubated for 18h with RBC from 12-month-old FVB mice. RBCs-12-m- Tgαq*44; aorta isolated from 4-m-FVB incubated for 18h with RBC from 12-month-old Tgαq*44 mice; Ach, acetylocholine; SNP, sodium nitroprusside; m-months.*

*6.9.2. Effects of RBCs isolated from Tgαq*44 mice and arginase inhibitors pretreatment on RBC-mediated effects on endothelium-dependent vasodilation*

The potential role of RBC arginase activity as a mechanism for endothelial dysfunction induced by RBCs was investigated. Moreover, the involvement of RBCs peroxynitrite in the endothelial dysfunction was analyzed by adding the peroxynitrite scanager-*5,10,15,20-Tetrakis (4-sulfonate phenyl) porphyrinato iron (III) chloride* (FeTPPS) to the co-incubation of RBCs with aortic rings.

Aortic rings isolated from healthy 4-month-old FVB mice, were pre-incubated for 18 h in the absence and the presence of nor-NOHA (Nω-Hydroxy-nor-L-arginine) *(Figure 19A)*, ABH (*2(S)-amino-6-boronohexanoic acid*) (Figure 19B), FeTTPs (*Figure 19 A*) or NAC (*N-acetylcysteine*) (*Figure* 19B)

As shown in *Figure 19* and *20* endothelial function was not affected by NAC, FeTTPs, nor-NOHA, but endothelial function was improved in response to incubation with ABH *Figures 20B* suggesting the role of arginase.

In all experimental groups of Tgαq*44 mice, endothelium-independent vasodilation induced by SNP was fully preserved compared with the age-matched FVB (control) mice *(Figure 19B, 19D, 20B, 20D).*

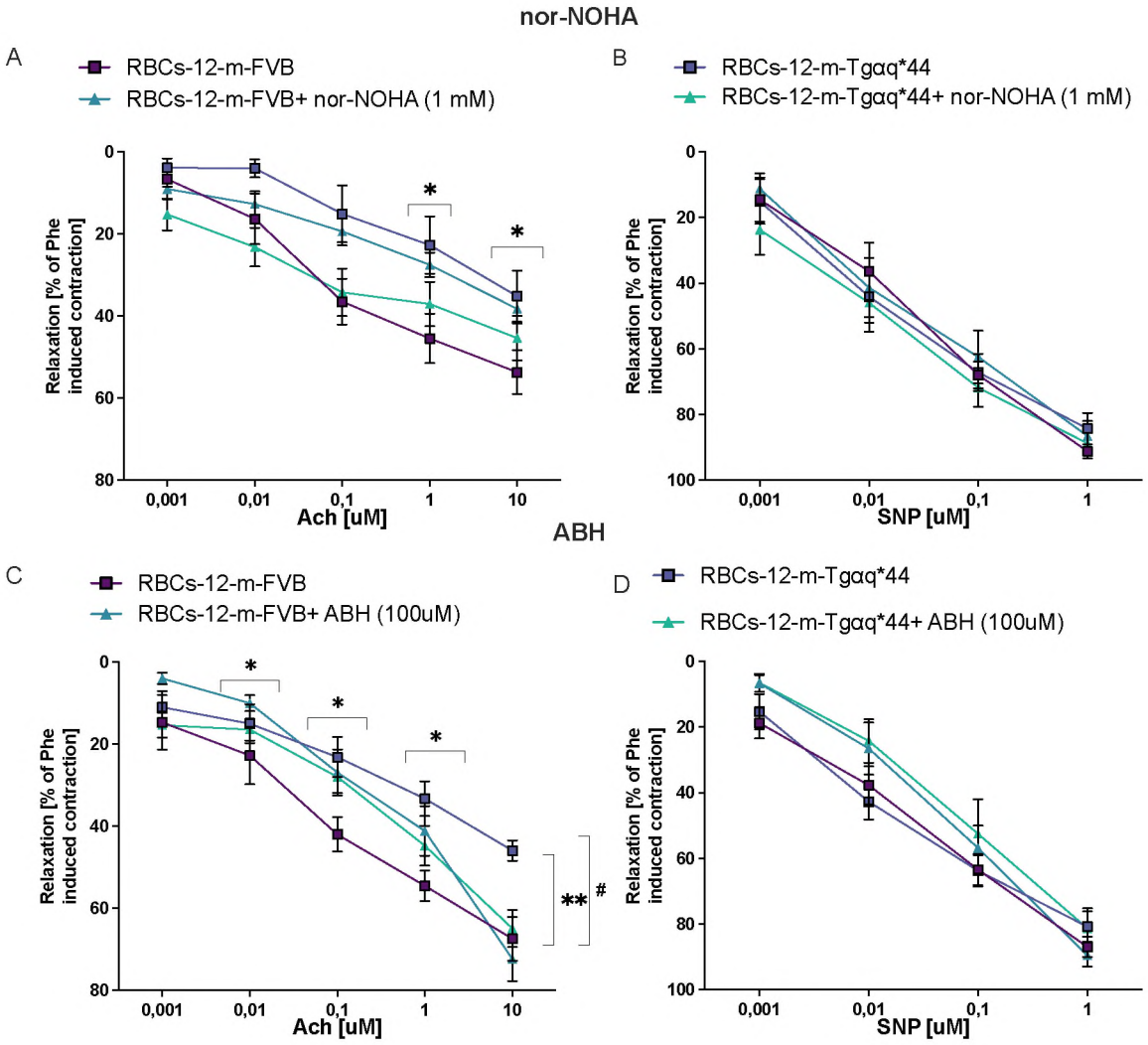

*Figure 19. Effects of different arginase inhibitors on RBC-mediated effects on endothelial function in aorta taken from 12-month-old Tgαq*44 and FVB mice. Effect of nor-NOHA/ ABH incubated with RBCs isolated from 12-month-old FVB and Tgαq*44 mice on endothelium-dependent relaxation induced by Ach (A, C) in aorta isolated from 4-month-old FVB mice are presented. Effect of nor-NOHA/ ABH incubated with RBCs isolated from 12-month-old FVB and Tgαq*44 mice on endothelium-independent relaxation induced by sodium nitroprusside (SNP) (B, D) in aorta isolated from 4-month-old FVB mice are presented. Controls were incubated with medium for 18h. Results presented as mean ± SEM, n=5-6. RBCs-12-m-FVB+nor-NOHA/ABH; aorta isolated from 4-m-FVB incubated with RBC from 12-month-old FVB mice in the present of nor-NOHA or ABH. RBCs-12-m- Tgαq*44; aorta isolated from 4-m-FVB incubated with RBC from 12-month-old Tgαq*44 mice in the present of nor-NOHA or ABH; nor-NOHA, (Nω-Hydroxy-nor-L-arginine); ABH, 2(S)-amino-6-boronohexanoic acid; Ach, acetylocholine; SNP, sodium nitroprusside; m-months.*

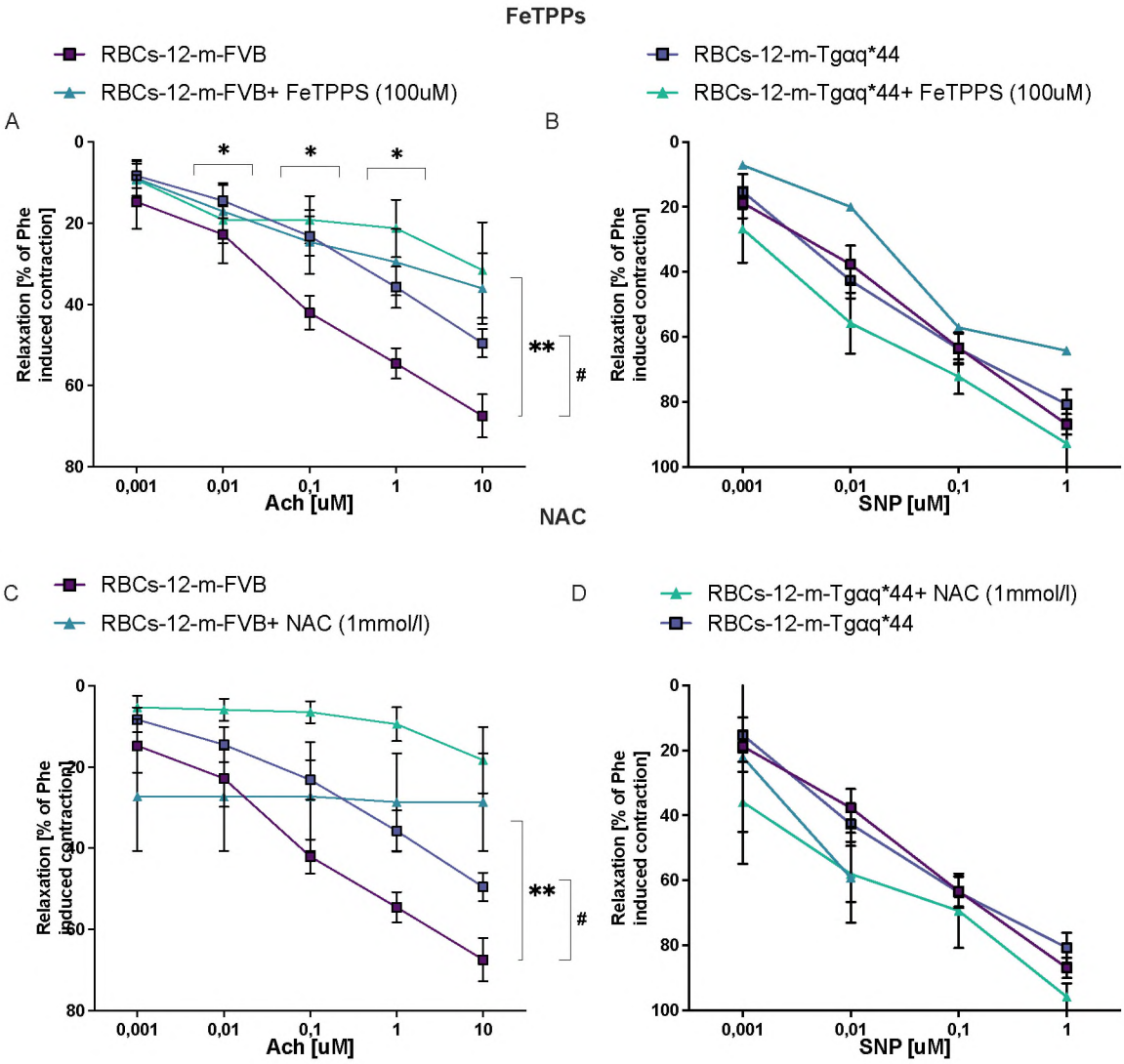

*Figure 20. Effects of different arginase inhibitors on RBC-mediated effects on endothelial function in aorta taken from 12-month-old Tgαq*44 and FVB mice. Effect of FeTPPS/NAC incubated with RBCs isolated from 12-month-old FVB and Tgαq*44 mice on endothelium-dependent relaxation induced by Ach (A, C) in aorta isolated from 4-month-old FVB mice are presented. Effect of FeTPPS/NAC incubated with RBCs isolated from 12-month-old FVB and Tgαq*44 mice on endothelium-independent relaxation induced by sodium nitroprusside (SNP) (B, D) in aorta isolated from 4-month-old FVB mice are presented. Controls were incubated with medium for 18h. Results presented as mean ± SEM, n=5-6. RBCs-12-m-FVB+ FeTPPS /NAC; aorta isolated from 4-m-FVB incubated for 18h with RBC from 12-month-old FVB mice in the present of FeTPPS or NAC. RBCs-12-m- Tgαq*44; aorta isolated from 4-m-FVB incubated for 18h with RBC from 12-month-old Tgαq*44 mice in the present of FeTPPS or NAC; FeTPPS, (Fe(III)5,10,15,20-tetrakis(4-sulfonatophenyl)porphyrinato chloride); NAC, (N-acetylcysteine), Ach, acetylocholine; SNP, sodium nitroprusside; m-months.*

*6.9.3. Alterations in blood count, erythrocyte deformability and GSH/GSSG ratio in RBCs in Tgαq*44 mice*

Automated blood counts analysis showed a reduced MCV level in 8-12-month-old Tgαq*44 mice as compared to the age-matched FVB *(Figure 21A)*, while RDW was significantly increased in 10-and 12-month-old mice Tgαq*44 relatively to age-matching control groups *(Figure 21B)*. Measurements of total glutathione, GSH, GSSG in RBCs showed no statistically significant differences in Tgαq*44 mice vs FVB mice [result not shown], whereas the GSH/GSSG ratio in RBCs was significantly lower in 12-month Tgαq*44 mice as compared to age-matching FVB mice *(Figure 21C)*.

Erythrocyte deformability measured at shear stress 20 Pa was markedly decreased in 12-month-old Tgαq*44 mice as compared to age-matching control groups *(Figure 21D)*.

There were no differences in EPO plasma concentration level in 4-,8-, and 12-month-old Tgαq*44 mice as compared to age-matched FVB mice *(Figure 21E)*.

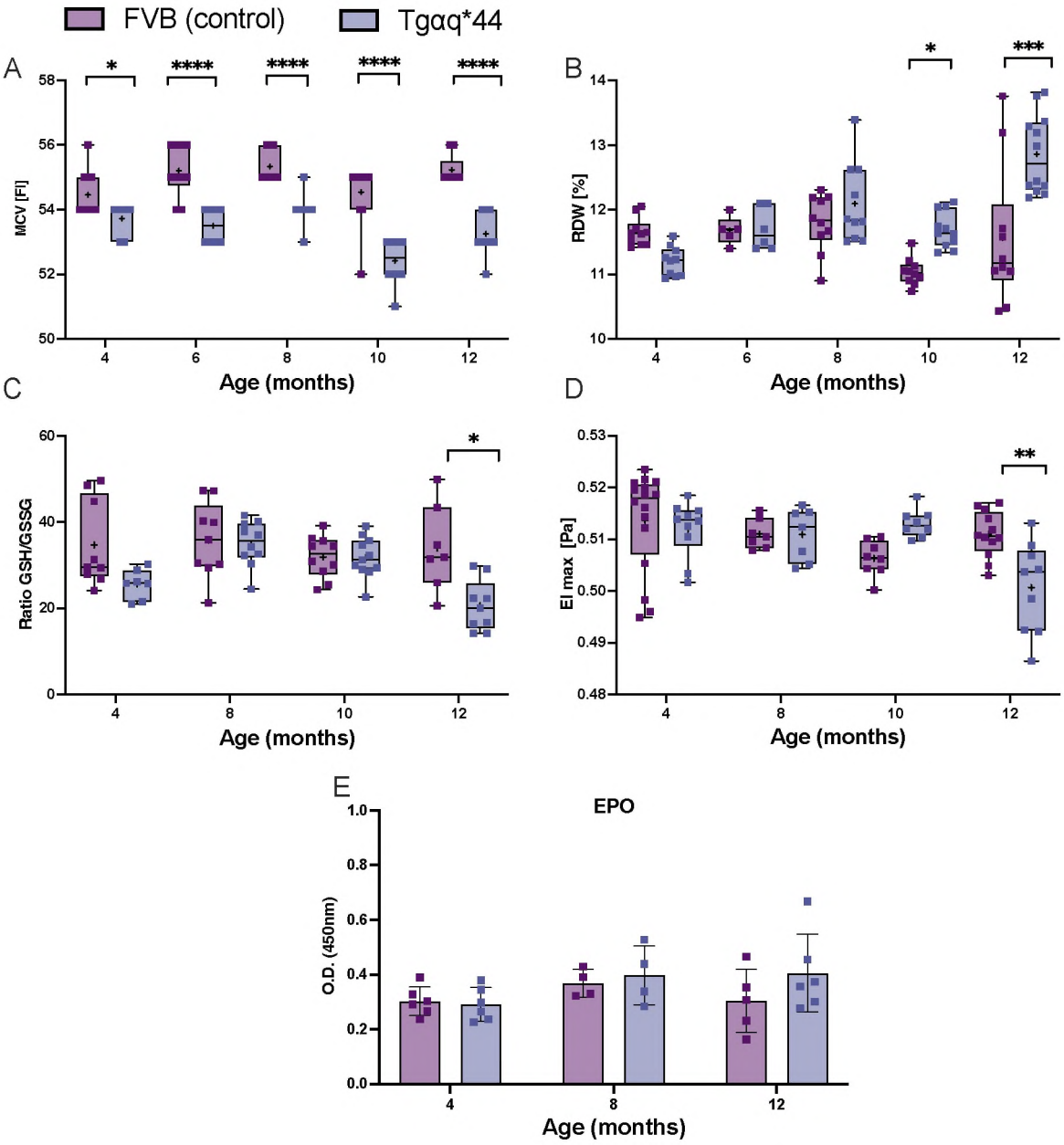

*Figure 21. Alterations in blood count, erythrocyte deformability and GSH/GSSG ratio in RBCs (oxidative stress) along the progression of HF in Tgαq*44 compared with an age-matched FVB mice. Mean corpuscular volume (MCV) (n=11-12) (A) red blood cell distribution width (RDW) (10-12) (B) in the blood, The glutathione redox ratio ($GSSG{\cdot}GSH^{-1}$) (n=7-10) (C) in the RBCs in 4-,8-,10- and 12-month-old Tgαq*44 mice vs FVB. RBCs deformability (n=7-12) (D) at the shear stress 20Pa (El max). EPO (erythropoietin) concentration RBCs in 4-,8-and 12-month-old Tgαq*44 mice vs FVB are presented. Normality was assessed using Shapiro-Wilk test. Results are presented as box plots (median, Q1, Q3, interquartile ranga). Q1, Q3 indicate 25th and 75th percentiles, respectively. *p<0.05, **p<0.01, ***p<0.001 ****p<0.0001, 2wayAnova, FVB vs Tgαq*44.*

PART III

ANG-(1-12)/ANG II/TXA$_2$ PATHWAY

IN PERIPHERAL CIRCULATION IN TGαQ*44 MICE

*6.10. Impaired endothelium-dependent vasodilation induced by Ang I, Ang II or Ang-(1–12) in the aorta isolated from Tgαq*44 mice as compared to age-matched FVB*

To test effects of exogenous angiotensin's, Ang I, Ang II and Ang-(1-12) were incubated with the **aorta** isolated from 4- and 12-months-old-Tgαq*44 and FVB mice for 18-24 hours.

In 12-month-old Tgαq*44 mice the decreased endothelium-dependent vasorelaxation was observed in response to Ang I, Ang II, and Ang- (1-12), as compared to non- stimulated aortic rings *(Figure 23)*, whereas, in 4-months-old Tgαq*44 mice *(Figure 22)*, only Ang-(1-12) induced the impaired vasodilatory endothelial response to Ach as compared to non-stimulated aortic rings (Fig.18). In contrast, there was no difference in endothelial independent vascular response to SNP after incubation with Ang I, Ang II or Ang-(1-12) in 4- *(Figure 22 B, D)* and 12- *(Figure 23 B, D)* Tgαq*44 or age-matched FVB.

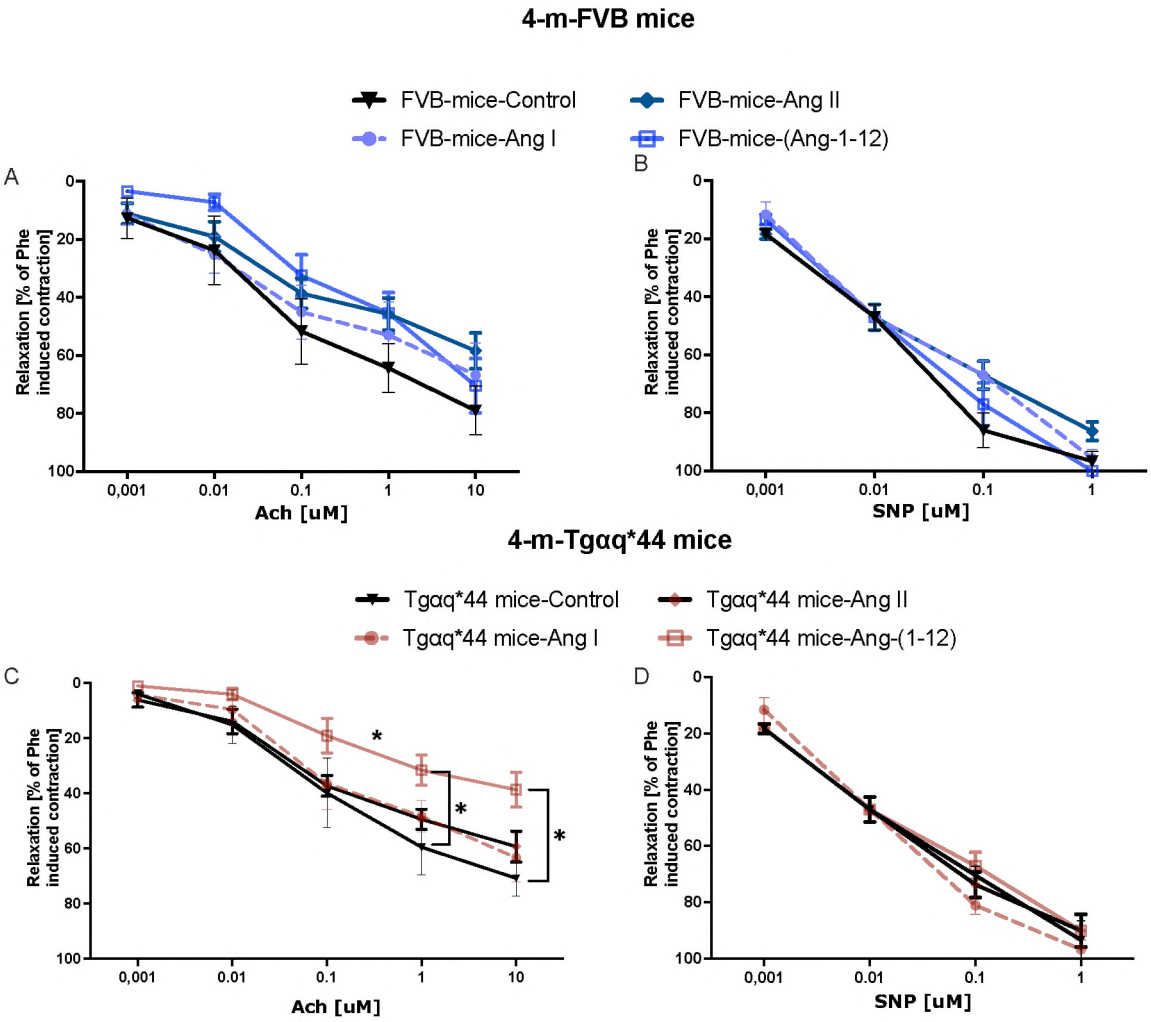

*Figure 22. Effects of exogenous Ang I, Ang II, and Ang-(1–12) on vascular endothelial function after incubation with Ang I, Ang II, and Ang-(1–12) for 18-24 hours in 4-month-old Tgq*44 mice and age-matched FVB. The vasodilation of the aorta rings in dose-response to Ach was assessed in 4-month-old Tgαq*44 mice versus age-matched FVB control after 18–24 h (measured ex vivo) incubation with Ang I, Ang II and Ang-(1–12). The results are presented as mean ± standard error of the mean SEM, n = 5–8 Key: *, P < 0.05; **, P < 0.01; ***, P < 0.001 in a one-way ANOVA. Ach, acetylocholine; SNP, sodium nitroprusside; Ang I, angiotensin I; Ang II, angiotensin II; Ang-(1-12), Angiotensin-(1-12); m-months.*

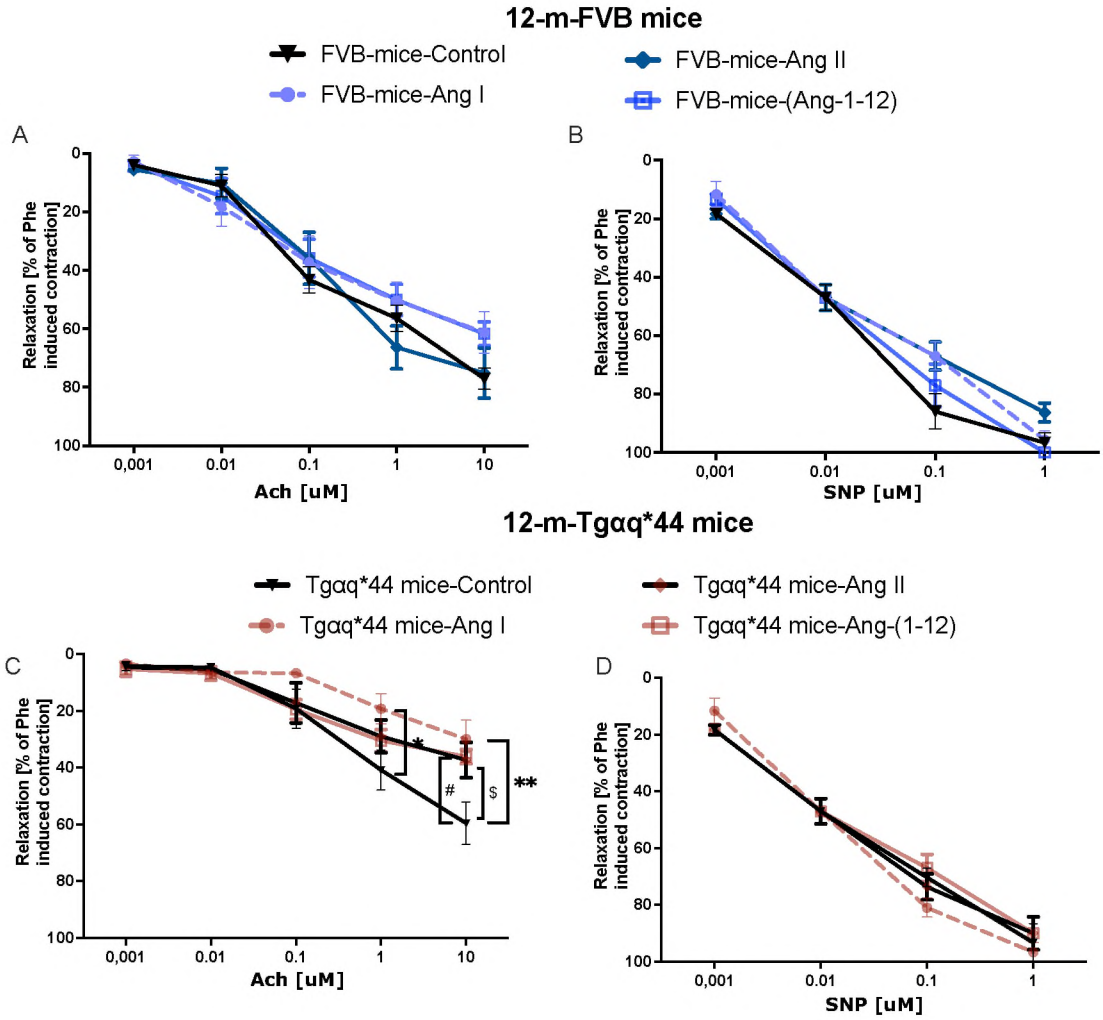

*Figure 23. Effects of exogenous Ang I, Ang II, and Ang-(1–12) on vascular endothelial function after incubation with Ang I, Ang II, and Ang-(1–12) for 18-24 hours in 12-month-old Tgq*44 mice and age-matched FVB. The vasodilation of the aorta rings in dose-response to Ach was assessed in 4-month-old Tgαq*44 mice versus age-matched FVB control after 18–24 h (measured ex vivo) incubation with Ang I, Ang II and Ang-(1–12). The results are presented as mean ± standard error of the mean SEM, n = 5–8 Key: *, P < 0.05; **, P < 0.01; ***, P < 0.001 in a one-way ANOVA. Ach, acetylocholine; SNP, sodium nitroprusside; Ang I, angiotensin I; Ang II, angiotensin II; Ang-(1-12), Angiotensin-(1-12); m-months.*

*6.11. mRNA expression levels of renin, chymase, ACE, ACE-2, AT_1 or AT_2 receptors in aorta from Tgαq*44 mice as compared with age-matched FVB mice*

To test if endothelial dysfunction is linked to changes in the expression of RAS pathway elements, mRNA expression of renin, chymase, ACE, ACE-2, AT_1 and AT_2 receptor were measured by qRT-PCR.

There were no differences in ACE-2 (*Figure 24A*), AT_1 (*Figure 24*C) and chymase (Cma1) (*Figure 24F*), mRNA levels in the isolated aorta in 4- and in 12-month-old Tgαq*44 mice as compared with age-matched FVB mice. However, the increased AT_2 and renin level (*Figure 24*D) and lower ACE level (*Figure 24A*), were shown in isolated aorta from 12-month-old Tgαq*44 mice as compared to aged-matched FVB mice. In contrast, 4-month-old Tgαq*44 mice and age-matched FVB mice did not show any differences in renin, ACE *(Figure 24E)*, ACE-2 *(Figure 24B)*, AT_1 *(Figure 24C)* AT_2 *(Figure 24D)* or chymase (Cma1) *(Figure 24F)* mRNA levels in the isolated aorta.

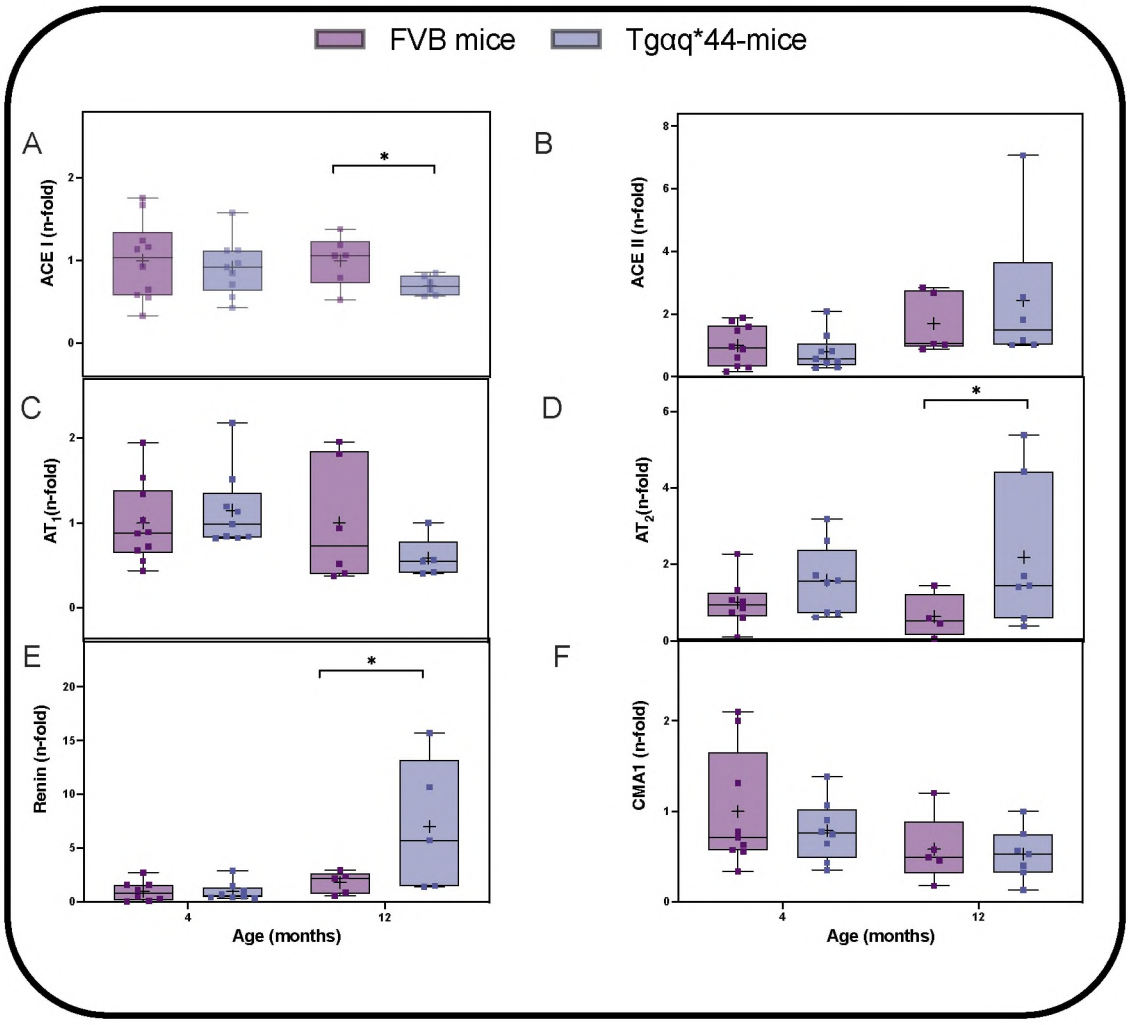

*Figure 24. Vascular mRNA expression of renin, chymase (CMA-1), ACE, ACE-2, AT_1 and AT_2 receptor in isolated aorta from Tgαq*44 mice compared with age-matched FVB mice. ACE (A),) ACE-2 (B), AT_1 (C), AT_2 (D), Renin (E), and chymase (CMA1) (F) mRNA levels in the aortic rings in Tgαq*44 mice were compared to age-matched FVB mice (n = 5–8). The results are presented as boxplots (median, Q1, Q3, and whiskers indicating minimum/maximum). Key: *, $P < 0.05$ for Tgαq*44 vs age matched FVB mice in a two-way ANOVA with post hoc Sidak test, n = 5–8, (mRNA measurements made in cooperation with Raquel Rodrigues-Diez, PhD, Spain).*

*6.12. Changes in angiotensin profile induced by Ang-(1–12), Ang I, or Ang II incubated with the aorta from Tgαq*44 mice as compared with age-matched FVB mice*

6.12.1. Changes in angiotensin profile induced by exogenous Ang I in the aorta

Ang I (100 nM) incubated with aortic rings for 18-24-hours induced Ang II, Ang IV, and Ang-(1–7) production in 4- and 12-month-old Tgαq*44 mice and in age-matched FVB mice. Ang-(1–12)-derived Ang-(1–7) production was significantly inhibited by an ACE-inhibitor (perindoprilat; 10 μM) in 12-month-old Tgαq*44 mice, reducing Ang-(1–7) concentration below the method's quantification limit (*Figure 25*).

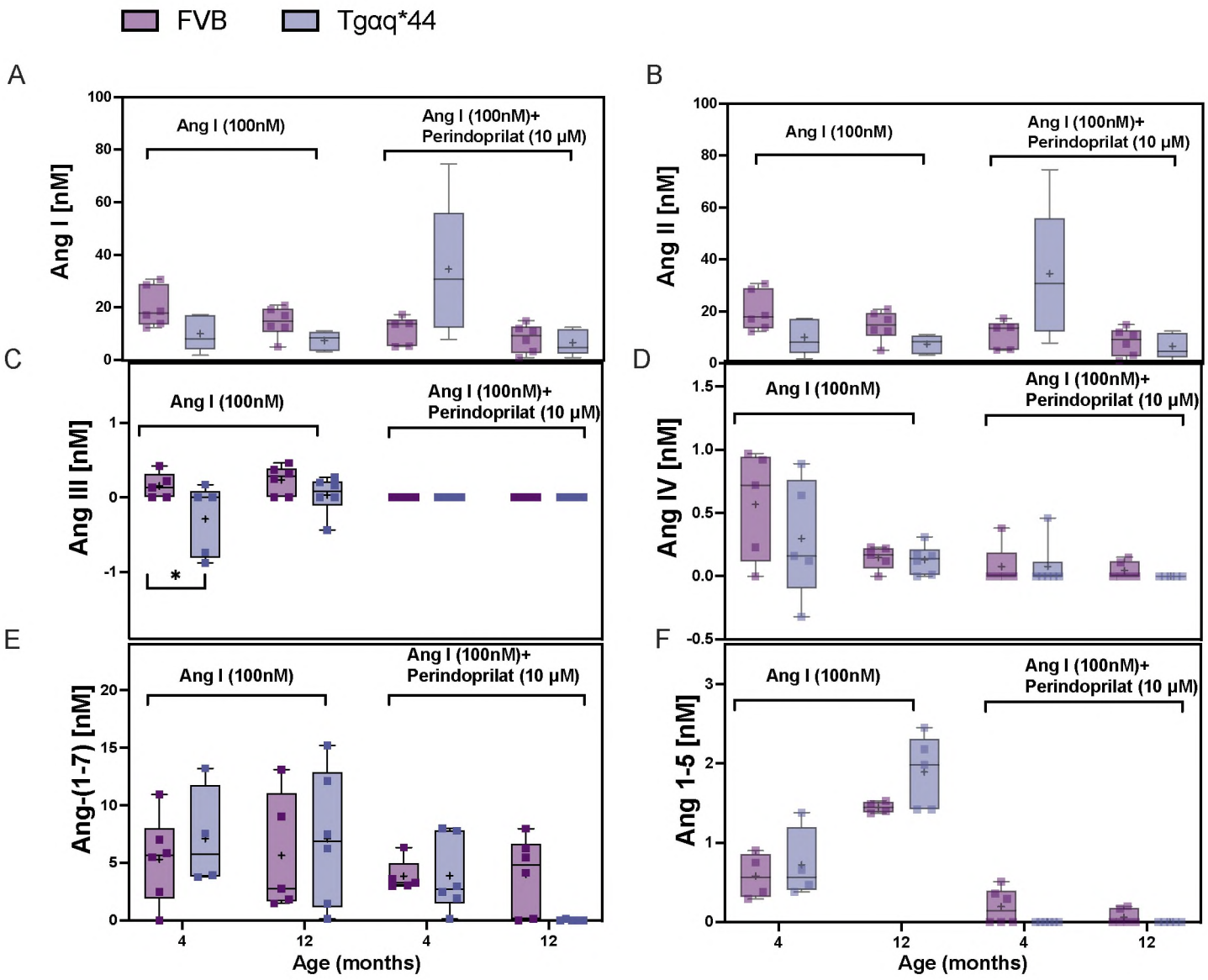

*Figure 25. Changes in angiotensin's profile production in the aorta isolated from Tgαq*44 mice and age- matched FVB mice after incubation with Ang I. Ang I (A), Ang II (B), Ang III (C), Ang IV (D), Ang-(1–7 (E) and Ang-(1–5) (F) concentrations in the medium after Ang I, 100 nM stimulation of aortic rings with and without an ACE-inhibitor (perindoprilat; 10 µM) for 18-24 h in 4- and 12-month-old Tgαq*44 mice compared to age-matched FVB mice are presented. The results are presented as boxplots (median, Q1, Q3, and whiskers indicating minimum/maximum): *, $P < 0.05$; **, $P < 0.01$ for Tgαq*44 vs age matched FVB mice in a two-way ANOVA with post hoc Sidak test, n = 5–8.*

6.12.2. Changes in angiotensin profile induced by exgogenous Ang II in the aorta

Ang II (100 nM) incubated with aortic rings for 18-24-hours induced Ang III, Ang IV, Ang-(1–7) and Ang-(1–5) production in 4- and 12-month-old Tgαq*44 mice as compared to age-matched FVB mice.

Moreover, **MLN (ACE-2 inhibitor)** applied with Ang II decreased concentration of Ang II, Ang III, Ang IV, Ang-(1–7) and Ang-(1–5) in 12-month-old Tgαq 44 mice and increased concentration of Ang I and III in 4-month-old Tgαq 44 mice as compared to age matched control groups (*Figure 26*).

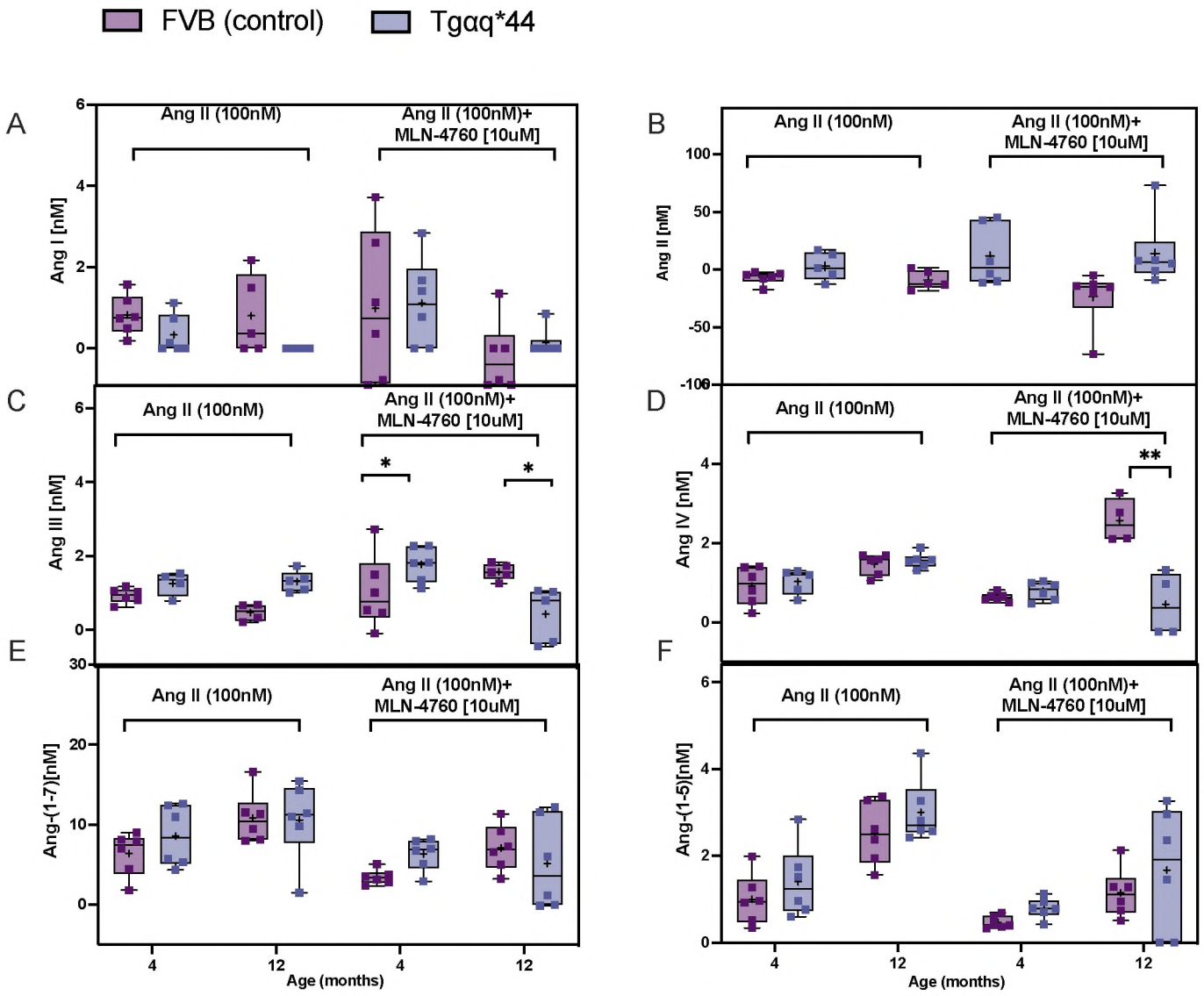

*Figure 26. Changes in angiotensin's profile production in the aorta isolated from Tgαq*44 mice and age-matched FVB mice after incubation with Ang II. Ang I (A), Ang II (B), Ang III (C), Ang IV (D), Ang-(1–7 (E) and Ang-(1–5) (F) concentrations in the medium after Ang II (100 nM) stimulation of aortic rings with and without an ACE-2 inhibitor (MLN-4760; 10 μM) for 18-24 h in 4- and 12-month-old Tgαq*44 mice compared to age-matched FVB mice are presented. The results are presented as boxplots (median, Q1, Q3, and whiskers indicating minimum/maximum). Key: *, P < 0.05; **, P < 0.01 for Tgαq*44 vs age matched FVB mice in a two-way ANOVA with post hoc Sidak test, n = 5–8.*

6.12.3. Changes in angiotensin profile induced by exogenous Ang-(1-12) in the aorta

Ang-(1–12) (100 nM) incubated with aortic rings for 18-24-hours induced Ang II, Ang IV and Ang-(1-12) production in 4- and 12-month-old Tgαq*44 mice as compared to age-matched FVB mice. In 4-months-old Tgαq*44 mice Ang-(1-12) caused increase of Ang II, Ang III, Ang IV, and Ang-(1–7) production in the aortic rings compared to age-matched FVB mice.

Moreover, **chymostatin (chymase inhibitor)** applied with Ang-(1-12) increased concentration of Ang III and Ang-(1-7) in 12-monh-old Tgαq*44 mice and the level of Ang IV in 4-monh-old Tgαq*44 (*Figure27*) as compared to age-matched controls. No changes were observed in Ang II concentration in the presence of chymostatin in all experimental groups of mice.

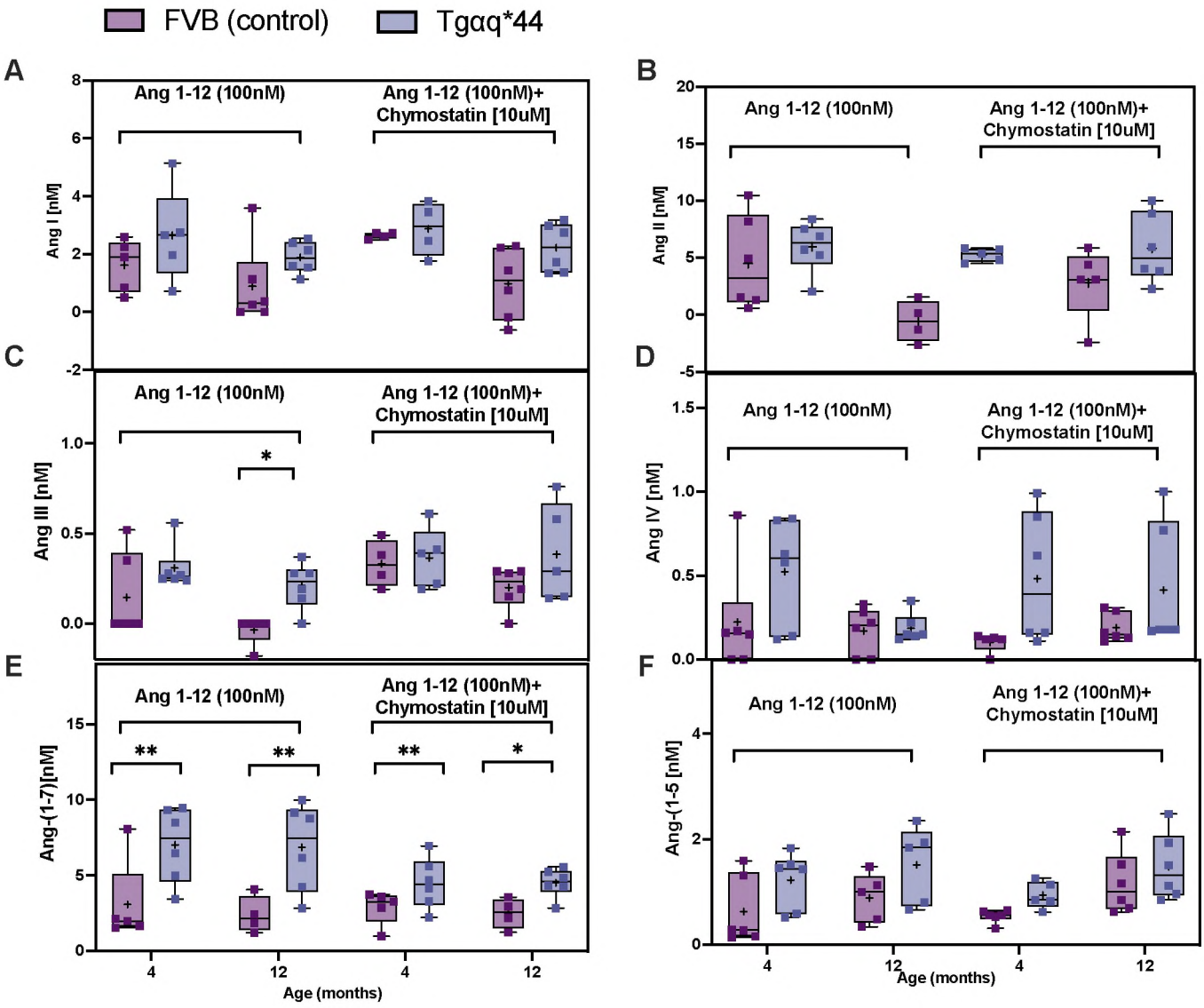

*Figure 27. Changes in angiotensin's profile production in the aorta isolated from Tgαq*44 mice and age-matched FVB mice after incubation with Ang-(1-12). Ang I (A), Ang II (B), Ang III (C), Ang IV (D), Ang-(1–7 (E) and Ang-(1–5) (F) concentrations in the medium after Ang-(1-12) (100 nM) stimulation of aortic rings with and without a chymase inhibitor (chymostatin; 10 μM) for 18-24 h in 4- and 12-month-old Tgαq*44 mice compared to age-matched FVB mice are presented. The results are presented as boxplots (median, Q1, Q3, and whiskers indicating minimum/maximum). Key: *, P < 0.05; **, P < 0.01 for Tgαq*44 vs age matched FVB mice in a two-way ANOVA with post hoc Sidak test, n = 5–8.*

*6.13. Changes in eicosanoids profile after incubation with Ang-(1–12), Ang I, or Ang II in the aorta of Tgαq*44 mice as compared with age-matched FVB*

There was a clear-cut difference in profile eicosanoids generated in response to Ang I, Ang II or Ang-(1-12) in aorta taken from 12- month-old Tgαq*44 mice as compared with 4-month-old Tgαq*44 mice. In each case, after incubation with Ang I, Ang II or Ang-(1-12) there was a higher concentration of TXB_2 generated in aortic rings from 12-month-old Tgαq*44 mice as compared with aortic rings taken from 4-month-old Tgαq*44 mice.

6.13.1. Changes in eicosanoids profile induced by exogenous Ang I in the aorta

The profile of eicosanoids released from aorta incubated with **Ang I** from 8-month-old **Tgαq*44 mice** did not differ in comparison with age-matched FVB mice. Only the concentration of PGE_2 was decreased in aortic rings incubated with Ang I. The concentration of 5-, 12- and 15-HETEs in aortic effluent was similar in 12-month-old Tgαq*44 mice as compared to age matched FVB mice.

In the presence of ACE-inhibitor (perindoprilat) Ang I induced changes in eicosanoids profile weren't modified significant in 4-and 12-month-old Tgαq*44 mice as well as age matched FVB mice (*Figure 28)*.

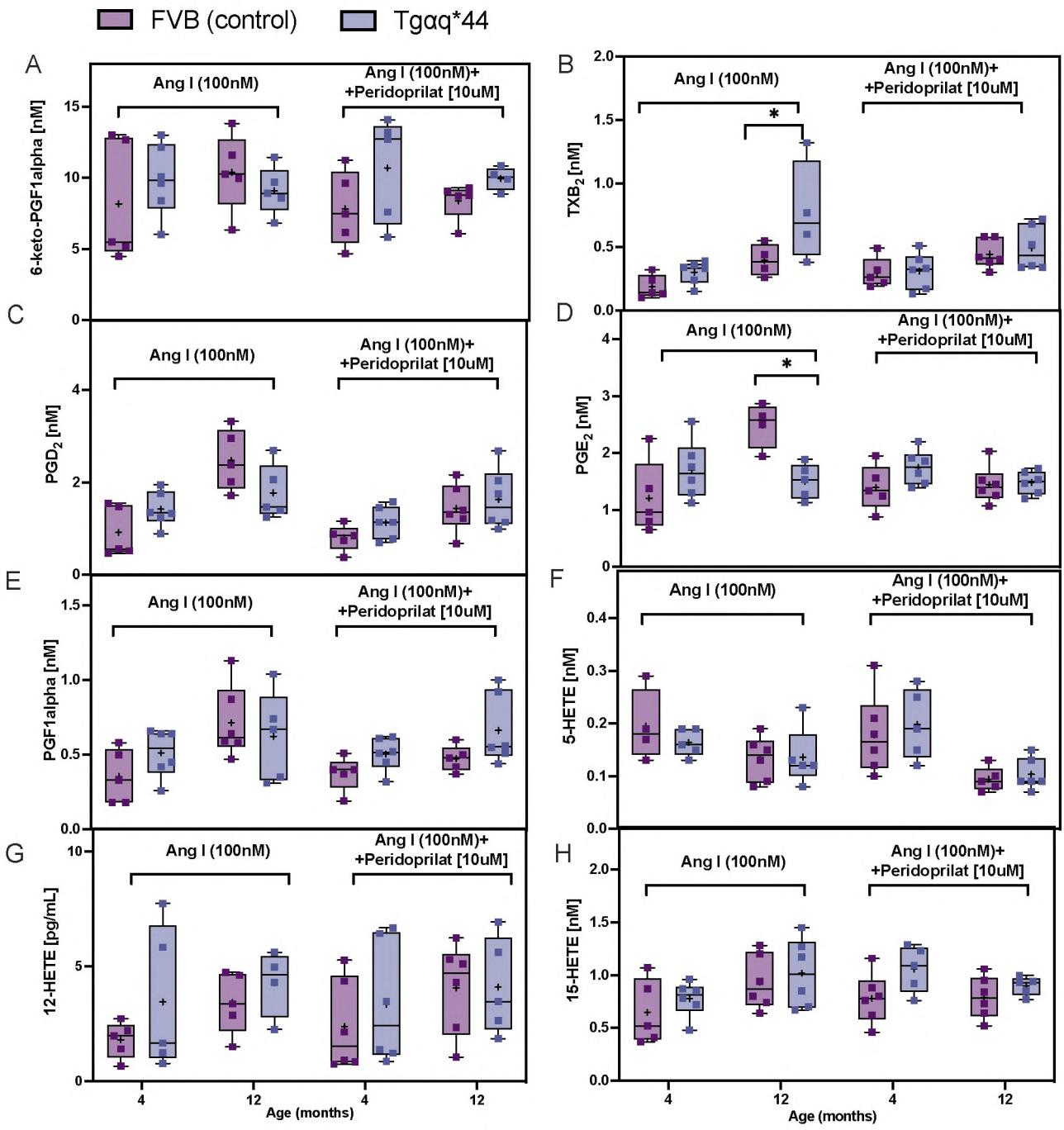

*Figure 28. Changes in eicosanoids production in the aorta rings isolated from Tgαq*44 mice and age-matched FVB mice after incubation with exogenous Ang I with and without an ACE- inhibitor (perindoprilat; 10 μM) for 18–24 h in 4- and 12-month-old Tgαq*44 mice compared to age-matched FVB mice. Eicosanoids production in the buffer after ex vivo stimulation of the aorta by Ang I (100 nM; 45 min), including 6-keto-PGF$_{1alfa}$ (A) TXB$_2$ (B), PGD$_2$ (D), PGE$_2$ (F), PGF$_{1alpha}$ (E), PGF2α (F) 5-HETE (F), 12-HETE (G) and 15-HETE (H), assessed in 4- and 12-month-old Tgαq*44 mice compared to age-matched FVB mice are presented. The results are presented as boxplots (median, Q1, Q3, with whiskers indicating minimum/maximum). Key: *, P < 0.05 for Tgαq*44 vs age matched FVB mice in a two-way ANOVA with post hoc Sidak test, n = 5–8.*

6.13.2. Changes in eicosanoids profile induced by exogenous Ang II in the aorta

The profile of eicosanoids released from aorta incubated with **Ang II** showed the increased concentration of PGD_2 (*Figure 29C*) in aortic rings in 12-months but not 4-month-old Tgαq*44 mice (*Figure 29)*. The concentration of 5-HETEs (*Figure 29F*) in aortic effluent was similar in 12-month-old Tgαq*44 mice as compared to age matched FVB mice, while the release of 12-and 15- HETE tended to increase.

In the presence of **ACE-2 inhibitor (MLN-4760)** Ang II induced changes in eicosanoids profile weren't modified significant in 4-and 12-month-old Tgαq*44 mice as well as age matched FVB mice (*Figure 29)*.

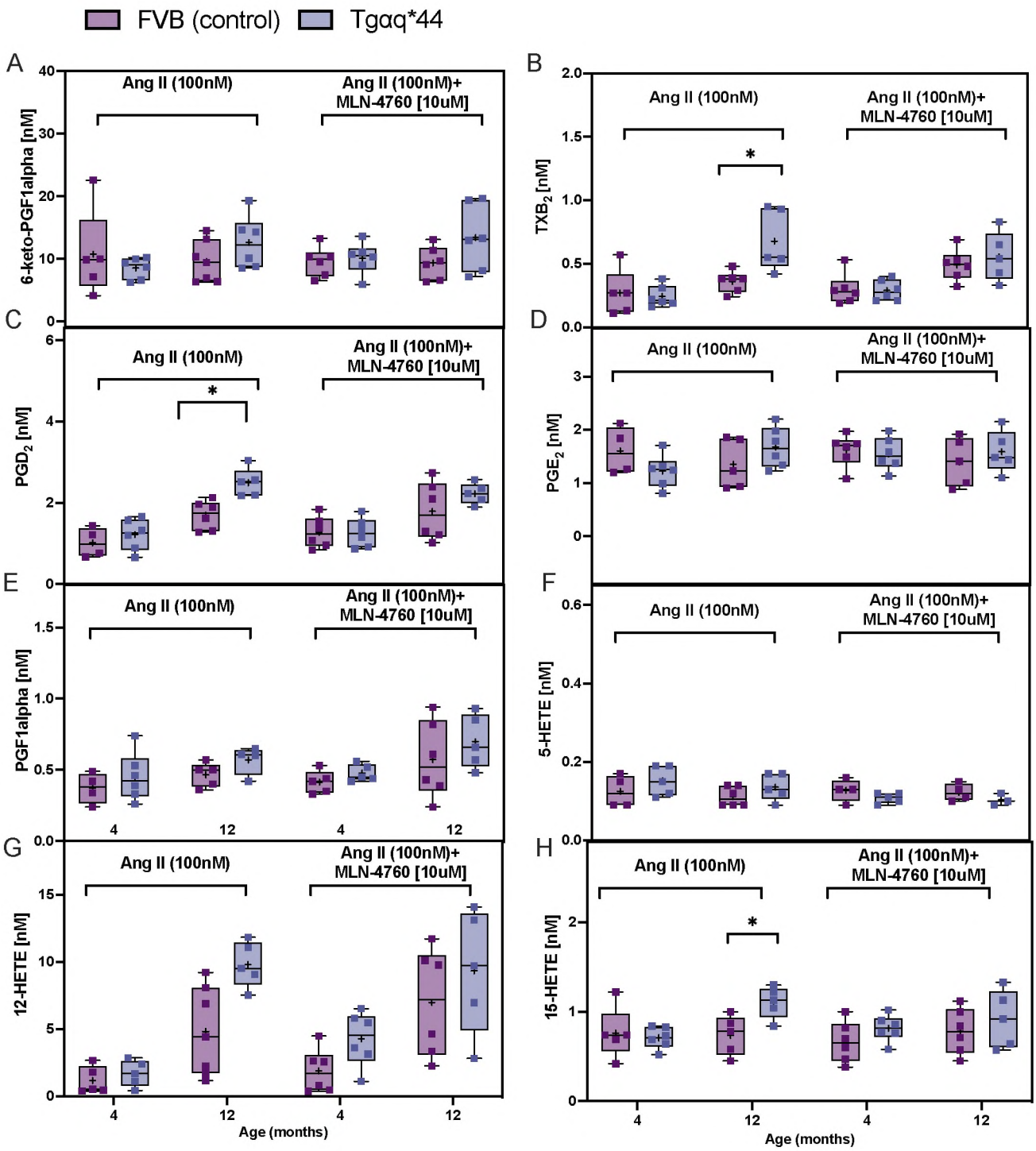

*Figure 29. Changes in eicosanoids production in the aorta rings isolated from Tgαq*44 mice and age-matched FVB mice after incubation with exogenous Ang II with and without an ACE-2 inhibitor (MLN-4760; 30 µM) for 18-24 h in 4- and 12-month-old Tgαq*44 mice compared to age-matched FVB mice. Eicosanoids production in the buffer after ex vivo stimulation of the aorta by Ang 1 (100 nM; 45 min), including 6-keto-PGF1alfa (A) TXB2 (B), PGD2 (D), PGE2 (F), PGF1alpha (E), PGF2α (F) 5-HETE (F), 12-HETE (G) and 15-HETE (H), assessed in 4- and 12-month-old Tgαq*44 mice compared to age-matched FVB mice are presented. The results are presented as boxplots (median, Q1, Q3, with whiskers indicating minimum/maximum). Key: *, $P < 0.05$ for Tgαq*44 vs age matched FVB mice in a two-way ANOVA with post hoc Sidak test, n = 5–8.*

6.13.3. Changes in eicosanoids profile induced by exogenous Ang-(1-12) in the aorta

As regards other eicosanoids, only **Ang-(1-12)** induced a consistent increase in 6-keto $PGF_{1\alpha}$, (*Figure 30A*) PGD_2 (*Figure 30C*), PGE_2 (*Figure 30D*) and $PGF_{1\alpha}$, (*Figure 30E*) generation by aorta, and this effect was only visible in 4-month-old Tgαq*44 mice, but not in 12-month-old Tgαq*44 mice as compared to age-matched FVB mice. Effects of Ang I, Ang II and Ang-(1-12) on PGD_2, $PGF_{2\alpha}$ and PGE_2 production by aorta were not consistent in Tgαq*44 mice (*Figure30*). The concentration of 5-, 12- and 15-HETEs in aortic effluent was similar in 12-month-old Tgαq*44 mice as compared to age matched FVB mice.

In the presence of **chymase inhibitor (chymostatin**) Ang-(1-12) induced changes in eicosanoids profile weren't modified significant in 4-and 12-month-old Tgαq*44 mice as well as age matched FVB mice (*Figure 30).*

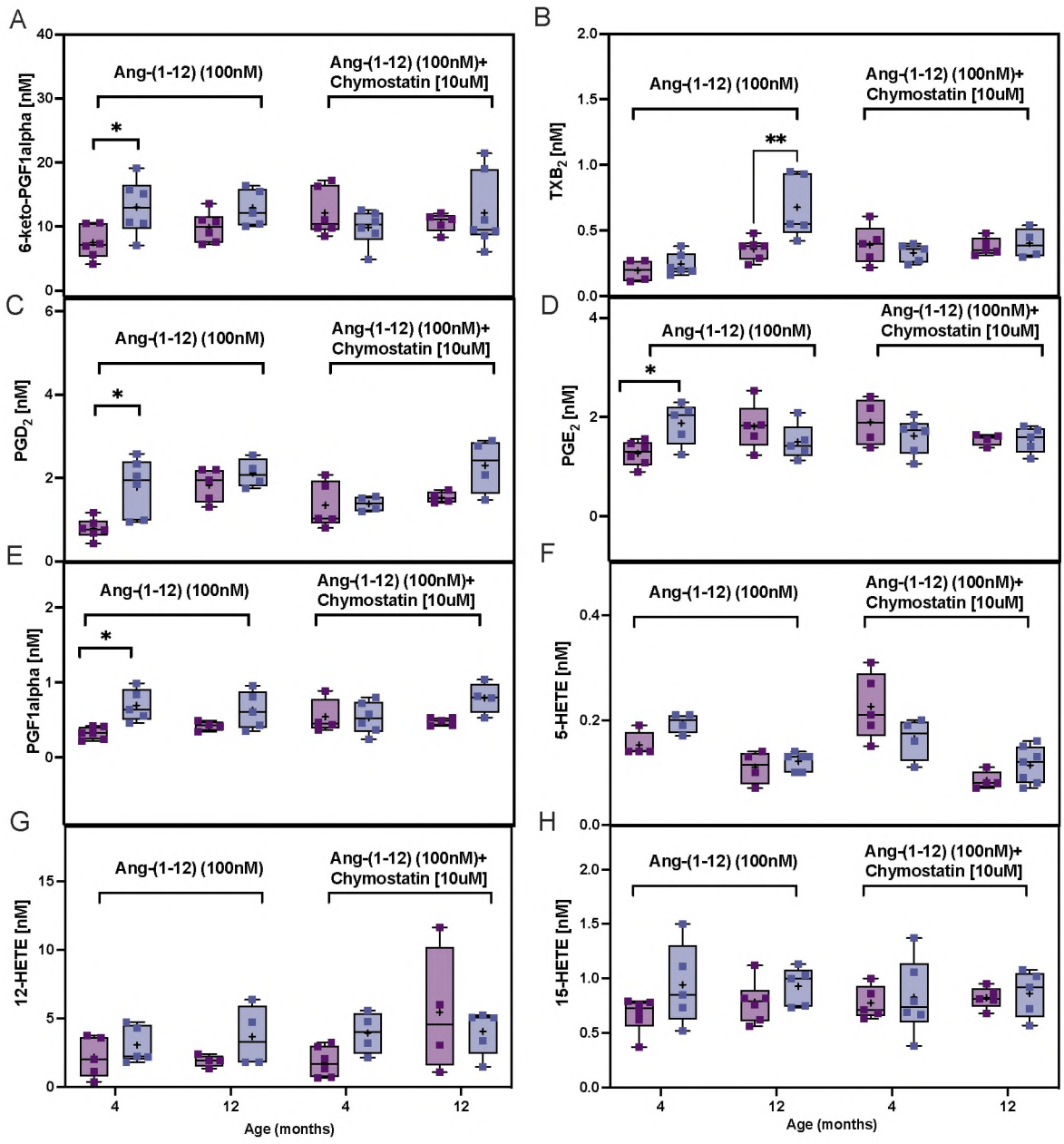

*Figure 30. Changes in eicosanoids production in the aorta rings isolated from Tgαq*44 mice and age-matched FVB mice after incubation with exogenous Ang-(1–12) (100 nM) with and without chymase inhibitor (chymostatin; 10 μM) for 18–24 h in 4- and 12-month-old Tgαq*44 mice compared to age-matched FVB mice. Eicosanoids production in the buffer after ex vivo stimulation of the aorta by Ang I (100 nM; 45 min), including 6-keto-PGF_{1alfa} (A) TXB_2 (B), PGD_2 (D), PGE_2 (F), PGF_{1alpha} (E), PGF2α (F) 5-HETE (F), 12-HETE (G) and 15-HETE (H), assessed in 4- and 12-month-old Tgαq*44 mice compared to age-matched FVB mice are presented. The results are presented as boxplots (median, Q1, Q3, with whiskers indicating minimum/maximum). Key: *, $P < 0.05$ for Tgαq*44 vs age matched FVB mice in a two-way ANOVA with post hoc Sidak test, n = 5-8.*

6.14. Effects of TP and AT1 antagonists on peripheral vascular endothelial dysfunction induced by Ang-(1–12) or Ang II in aorta from 4-month-old FVB mice

To assess the possible role of Ang II and TXA_2 as a mechanism behind the induction of aortic endothelial dysfunction, the ***TP and AT_1 antagonists were added to the 24 hours incubation of aortic rings.*** Results showed no difference in endothelial dependent- and independent- vasodilation in response to Ang II and Ang-(1-12) with or without ***TP and AT_1 antagonists*** in 4-month-old FVB mice *(Figure 31).* Of note, endothelium-dependent vasodilatation induced by SNP was fully preserved in aorta isolated from 4-month-old Tgαq*44 mice *(Figure 31 B and D).*

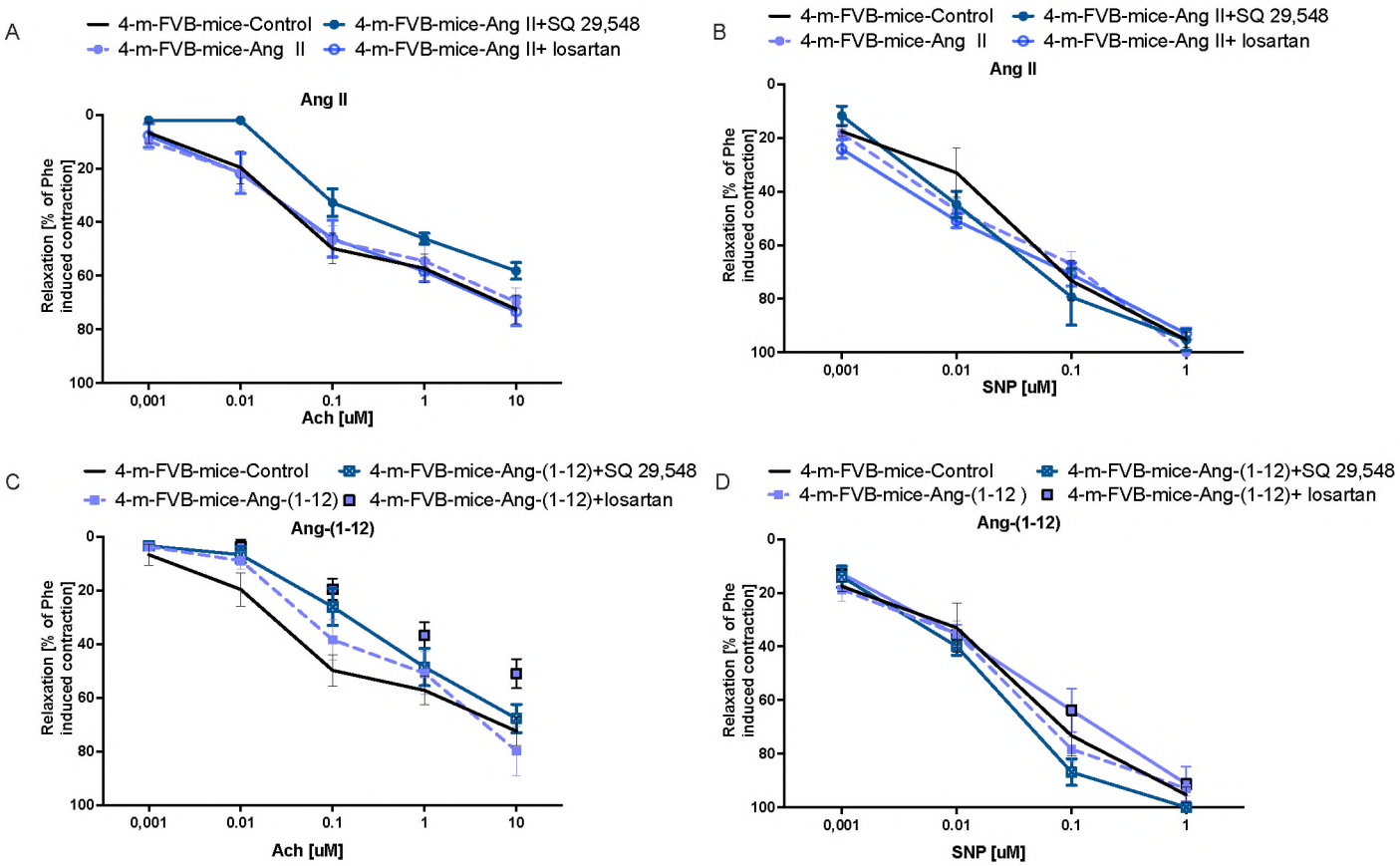

Figure 31. Peripheral vascular endothelial dysfunction in aorta from 4-month-old FVB mice incubated with Ang II (A, B), Ang-(1–12) (C, D), in the presence or absence of TP and AT_1 antagonist are presented. The relaxation of the aorta rings in response to increasing concentration Ach (A, C) and SNP (B, D) was assessed in aorta isolated from 4-month-old FVB mice after incubation for 18–24h ex vivo *with Ang II (100nM), Ang-(1–12); (100nM), Ang II+SQ 29548 (300 µM), Ang II+losartan (10 nM), Ang-(1–12)+SQ 29548 (300 µM), or Ang-(1–12)+losartan (10 nM). The results are presented as mean ± SEM. Key: */# $P<0.05$; **/##, $P<0.01$; ***, $P<0.001$ two-way ANOVA, n = 5–8. Ach, acetylocholine; SNP, sodium nitroprusside; m-months.*

*6.15. Effects of TP and AT1 antagonists on peripheral vascular endothelial dysfunction induced by Ang-(1–12) or Ang II in aorta from 4-month-old Tgαq*44 mice.*

Ang-(1–12) **(100 nM) induced** inhibion of endothelium-dependent vasodilation by ACh in the aortic rings **after 24-hrs incubation which was not prevented by a TP antagonist (**SQ 29548; 300 μM) in 4-month-old Tgαq*44 mice. However, the reduction in endothelium-dependent vasodilation after **24-hrs incubation with** Ang-(1–12) was prevented by losartan in aortic rings isolated from 4-month-old-Tgαq*44 mice (Figure 32 A and C). Again, endothelium-dependent vasodilatation induced by SNP was fully preserved in aorta isolated from 4-month-old Tgαq*44 mice (Figure 32 B and D).

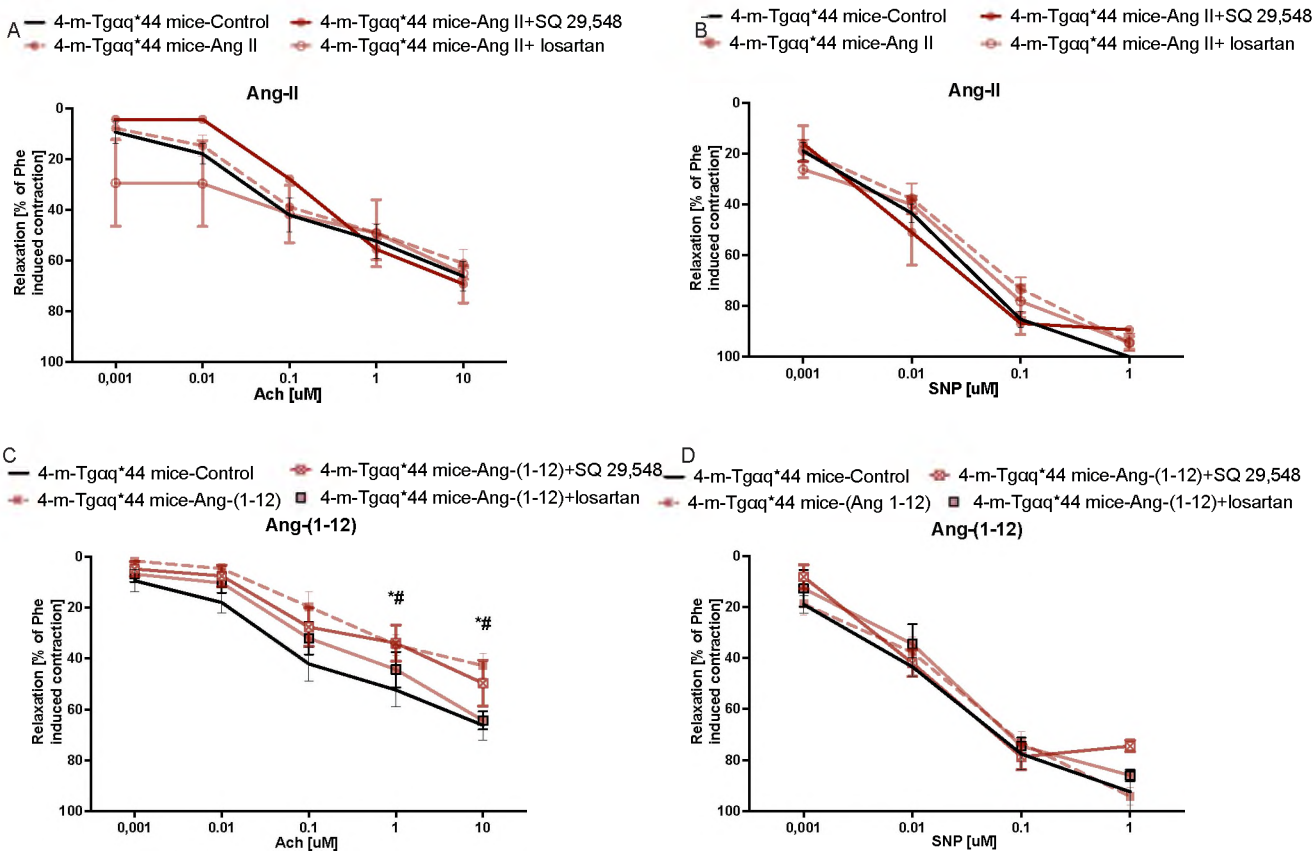

*Figure 32. Peripheral vascular endothelial dysfunction in aorta from 4-month-old Tgαq*44 mice incubated with Ang II (A-B), Ang-(1–12) (C-D), in the presence or absence of TP and AT_1 antagonist are presented. The relaxation of the aorta rings in response to increasing concentration Ach (A, C) and SNP (B, D) was assessed in aorta isolated from 4-month-old Tgαq*44 mice after incubation for 18–24h* ex vivo *with Ang II (100nM), Ang-(1–12; (100nM), Ang II+SQ 29548 (300 μM), Ang II+losartan (10 nM), Ang-(1–12) +SQ 29548 (300 μM), or Ang-(1–12)+losartan (10 nM). The results are presented as mean ± SEM. Key: */# P < 0.05; **/##, P < 0.01; ***, P < 0.001 two-way ANOVA, n = 5–8. Ach, acetylocholine; SNP, sodium nitroprusside; m-months.*

6.16. Effects of TP and AT1 antagonists on peripheral vascular endothelial dysfunction induced by Ang-(1–12) or Ang II in aorta from 12-month-old FVB mice

Endothelium-dependent vasodilation responses to Ang II and Ang-(1-12) were not modified by ***TP and AT_1 antagonists*** in 12-month-old FVB mice *(Figure 33)*. Endothelium-independent vasodilatation induced by SNP was fully preserved in aorta isolated from 12-month-old FVB mice *(Figure 33 B and D)*.

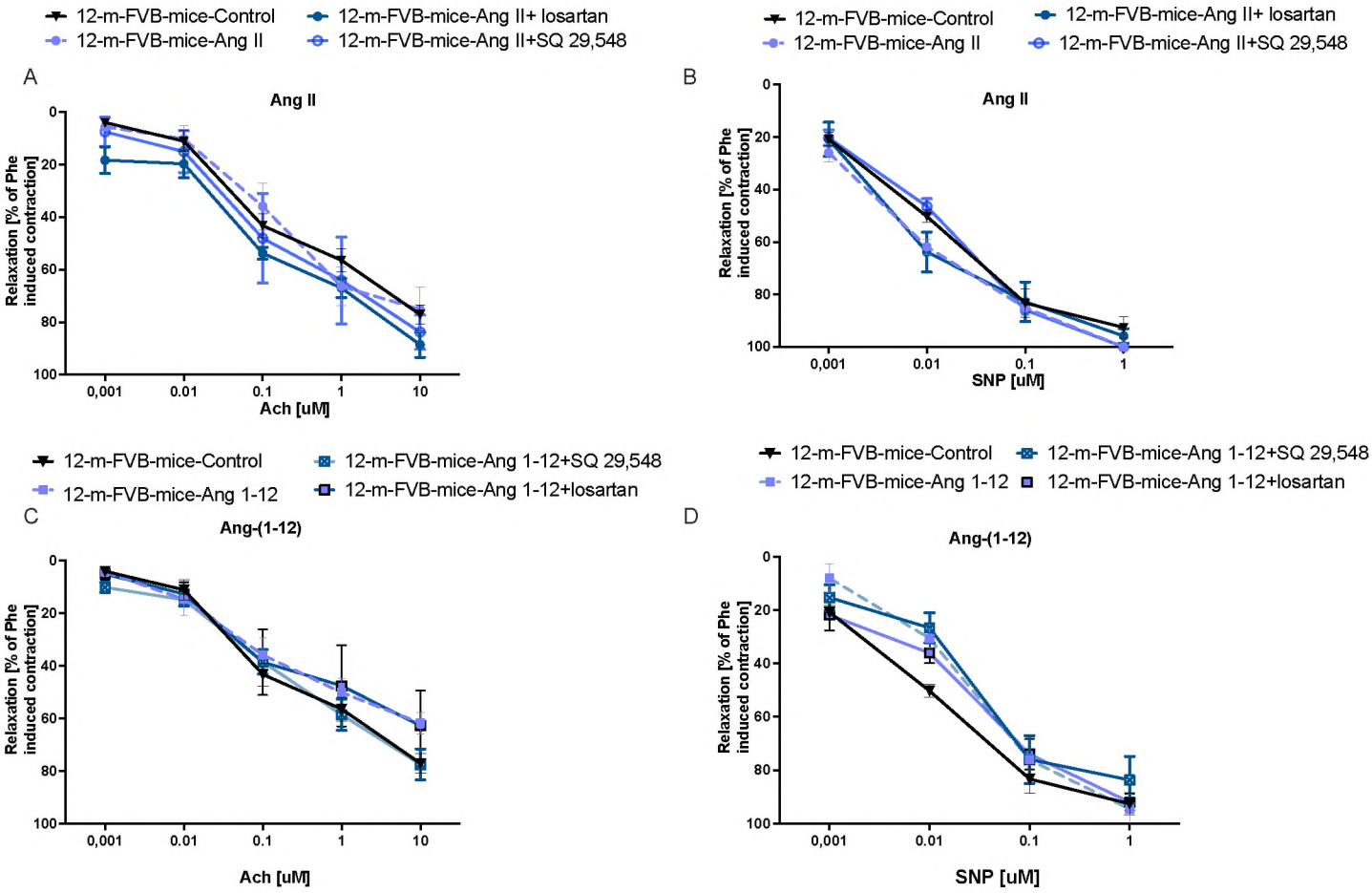

Figure 33. Peripheral vascular endothelial dysfunction in aorta from 12-month-old FVB mice incubated with Ang II (A-B), Ang-(1–12) (C-D), in the presence or absence of TP and AT_1 antagonist are presented. The relaxation of the aorta rings in response to increasing concentration Ach (A, C) and SNP (B, D) was assessed in aorta isolated from 12-month-old FVB mice after incubation for 18–24h ex vivo *with Ang II (100nM), Ang-(1–12; (100nM), Ang II+SQ 29548 (300 µM), Ang II+losartan (10 nM), Ang-(1–12)+SQ 29548 (300 µM), or Ang-(1–12)+losartan (10 nM). The results are presented as mean ± SEM. Key: */# P < 0.05; **/##, P < 0.01; ***, P < 0.001 two-way ANOVA, n = 5–8. Ach, acetylocholine; SNP, sodium nitroprusside; m-months.*

*6.17. Effects of TP and AT1 antagonists on peripheral vascular endothelial dysfunction induced by Ang-(1–12) or Ang II in aorta from 12-month-old Tgαq*44 mice*

The reduction in endothelium-dependent vasodilation after **24-hours incubation with** Ang-(1–12) was prevented by losartan and SQ 29548 in isolated aortic rings from 12-month-old-Tgαq*44. Similarly, the reduction in endothelium-dependent vasodilation after **24-h incubation with** Ang II (100nM) was prevented by losartan (10 µM) and SQ 29548 (300 µM) in the isolated aorta from 12-month-old-Tgαq*44 mice *(Figure 34)*. Endothelium-independent vasodilatation induced by SNP was fully preserved in aorta isolated from 4-month-old Tgαq*44 mice *(Figure 34B and D)*.

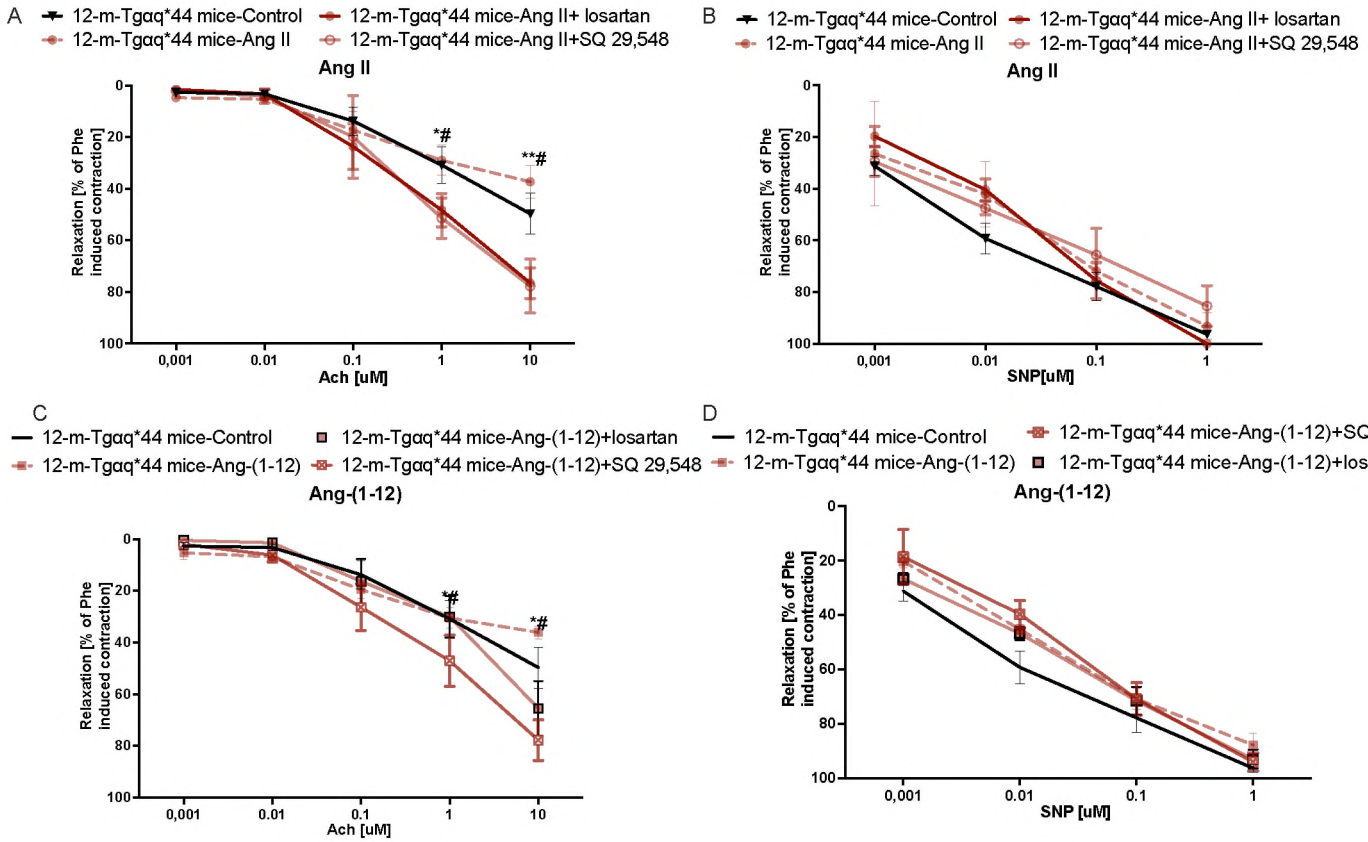

*Figure 34. Peripheral vascular endothelial dysfunction in aorta from 12-month-old Tgαq*44 mice incubated with Ang II (A-B), Ang-(1–12) (C-D), in the presence or absence of TP and AT_1 antagonist are presented. The relaxation of the aorta rings in response to increasing concentration Ach (A, C) and SNP (B, D) was assessed in aorta isolated from 12-month-old Tgαq*44 mice after incubation for 18–24h* ex vivo *with Ang II (100nM), Ang-(1–12; (100nM), Ang II+SQ 29548 (300 µM), Ang II+losartan (10 nM), Ang-(1–12)+SQ 29548 (300 µM), or Ang-(1–12)+losartan (10 nM). The results are presented as mean ± SEM. Key: */# P < 0.05; **/##, P < 0.01; ***, P < 0.001 two-way ANOVA, n = 5–8. Ach, acetylocholine; SNP, sodium nitroprusside; m-months.*

7. DISCUSSION

A number of recent studies have implicated that alterations in RBCs function contribute to endothelial dysfunction in various diseases, such as diabetes, preeclampsia, hypercholesteremia, or even COVID-19 (Collado *et al.*, 2021; Mahdi, Collado, *et al.*, 2021a) but it was not known whether RBCs alteration play a role in the pathophysiology of endothelial dysfunction in HF. Similarly, multiple rapports demonstrated the involvement of Ang-(1-12)-chymase dependent conversion to Ang II in cardiac remodeling (Ahmad *et al.*, 2011, 2013; Ahmad and Ferrario, 2018), but it was not known whether Ang-(1-12)-dependent pathway play a role in the development of endothelial dysfunction in HF (Ahmad *et al.*, 2021).

In this Ph.D. thesis, the effect of erythopathy and of Ang-(1–12)-dependent pathway on endothelial function was investigated using a unique model of HF (Tgαq*44).

The major finding in the present Ph.D. thesis where the following;

1) Peripheral endothelial dysfunction occurred in the transition-phase of HF and was featured by impaired endothelial-dependent vasodilation induced by Ach in the aorta but not by impaired flow-mediated vasodilation in the mesenteric or femoral artery and at the end-stage of HF was associated by a fall in systemic NO bioavailability, HbNO content in RBCs and in the aorta with impaired nitric oxide (NO) production, increased superoxide anion (O^{2-}) and increased eicosanoid production
2) RBCs isolated from 12-month-old Tgαq*44 mice induced endothelial dysfunction in aorta taken from 12-month-old FVB mice which was attenuated by arginase I and II inhibitor but not by ROS scavenging.
3) In response to Ang-(1-12), TXA_2 production were upregulated in aortic rings isolated from 12-month-old-Tgαq*44-mice, but not from 4-month-old-Tgαq*44 mice or age-matched FVB mice.

4) Impaired endothelium-dependent vasodilation caused by Ang-(1–12) in the aorta isolated from 12-month-old-Tgαq*44-mice were reversed by TXA_2 receptor (SQ 29548) or Ang receptor type I (losartan) antagonists.

Collectively results of present Ph.D. thesis indicated novel mechanisms by which RBCs and intravascular Ang-(1–12)/Ang II/ pathway could contribute to the development of endothelial dysfunction in HF.

*7.1. Progression of endothelial dysfunction in the murine model of HF (Tgαq*44 mice)*

Endothelial dysfunction in the peripheral circulation has a predictive value, regardless of whether the HF is of ischemic or non-ischemic origin (Fischer *et al.*, 2005). Despite the abundance of literature on mechanisms of peripheral endothelial dysfunction in HF of ischemic origin (Alem, 2019) little is known about the mechanism of endothelial dysfunction in non-ischemic HF.

In this Ph.D. thesis the development of peripheral endothelial dysfunction along the progression of HF in Tgαq*44 mice in comparison with age-matched FVB mice were characterized. The model of Tgαq*44 mice was previously characterized extensively by prof. Chłopicki group (Drelicharz *et al.*, 2008, 2009; Berkowicz *et al.*, 2018; Tyrankiewicz *et al.*, 2018b), but peripheral endothelial dysfunction was not studied as yet. *Figure 36* summarizes the major findings related to the pathophysiology of HF in Tgαq*44 mice revealed in previous reports as well as novel results reported in this Ph.D. thesis, which are discussed further below.

Tgαq*44 mice model was developed due to cardiomyocyte-specific overactivation of Gαq protein that imitates cardiac response to neurohormonal activation by RAAS, sympathetic and endothelin-1-dependent system. Tgαq*44 mice model display three stages of HF, the early stage in 4–6-month-old mice, the transition stage appeared in 8-10-month-old mice and the end stage occurred in 12–14-month-old mice (Tyrankiewicz *et al.*, 2018a). The early phase of HF

at the age of 4-month-old Tgαq*44 mice is characterized by diastolic dysfunction with preserved global cardiac performance, fibrosis, cardiomyocyte hypertrophy and activation of hypertrophic genes (ANP, BNP, MHC-β) (U. Mende *et al.*, 2001; Drelicharz *et al.*, 2008; Olkowicz, Chlopicki and Smolenski, 2017). In the transition phase of HF, a progressive impairment of the basal systolic and diastolic cardiac performance with a preserved global cardiac response appears in 10-months-old Tgαq*44 mice. At the end-stage of HF in 12-14 months-old Tgαq*44 mice change concerned ventricular enlargement with pulmonary edema, impaired cardiac performance, loss of the cardiac reserve in response to dobutamine, and disruptions in ACE/ACE-2 balance (Tyrankiewicz et al. 2021).

Experimental approach adopted in the present PhD thesis to characterize endothelial dysfunction in Tgαq*44 mice was based on the functional, biochemical and molecular methods to have a more comprehensive insight in the progression of endothelial function that one might have used one method only. On a functional level, MRI, as well as wire and culture myographs, were used. The biochemical level production of NO/O^{2-} and eicosanoidas was assessed using EPR and HPLC, respectively. On the molecular level, RT-PCR and Western Blot were used to determine gene and protein expression, respectively.

Results presented equivocally demonstrated that endothelial dysfunction developed in murine model of HF in 8-month-old Tgαq*44 mice as detected by *in vivo* MRI which appeared more sensitive to detect the early phase of endothelial dysfunction than *ex vivo* approach. E*x vivo* measurement confirm endothelial dysfunction in 10-month-old Tgαq*44 mice which at the end-stage HF was associated with impaired NO production, increased O^{2-} and eicosanoids production in the aorta.

Those findings are in line with previous studies (Zuchi *et al.*, 2020), which showed that endothelial dysfunction in response to Ach was not observed in early HF in rats but was present in the later phases of HF development (Zuchi *et al.*, 2020) Moreover, SNP response in aorta (*ex*

vivo) was fully preserved along the progression of HF in Tgαq*44 mice. The results from patients with HF demonstrated decreased responsiveness to nitroglycerin (Katz *et al.*, 1992; Zuchi *et al.*, 2020) or no difference in the vasodilator response to SNP, suggesting that the impairment of endothelium-independent response in HF, might depend on the stage of HF or other factors. Nevertheless, in Tgαq*44 mice reduced relaxation response to Ach was not related to the reduction in the responsiveness of the vascular smooth muscle as evidence by preserved SNP responses.

Reduced Ach-induced NO-dependent vasodilation in the aorta was associated with a progressive decrease in plasma nitrate content, but nitrite concentration remained stable in 8- to 12-month-old Tgαq*44 mice compared to age-matched control groups. These results suggest that the nitrate-nitrite-NO reductive pathway could have been activated, as a compensatory source that maintained NO bioavailability. Indeed, HbNO content in RBC decrease at the end-stage of HF in 12-month-old Tgαq*44 mice confirming a systemic decreased in NO bioavailability in 12-month-old Tgαq*44, but not in younger Tgαq*44 mice.

Importantly, impaired NO production in the aorta detected at the stage of advanced HF was associated with increased O^{2-} detected by EPR confirming the presence of oxidative stress a hallmark of endothelial dysfunction in many cardiovascular diseases including HF (Sun *et al.*, 2020).

Concomitantly, in 12-month-old Tgαq*44 mice endothelial dysfunction was featured by upregulated COX-2, increased generation of cyclooxygenase-derived eicosanoids such as PGE_2, PGD_2, PGF_{1a}, and PGI_2 -that may play a compensatory role (Félétou, Huang and Vanhoutte, 2011; Ricciotti and Fitzgerald, 2011). Interestingly, according, to previously study PGF_{1a} may be beneficial to the vascular endothelium by promoting the release of nitric oxide (Korzekwa *et al.*, 2007). On the other hand, increased vascular TXB_2 could contribute to

vascular inflammation (Ricciotti and Fitzgerald, 2011) but TXB_2 was not detected when aorta was incubated without any additional stimulation *ex vivo*.

Taken together, in the murine model of HF (Tgαq*44) endothelial dysfunction was detected *in vivo* in the transition phase of HF in 8-month-old Tgαq*44 mice but clearly, some heterogeneity in endothelial response to HF progression as well as different sensitivity of various methods used to detect endothelial dysfunction was observed. Firstly, only using MRI *in vivo* was the endothelial dysfunction detected in 8-month-old Tgαq*44 mice. Whereas, using an *ex vivo* myography experimental setup endothelial dysfunction was observed in 10-month-old Tgαq*44 mice. Additionally, impaired NO production in the aorta and other alterations in biochemical phenotype in the aorta as well as a fall in systemic NO bioavailability was detected in 12-month-old Tgαq*44 mice. Finally, FMD *in vivo* in femoral artery, as well as *ex vivo* in mesenteric artery, was preserved in Tgαq*44 mice as compared to the control group.

Previous studies reported (Barton *et al.*, 1997a, 1997b; Vercauteren *et al.*, 2006; Sallam and Laher, 2020) some conflicting results as regards the presence or absence of endothelial dysfunction in various vascular beds in various models. For example, along aging, in aorta, relaxations to acetylcholine, basal NO release, and expression of eNOS mRNA were reduced, whereas in femoral arteries, relaxation to acetylcholine was fully preserved, and only basal release of NO was attenuated (Barton *et al.*, 1997a). In turn, in db/db mice vasodilatory response to ACh was impaired in the femoral arteries in contrast to the aorta (Sallam and Laher, 2020). Of note, vasodilatory mechanisms of FMD response may differ than those implicated in Ach-induced responses. In addition to the two main compounds (NO, prostacyclin), vascular relaxation can be mediated by EDHF. Finally, in the model of HF induced by myocardial infarction (Maupoint et al. 2016; Vercauteren et al. 2006). FMD in the femoral artery was impaired, while the response to Ach was only moderately affected suggesting that the difference

in response might also relate to the stimulus used. On the other hand, other publications reported an impairment of FMD in the mesenteric artery in animals with HF.

These results may underscore the heterogenous response of the endothelium to HF progression in the macro and the microvasculature, in ischemic and non-ischemic HF or indicate different responsiveness of the flow-mediated vasodilation as compared with agonist-induced vasodilation related to difference mechanisms involved in the respective vasodilation (Maupoint *et al.*, 2016; Alem, 2019; Giannitsi *et al.*, 2019; Zuchi *et al.*, 2020; Reina-Couto *et al.*, 2021)

	Tgαq*44		Myocardial infarction in mouse	
	Ach	Flow	Ach	Flow
Aorta	Impaired ↓NO	Data not shown	Impaired ↓NO	Data not shown
Mesenteric artery	Data not show	Preserved ↑*EDHF*	Preserved ↑EDNF	Impaired ↓NO
Femoral artery	Data not shown	Preserved ↑*EDHF*	Data not shown	Data not shown

Figure 35. Comparison of endothelial function in different vessels in Tgαq*44 mice with HF versus mice with myocardial infarction. Based on (Widder* et al., *2004; Maupoint* et al., *2016)

Despite these discrepancies, our results allow us to conclude that MRI *in vivo* was more sensitive to detect endothelial dysfunction than any other approach used (detected endothelial dysfunction in 8-month-old Tgαq*44), while *ex vivo* measurements in isolated vessels revealed endothelial dysfunction later (in 10-month-old Tgαq*44). Finally, biochemical measurements in the aorta (NO/ROS, eicosanoids) and systematically (NO bioavailability) were supportive but only when endothelial dysfunction was severe.

As regards the mechanism involved in the progression of endothelial dysfunction in HF in Tgαq*44, our results seem to exclude the direct effect of **hemodynamic factors** on peripheral endothelial dysfunction. Cardiac function was impaired quite early in Tgαq*44 mice

and even 4-month-old Tgαq*44 mice displayed impaired systolic and diastolic cardiac function (Tyrankiewicz *et al.*, 2013, 2021). While endothelial dysfunction was present in 8-month-old Tgαq*44 mice when studied *in vivo* and it was detected even later when studied *ex vivo* (10-month-old Tgαq*44 mice). Therefore, our data does not seem to support a direct triggering role of hemodynamic factors on the mechanism of peripheral endothelial dysfunction in the aorta in Tgαq*44 mice. Of course, we could not exclude that hemodynamic factors could contribute to endothelial dysfunction in the late stage of HF in 14-month-old Tgαq*44 mice (Ricciotti and Fitzgerald, 2011; Alem, 2019)

Similarly, **systemic or local inflammation** often altered in HF (Alem, 2019; Sun *et al.*, 2020), which may contribute to endothelial dysfunction in HF did not seem to be of importance in the pathophysiology of endothelial dysfunction in Tgaq*44 mice. In fact, TNF-α and IL-6 expression in aorta determined by RT-qPCR did not change along the progression of HF, excluding the role of vascular TNF-α or IL-6 –dependent vascular inflammation as a major mechanism in the pathogenesis of peripheral endothelial dysfunction in Tgαq*44 mice, in contrast, for example, to hypertensive vascular remodeling (Reina-Couto et al. 2021). Furthermore, the concentration of various cytokines in plasma in Tgαq*44 mice at the age of 12-months was comparable to age-matched FVB mice. There were no differences in the plasma level of Tumor Necrosis Factor-alpha (TNF-a), Interleukin-1β (IL-1β), IL-2, IL-3, IL-4, IL-5, IL-6, IL-9, Interferon-gamma (IFNγ) in 12-month-old Tgαq*44 mice when compared to age-matched FVB mice. Therefore, our findings contradict previous ones which show that inflammation could contribute to endothelial dysfunction in the peripheral vessels in HF (Alem, 2019; Sun *et al.*, 2020). Moreover, in rats with HF, an anti-inflammatory drug improved endothelial function in peripheral vessels (Daiber *et al.*, 2017; Sun *et al.*, 2020) further supporting a role of inflammation in endothelial dysfunction in some models. Clearly, these

discrepancies might be explained by various etiology of HF in our work and in the work of others (Alem, 2019; Giannitsi *et al.*, 2019; Zuchi *et al.*, 2020).

Taken together, our results seemed to exclude the role of systemic and local inflammation, and hemodynamic factors in the pathophysiology of endothelial dysfunction in HF in Tgαq*44 mice. That is why in this PhD thesis others possible mechanisms were investigated. In particular a possible role of intravascular Ang-(1-12)/Ang II pathway or alterations in erythrocytes in the development of endothelial dysfunction in murine model of HF (Tgαq*44) was analyzed.

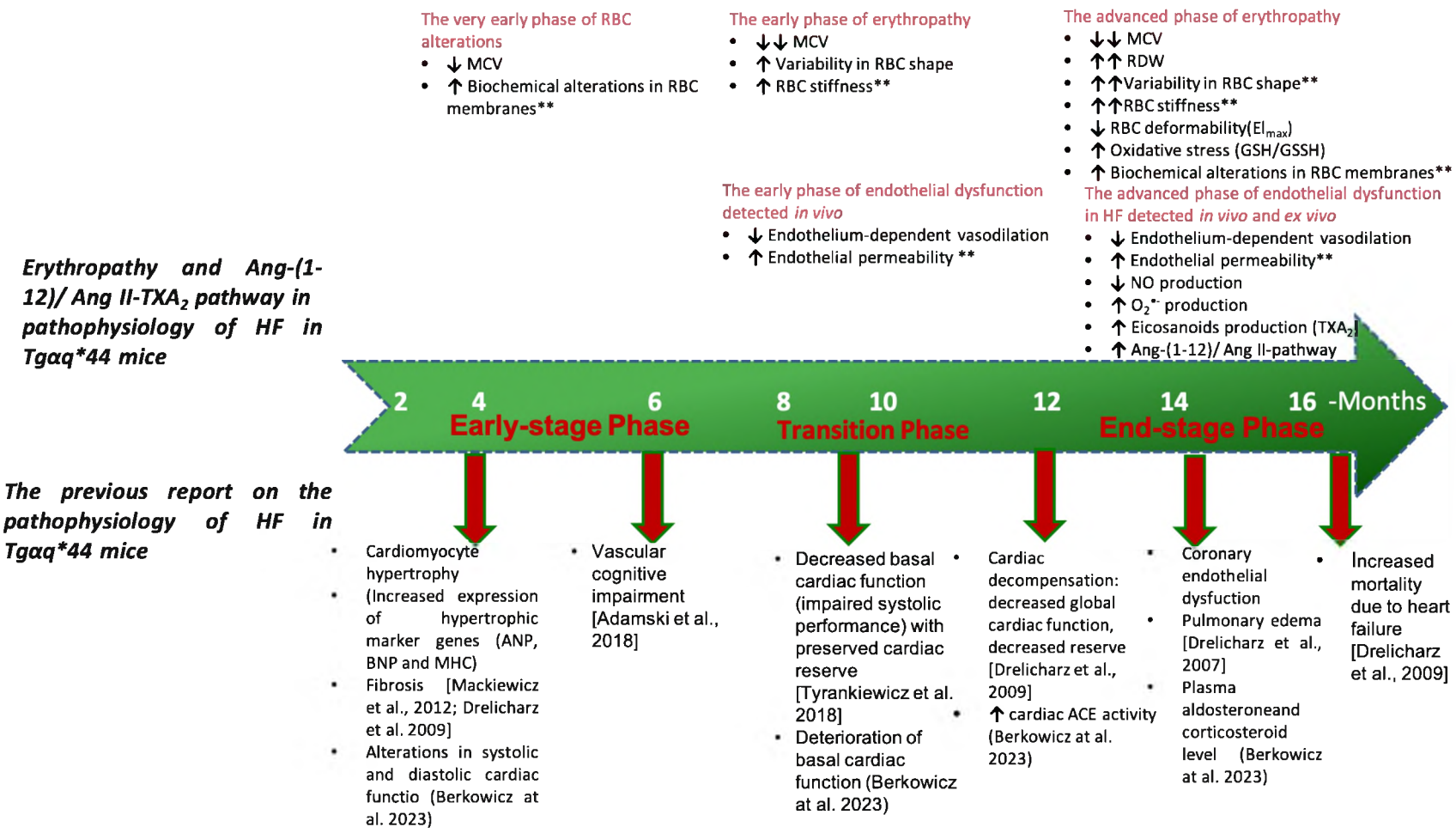

*Figure 36. Previous published report on pathophysiology of HF in Tgαq*44 mice model. ** Results previously published in (Mohaissen et al., 2022).*

*7.2. Ang 1-12/Ang II/TXA2 pathway the murine model of HF (Tgαq*44 mice)*

Previous research (Varagic *et al.*, 2013; Ferrario *et al.*, 2019) found evidence of a possible role of the Ang 1-12 tissue system in cardiovascular diseases, but their reports were mostly focused on cardiac remodeling (Ahmad *et al.*, 2010, 2011; Ahmad and Ferrario, 2018), but not on peripheral endothelial dysfunction. Interestingly, previously it was reported in the work by Tyrankiewicz et al., that in Tgαq*44 mice, Ang-(1-12) was increased in plasma and in the aorta in the transition phase of HF and was associated with Ang II pathway upregulation in plasma and in aorta (Tyrankiewicz *et al.*, 2019) suggesting a possible role of Ang-(1-12)/Ang II pathway not only in the systemic neurohormonal activation but also in vascular response to HF progression.

Therefore, one of the aims of this Ph.D. thesis was to test whether elevated levels of Ang-(1-12) in plasma could indeed be involved in the development of peripheral endothelial dysfunction in HF in Tgαq*44. The approach adopted in this work was based on the addition of exogenous Ang-(1-12), Ang I, Ang II, and incubation with isolated aorta to provide a better experimental setup to assess possible intravascular conversion of Ang-(1-12). Using these approaches, it was firstly confirmed that the phenotype of endothelial dysfunction in Tgαq*44 mice was maintained over 24-h incubation but deteriorated in response to the addition of exogenous Ang-(1-12). Ang I and Ang II were given for comparison. The consistent effect of Ang-(1-12) in young and old Tgαq*44 mice suggests a possible pathophysiological role of intravascular conversion of Ang-(1-12). Ang I and II deteriorated endothelial function only in 12-month-old Tgαq*44 mice, but not in 4-month-old Tgαq*44 mice. It was previously shown that Ang-(1-12) is a renin-independent precursor for Ang II which is (Mehta and Griendling, 2007) a key driver for the development of endothelial dysfunction. Ang-(1-12) induced effects could have been linked to altered expression of RAS components (Ahmad and Ferrario, 2018). Previous study demonstrated, that arterial aging was linked to a reduced ACE-2-MasR axis and

an enhanced PRR-ACE-Ang II-AT_1R axis in mice (Yoon *et al.*, 2016). However, here the expression of angiotensinogen, chymase, ACE-2, and AT_1 receptor did not change, indicating that changes in the vascular Ang-(1-12)/Ang II pathway in Tgαq*44 animals were linked to functional changes most likely of intravascular Ang-(1-12) conversion and signaling.

Interestingly, in contrast to aortic rings incubated for 1 hour without stimulation (see *Chapter 7.1*), 24-hour incubation with Ang I, Ang II and Ang-(1-12) resulted in the increased production TXA_2 in 12-month-old Tgαq*44 mice but not in 4-month-old Tgαq*44 mice when compared to age-matched FVB mice. These results indicated a possible role of TXA_2 in endothelial dysfunction in Tgαq*44 mice. Interactions between TXA_2 and the renin-angiotensin system have been previously suggested (Francois *et al.*, 2004). For example, Ang II stimulates TxA_2 synthesis in vascular tissue (Francois *et al.*, 2004) Other studies suggested that TXA_2 and ET_1 are important mediators affecting the renal vascular resistance produced by Ang II (Cediel et al. 2002; Francois et al. 2004). Furthermore, there is evidence for common actions of Ang II and TXA_2 to promote systemic and renal vasocontraction, vascular smooth muscle proliferation and sodium hemostasis. Finally, Ang II infusion stimulated the production of different eicosonoids, including TXA_2 and PGH_2, in vascular and renal tissue (Francois *et al.*, 2004).

The important finding of this PhD was to show that endothelial dysfunction in aorta induced by Ang II or Ang-(1-12) was reversed in the presence of TP antagonist (SQ-29548) or AT1 antagonist (losartan) in 12-month-old Tgαq*44 mice. Those results indicating the involvement of vascular TXA_2 overproduction in Ang-(1-12)/Ang II pathway at the late stage Interestingly, neither chymostatin nor peridoprylat did not inhibit completely TXA_2 production induced by exogenous Ang I and Ang-(1-12), suggesting ACE- and chymase-independent pathway of TXA_2 production in response to Ang I and Ang-(1-12). However, the lack of effect of this inhibitor maybe also due to the low experimental group n=5-6.

Thromboxane (TP) antagonists can prevent aging-related vasoconstriction mediated by prostanoids as well as cardiovascular risk factors linked to elevated oxidative stress, which upregulates COX-1 and/or induces COX-2 (Félétou *et al.*, 2010; Smyth, 2010). This could suggest a potential contribution of TP to the pathogenesis of cardiovascular system.

Of note, the pharmacological effects assessed using TP receptor could be related not only to TXA_2 synthesis but also related to changes in PGH_2, PGE_2 and PGI_2 synthesis (Francois et al., 2004).On the other hand, we could not exclude the role of PGH_2, that is considered as a TP receptor agonist (Davì, Santilli and Vazzana, 2012), and PGH_2 generation was also linked to oxidant stress present in peripheral vasculature in Tgαq*44 mice (Mohaissen et al., 2022).

Altogether, intravascular chymase-independent Ang-(1-12)/AngII/TXA_2 pathway could be involved in the development of peripheral endothelial dysfunction in HF in Tgαq*44 mice but further research are needed to fully understand the process of intravascular conversion of Ang-(1-12) to Ang II and to confirm the mechanisms involved in *in vivo* experiments.

*7.3. Erytropathy in the murine model of HF (Tgαq*44 mice)*

RBCs play a major role in the oxygen transporter and contribute in balancing oxygen supply with metabolic requirements (Pernow *et al.*, 2019; Mahdi, Kövamees and Pernow, 2020; Mahdi *et al.*, 2021). RBCs are also involved in other processes like antigen recognition, phagocytosis, defences against infection immune adhesion, redox balance as well as physiological regulation of blood flow in microcirculation and thus cardiovascular function (Yang *et al.*, 2018). Interestingly, several recently published studies have shown that alterations in RBCs function could contribute to the development of cardiovascular injury or endothelial dysfunction in diabetes types II (Pernow *et al.*, 2019; Mahdi, Kövamees and Pernow, 2020; Mahdi *et al.*, 2021), pre-eclampsia and dyslipidemia, but whether alterations in RBCs could be involved in endothelial dysfunction in heart failure has not been investigated.

Therefore, one of the major aims of Ph.D. thesis was to characterize the alterations in RBCs and the relationship of these alterations with the development of endothelial dysfunction along the progression of HF in Tgαq*44 mice to understand if erythropathy may contribute to endothelial dysfunction in this model. The methodological approach adopted in this Ph.D. was taken from the methodology of Pernow et al. (Pernow and Jung, 2013; Yang *et al.*, 2018; Pernow *et al.*, 2019; Mahdi, Collado, *et al.*, 2021b). Based on that methodology, authors showed that RBC taken from diabetic animals incubated with aorta perfused via coronary circulation of healthy mice induced endothelial dysfunction (Pernow and Jung, 2013; Ahmad and Ferrario, 2018; Zhou, Yang and Pernow, 2018; Pernow *et al.*, 2019). Results obtained in this Ph.D. thesis demonstrated that endothelium-dependent relaxation was impaired in aortic segments when incubated with RBCs isolated from Tgαq*44 mice, but this was not the case when RBCs were isolated from FVB mice.

To understand a possible mechanism by which RBCs could impair endothelium-dependent vasodilatation, the effect of different scavengers and arginase inhibitors on endothelial function was tested**.** RBC suspensions were incubated with an arginase inhibitor (nor-NOHA, ABH), peroxynitrite scavenger (FeTPPs), or scavengers of ROS (NAC) (Yang *et al.*, 2013, 2018).

The impairment of endothelial function induced by RBCs was **not** affected by NAC, FeTTPs, nor-NOHA. Those results are in line with the previous findings which demonstrated that peroxynitrite scavenger didn't improve the endothelial dysfunction induced by RBCs isolated from diabetes mice (Mahdi *et al.*, 2020). However, the incubation with ABH but not nor-NOHA revealed an improvement in the endothelial depended function upon exposure of RBCs. ABH is an inhibitor of arginase types I and II in contrast to nor-NOHA that inhibits arginase II much stronger (Pernow and Jung, 2013; Mahdi, Kövamees and Pernow, 2020). This might be the main reason of the difference of action between ABH and nor-NOHA effect.

Pernow et al. (Pernow and Jung, 2013; Zhou, Yang and Pernow, 2018; Pernow *et al.*, 2019; Mahdi, Kövamees and Pernow, 2020) showed that RBCs expressed only arginase I, so it can be concluded that this isoform was responsible for the functional effect of arginase in the work of Pernow group (Zhou, Yang and Pernow, 2018) as well as in our experiments. Of note, it was previously shown that Nor-NOHA and ABH are structurally different arginase inhibitors the nor-NOHA has a guanidinium chain, while ABH binds as a tetrahedral boronate anion (Yang *et al.*, 2018) that which might explain their difference in the selectivity towards arginase I and II.

Taken together, the presented results demonstrated the importance of arginase in the mechanisms of endothelial dysfunction in Tgαq*44 mice and stay in line with other studies suggesting increased arginase activity as an important regulator of NO formation and ROS production in diabetes (Yang *et al.*, 2018).

To understand nature of RBCs alterations that occurs along the progression of HF in Tgαq*44 mice biochemical and blood count parameters of RBCs were measured. Results have shown mild alteration in RBCs in early stage of HF, like reduction in MCV (suggesting early RBC anisocytosis in HF), slightly RBC shape alteration but severe changes of RBCs parameters were present in late stage of HF including RDW. In fact, increased RDW was noted in 10-month-old Tgαq*44 mice indicating a greater variation in erythrocyte size without changes in reticulocyte count.

GSH/GSSH ratio represents an index of the redox state and was altered in late not early phases of HF. Given the high intracellular concentration of GSH and active PPP synthesis in RBC, this index could represent quite a late stage of alterations in erythropaty in HF, as compared with others parameters of RBCs studied in this Ph.D. thesis.

A decrease in phospholipid content and unsaturated lipids in RBC were also altered but the data are not shown here (Mohaissen *et al.*, 2022). In turn, AFM-based measurements of RBC

elasticity (*Figure 37*), demonstrated clear-cut changes in RBC elasticity and shape measured by AFM that were observed at the age of 8 months in Tgαq*44 mice and progressed to the severe alterations in 12-month-old Tgαq*44 mice.

Overall, the presented results show that in Tgαq*44 mice, the first signs of HF-linked erythropathy occurred at a very early stage in the course of HF in this model, and HF-linked erythropathy was substantially progressing along the progression of HF.

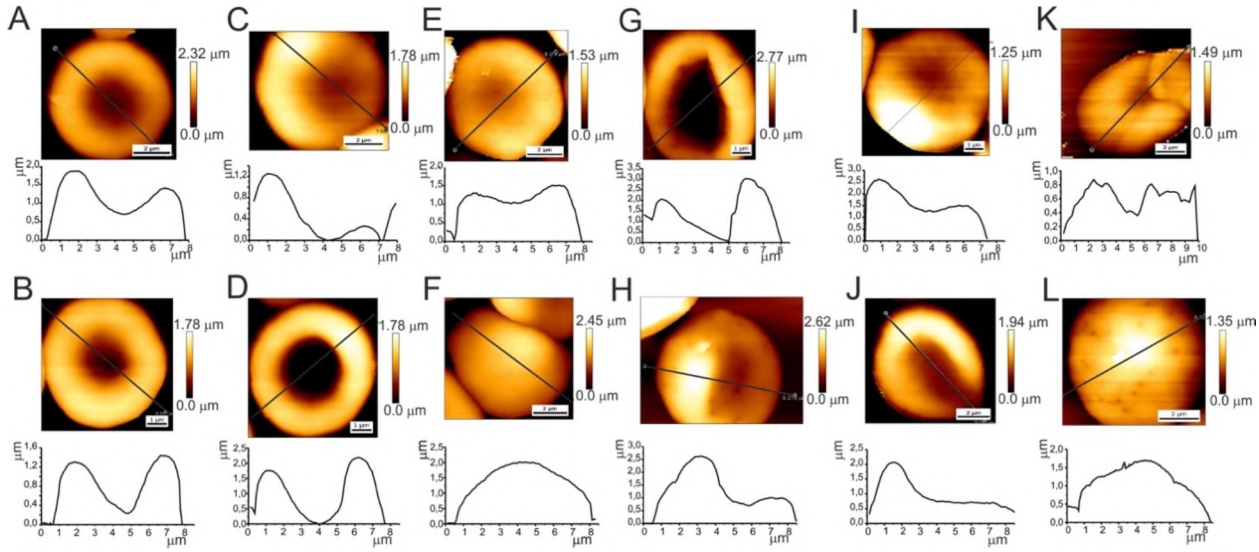

Figure 37. Variability of RBC shape during HF progression in Tgαq*44 mice versus age-matched FVB mice. Examples of RBC images taken for 4-month-old (A), 12-month-old (B) FVB mice (control sample), 4- month-old Tgαq*44 mice (C-D), 6- month-old Tgαq*44 (E-F), 8- month-old Tgαq*44 mice (G-H) 10- month-old Tgαq*44 mice (I-J), 12- month-old Tgαq*44 mice (K-L). Plots below AFM images show cross-sections along the marked lines. Figure based on (Mohaissen et al., 2022)

Enhanced generation of **reactive oxygen** and **inflammation** may influence erythrocyte homeostasis and survival. Therefore, we tested whether impaired erytropoietin or chronic systemic inflammation may contribute to erythropathy with increased RDW in Tgαq*44 mice. We measured plasma erythropoietin in Tgαq*44 mice at the age of 4-,8- and 12-month-old mice in comparison with age-matched FVB mice. Our results showed no differences in the EPO plasma concentration in 4-,8- and 12-month-old Tgαq*44 mice when compared to age-matched FVB mice. Based on those results, EPO does not seem to be the driver for RDW in HF in Tgαq*44 mice.

In the present Ph.D. thesis results showed that endothelial dysfunction and RBC alterations occurred very early in HF pathophysiology and progressed with HF progression. Moreover, it was demonstrated that Ang-(1-12) induced endothelial dysfunction in the aorta was mediated by Ang II/TXA_2 pathway in the late stage of HF in Tgαq*44 mice.

8. *Conclusions*

- Peripheral endothelial dysfunction occurred in the transition-phase of HF and was featured by impaired endothelial-dependent vasodilation induced by Ach in the aorta while FMD in the mesenteric or femoral artery was preserved, suggesting **heterogeneity** of the endothelial response to HF progression, in terms of vascular bed and stimulus.
- Endothelial dysfunction in the aorta in Tgαq*44 mice was associated with erythropathy on functional, structural, and biochemical (arginase activity) levels suggesting involvement of RBCs in systemic endothelial dysfunction.
- Endothelial dysfunction in aorta in Tgαq*44 mice could be also mediated by intravascular Ang-(1-12)/ Ang II-TXA_2 pathway in the late stage of HF and the conversion of Ang-(1-12) to Ang II seems to be chymase-independent.
- **Altogether, using a comprehensive methodology involving among others MRI based assessment of endothelial dysfunction *in vivo* and other complementary methods novel possible mechanism of peripheral endothelial dysfunction in Tgαq*44 mice was suggested. Those mechanism include erythropathy that could be involved in an early phase of HF and intravascular Ang-(1-12)/Ang II/TXA_2 pathway that could be only involved in the late stage of HF.**

9. Bibliography

- Ahmad, S. *et al.* (2010) 'Chymase-dependent generation of Angiotensin II from Angiotensin-(1–12) in human atrial tissue', *The FASEB Journal*, 24(S1). Available at: https://doi.org/10.1096/fasebj.24.1_supplement.605.4.
- Ahmad, S. *et al.* (2011) 'Chymase-dependent generation of angiotensin II from angiotensin-(1-12) in human atrial tissue', *PLoS ONE*, 6(12). Available at: https://doi.org/10.1371/journal.pone.0028501.
- Ahmad, S. *et al.* (2013) 'Chymase mediates angiotensin-(1-12) metabolism in normal human hearts', *Journal of the American Society of Hypertension*, 7(2). Available at: https://doi.org/10.1016/j.jash.2012.12.003.
- Ahmad, S. *et al.* (2014) 'Angiotensin-(1-12): a chymase-mediated cellular angiotensin II substrate.', *Current hypertension reports*, 16(5), p. 429. Available at: https://doi.org/10.1007/s11906-014-0429-9.
- Ahmad, S. *et al.* (2021) 'Newly developed radioimmunoassay for Human Angiotensin-(1–12) measurements in plasma and urine', *Molecular and Cellular Endocrinology*, 529. Available at: https://doi.org/10.1016/j.mce.2021.111256.
- Ahmad, S. and Ferrario, C.M. (2018) 'Chymase inhibitors for the treatment of cardiac diseases: a patent review (2010–2018)', *Expert Opinion on Therapeutic Patents*. Available at: https://doi.org/10.1080/13543776.2018.1531848.
- Alem, M.M. (2019) 'Endothelial dysfunction in chronic heart failure: Assessment, findings, significance, and potential therapeutic targets', *International Journal of Molecular Sciences*. Available at: https://doi.org/10.3390/ijms20133198.
- Ames, M.K., Atkins, C.E. and Pitt, B. (2019) 'The renin-angiotensin-aldosterone system and its suppression', *Journal of Veterinary Internal Medicine*. Available at: https://doi.org/10.1111/jvim.15454.
- Arbel, Y. *et al.* (2013) 'Red blood cell distribution width and the risk of cardiovascular morbidity and all-cause mortality: A population-based study', *Thrombosis and Haemostasis*, 111(2). Available at: https://doi.org/10.1160/TH13-07-0567.
- Arnold, A.C. *et al.* (2010) 'Angiotensin-(1-12) requires angiotensin converting enzyme and AT 1 receptors for cardiovascular actions within the solitary tract nucleus', *American Journal of Physiology - Heart and Circulatory Physiology*, 299(3). Available at: https://doi.org/10.1152/ajpheart.00345.2010.
- Avendaño, M.S. *et al.* (2018) 'MPGES-1 (Microsomal prostaglandin E synthase-1) mediates vascular dysfunction in hypertension through oxidative stress', *Hypertension*, 72(2). Available at: https://doi.org/10.1161/HYPERTENSIONAHA.118.10833.
- Bar, A. *et al.* (2015) 'MRI-based assessment of endothelial function in mice in vivo', *Pharmacological Reports*. Available at: https://doi.org/10.1016/j.pharep.2015.05.007.
- Bar, A. *et al.* (2019) 'Degradation of Glycocalyx and Multiple Manifestations of Endothelial Dysfunction Coincide in the Early Phase of Endothelial Dysfunction

Before Atherosclerotic Plaque Development in Apolipoprotein E/Low-Density Lipoprotein Receptor-Deficient Mice', *Journal of the American Heart Association*, 8(6). Available at: https://doi.org/10.1161/JAHA.118.011171.

- Bar, A. *et al.* (2020) 'In vivo magnetic resonance imaging-based detection of heterogeneous endothelial response in thoracic and abdominal aorta to short-term high-fat diet ascribed to differences in perivascular adipose tissue in mice', *Journal of the American Heart Association*, 9(21). Available at: https://doi.org/10.1161/JAHA.120.016929.
- Barton, M. *et al.* (1997a) 'Anatomic Heterogeneity of Vascular Aging', *Hypertension*, 30(4). Available at: https://doi.org/10.1161/01.hyp.30.4.817.
- Barton, M. *et al.* (1997b) 'Anatomic heterogeneity of vascular aging: Role of nitric oxide and endothelin', *Hypertension*, 30(4). Available at: https://doi.org/10.1161/01.HYP.30.4.817.
- Bauersachs, J. *et al.* (1999) 'Endothelial dysfunction in chronic myocardial infarction despite increased vascular endothelial nitric oxide synthase and soluble guanylate cyclase expression: Role of enhanced vascular superoxide production', *Circulation*, 100(3). Available at: https://doi.org/10.1161/01.CIR.100.3.292.
- Benjamin, N. *et al.* (1995) 'Measuring forearm blood flow and interpreting the responses to drugs and mediators', *Hypertension*, 25(5). Available at: https://doi.org/10.1161/01.HYP.25.5.918.
- Berkowicz, P. *et al.* (2018) 'Cardiac transcriptome profiling of Tgαq*44 mice using next generation sequencing', *Journal of Molecular and Cellular Cardiology*, 120. Available at: https://doi.org/10.1016/j.yjmcc.2018.05.138.
- Beyer, A.M. and Gutterman, D.D. (2012) 'Regulation of the human coronary microcirculation', *Journal of Molecular and Cellular Cardiology*. Available at: https://doi.org/10.1016/j.yjmcc.2011.10.003.
- Błyszczuk, P. and Szekanecz, Z. (2020) 'Pathogenesis of ischaemic and non-ischaemic heart diseases in rheumatoid arthritis', *RMD Open*. Available at: https://doi.org/10.1136/rmdopen-2019-001032.
- Briones, A.M. *et al.* (2009) 'Atorvastatin prevents angiotensin II-induced vascular remodeling and oxidative stress', *Hypertension*, 54(1). Available at: https://doi.org/10.1161/HYPERTENSIONAHA.109.133710.
- Buczek, E. *et al.* (2018) 'Alterations in NO- and PGI2- dependent function in aorta in the orthotopic murine model of metastatic 4T1 breast cancer: Relationship with pulmonary endothelial dysfunction and systemic inflammation', *BMC Cancer*, 18(1). Available at: https://doi.org/10.1186/s12885-018-4445-z.
- Buys, E. and Sips, P. (2014) 'New insights into the role of soluble guanylate cyclase in blood pressure regulation', *Current Opinion in Nephrology and Hypertension*. Available at: https://doi.org/10.1097/01.mnh.0000441048.91041.3a.
- Cediel, E. *et al.* (2002) 'Role of endothelin-1 and thromboxane A2 in renal vasoconstriction induced by angiotensin II in diabetes and hypertension', *Kidney International, Supplement*, 62(82). Available at: https://doi.org/10.1046/j.1523-1755.62.s82.2.x.

- Chen, J. *et al.* (2021) 'The protective role of SOD1 overexpression in central mediation of bradycardia following chronic intermittent hypoxia in mice', *American Journal of Physiology - Regulatory Integrative and Comparative Physiology*, 320(3). Available at: https://doi.org/10.1152/AJPREGU.00147.2020.
- Chiu, J.J. and Chien, S. (2011) 'Effects of disturbed flow on vascular endothelium: Pathophysiological basis and clinical perspectives', *Physiological Reviews*. Available at: https://doi.org/10.1152/physrev.00047.2009.
- Chlopicki, S. *et al.* (2005) 'Compensation of endothelium-dependent responses in coronary circulation of eNOS-deficient mice', *Journal of Cardiovascular Pharmacology*, 46(1). Available at: https://doi.org/10.1097/01.fjc.0000164093.88821.00.
- Collado, A. *et al.* (2021) 'MicroRNA: A mediator of diet-induced cardiovascular protection', *Current Opinion in Pharmacology*. Available at: https://doi.org/10.1016/j.coph.2021.07.022.
- Daiber, A. *et al.* (2017) 'Targeting vascular (endothelial) dysfunction', *British Journal of Pharmacology*. Available at: https://doi.org/10.1111/bph.13517.
- Daiber, A. and Chlopicki, S. (2020) 'Revisiting pharmacology of oxidative stress and endothelial dysfunction in cardiovascular disease: Evidence for redox-based therapies', *Free Radical Biology and Medicine*. Available at: https://doi.org/10.1016/j.freeradbiomed.2020.02.026.
- Danesh, J. *et al.* (2000) 'Haematocrit, viscosity, erythrocyte sedimentation rate: Meta-analyses of prospective studies of coronary heart disease', *European Heart Journal*. Available at: https://doi.org/10.1053/euhj.1999.1699.
- Davì, G., Santilli, F. and Vazzana, N. (2012) 'Thromboxane receptors antagonists and/or synthase inhibitors', *Handbook of Experimental Pharmacology*, 210. Available at: https://doi.org/10.1007/978-3-642-29423-5_11.
- Davies, P.F. (2009) 'Hemodynamic shear stress and the endothelium in cardiovascular pathophysiology', *Nature Clinical Practice Cardiovascular Medicine*. Available at: https://doi.org/10.1038/ncpcardio1397.
- Dell'italia, L.J., Collawn, J.F. and Ferrario, C.M. (2018) 'Multifunctional role of chymase in acute and chronic tissue injury and remodeling', *Circulation Research*. Available at: https://doi.org/10.1161/CIRCRESAHA.117.310978.
- Dikalov, S., Griendling, K.K. and Harrison, D.G. (2007) 'Measurement of reactive oxygen species in cardiovascular studies', *Hypertension*. Available at: https://doi.org/10.1161/01.HYP.0000258594.87211.6b.
- Dobbie, L.J. *et al.* (2020) 'Validation of semi-automated flow-mediated dilation measurement in healthy volunteers', *Blood Pressure Monitoring*, 25(4). Available at: https://doi.org/10.1097/MBP.0000000000000448.
- Doggrell, S.A. and Wanstall, J.C. (2004) 'Vascular chymase: Pathophysiological role and therapeutic potential of inhibition', *Cardiovascular Research*. Available at: https://doi.org/10.1016/j.cardiores.2003.11.029.

- Drelicharz, L. *et al.* (2008) 'NO and PGI2 in coronary endothelial dysfunction in transgenic mice with dilated cardiomyopathy', *Basic Research in Cardiology*, 103(5). Available at: https://doi.org/10.1007/s00395-008-0723-2.
- Drelicharz, Ł. *et al.* (2009) 'Application of magnetic resonance imaging in vivo for the assessment of the progression of systolic and diastolic dysfunction in a mouse model of dilated cardiomyopathy.', *Kardiologia polska*, 67(4), pp. 386–95. Available at: http://www.ncbi.nlm.nih.gov/pubmed/19492251 (Accessed: 30 July 2019).
- Dupouy, P. *et al.* (1993) 'Assessment of coronary vasomotion by intracoronary ultrasound', *American Heart Journal*, 126(1). Available at: https://doi.org/10.1016/S0002-8703(07)80012-3.
- Durand, M.J. and Gutterman, D.D. (2013) 'Diversity in mechanisms of endothelium-dependent vasodilation in health and disease', *Microcirculation*. Available at: https://doi.org/10.1111/micc.12040.
- Dybas, J. *et al.* (2020) 'Age–related and atherosclerosis–related erythropathy in ApoE/LDLR−/− mice', *Biochimica et Biophysica Acta - Molecular Basis of Disease*, 1866(12). Available at: https://doi.org/10.1016/j.bbadis.2020.165972.
- Dybas, J. *et al.* (2022) 'Trends in biomedical analysis of red blood cells – Raman spectroscopy against other spectroscopic, microscopic and classical techniques', *TrAC - Trends in Analytical Chemistry*. Available at: https://doi.org/10.1016/j.trac.2021.116481.
- Félétou, M. *et al.* (2010) 'TP receptors and oxidative stress. Hand in hand from endothelial dysfunction to atherosclerosis', in *Advances in Pharmacology*. Available at: https://doi.org/10.1016/B978-0-12-385061-4.00004-0.
- Félétou, M., Huang, Y. and Vanhoutte, P.M. (2011) 'Endothelium-mediated control of vascular tone: COX-1 and COX-2 products', *British Journal of Pharmacology*. Available at: https://doi.org/10.1111/j.1476-5381.2011.01276.x.
- Ferrario, C.M. (2006) 'Angiotensin-converting enzyme 2 and angiotensin-(1-7): An evolving story in cardiovascular regulation', in *Hypertension*. Available at: https://doi.org/10.1161/01.HYP.0000196268.08909.fb.
- Ferrario, C.M. *et al.* (2019) 'Activation of the Human Angiotensin-(1-12)-Chymase Pathway in Rats With Human Angiotensinogen Gene Transcripts', *Frontiers in Cardiovascular Medicine*, 6. Available at: https://doi.org/10.3389/fcvm.2019.00163.
- Ferrario, C.M. *et al.* (2021) 'Angiotensin (1-12) in Humans With Normal Blood Pressure and Primary Hypertension', *Hypertension*, 77(3). Available at: https://doi.org/10.1161/HYPERTENSIONAHA.120.16514.
- Fischer, D. *et al.* (2005) 'Endothelial dysfunction in patients with chronic heart failure is independently associated with increased incidence of hospitalization, cardiac transplantation, or death', *European Heart Journal*, 26(1). Available at: https://doi.org/10.1093/eurheartj/ehi001.

- Fortini, F. *et al.* (2021) 'Well-known and novel players in endothelial dysfunction: Updates on a notch(ed) landscape', *Biomedicines*. Available at: https://doi.org/10.3390/biomedicines9080997.
- Fountain, J.H. and Lappin, S.L. (2018) *Physiology, Renin Angiotensin System*, *StatPearls*.
- Francois, H. *et al.* (2004) 'Role for Thromboxane Receptors in Angiotensin-II-Induced Hypertension', *Hypertension*, 43(2). Available at: https://doi.org/10.1161/01.HYP.0000112225.27560.24.
- Franczuk, P. *et al.* (2015) 'Could an analysis of mean corpuscular volume help to improve risk stratification in non-anemic patients with acute myocardial infarction?', *Cardiology Journal*, 22(4). Available at: https://doi.org/10.5603/CJ.a2015.0031.
- Frolow, M. *et al.* (2015) 'Comprehensive assessment of vascular health in patients; Towards endothelium-guided therapy', *Pharmacological Reports*. Available at: https://doi.org/10.1016/j.pharep.2015.05.010.
- Garland, C.J., Hiley, C.R. and Dora, K.A. (2011) 'EDHF: Spreading the influence of the endothelium', *British Journal of Pharmacology*. Available at: https://doi.org/10.1111/j.1476-5381.2010.01148.x.
- Gaubert, M.L. *et al.* (2007) 'Endothelium-derived hyperpolarizing factor as an in vivo back-up mechanism in the cutaneous microcirculation in old mice', *Journal of Physiology*, 585(2). Available at: https://doi.org/10.1113/jphysiol.2007.143750.
- Gevaert, A.B. *et al.* (2017) 'Targeting Endothelial Function to Treat Heart Failure with Preserved Ejection Fraction: The Promise of Exercise Training', *Oxidative Medicine and Cellular Longevity*. Available at: https://doi.org/10.1155/2017/4865756.
- Giannitsi, S. *et al.* (2019) 'Endothelial dysfunction and heart failure: A review of the existing bibliography with emphasis on flow mediated dilation', *JRSM Cardiovascular Disease*, 8. Available at: https://doi.org/10.1177/2048004019843047.
- Gwozdzinski, K., Pieniazek, A. and Gwozdzinski, L. (2021) 'Reactive Oxygen Species and Their Involvement in Red Blood Cell Damage in Chronic Kidney Disease', *Oxidative Medicine and Cellular Longevity*. Available at: https://doi.org/10.1155/2021/6639199.
- Hambrecht, R. *et al.* (1998) 'Regular physical exercise corrects endothelial dysfunction and improves exercise capacity in patients with chronic heart failure', *Circulation*, 98(24). Available at: https://doi.org/10.1161/01.CIR.98.24.2709.
- Hamzaoui, M. *et al.* (2021) 'Soluble Epoxide Hydrolase Inhibition Prevents Experimental Type 4 Cardiorenal Syndrome', *Frontiers in Molecular Biosciences*, 7. Available at: https://doi.org/10.3389/fmolb.2020.604042.
- Helms, C.C., Gladwin, M.T. and Kim-Shapiro, D.B. (2018) 'Erythrocytes and Vascular Function: Oxygen and Nitric Oxide.', *Frontiers in physiology*, 9, p. 125. Available at: https://doi.org/10.3389/fphys.2018.00125.

- Hempe, J.M. and Ory-Ascani, J. (2014) 'Simultaneous analysis of reduced glutathione and glutathione disulfide by capillary zone electrophoresis', *Electrophoresis*, 35(7). Available at: https://doi.org/10.1002/elps.201300450.
- Higashi, Y. *et al.* (2001) 'A noninvasive measurement of reactive hyperemia that can be used to assess resistance artery endothelial function in humans', *American Journal of Cardiology*, 87(1). Available at: https://doi.org/10.1016/S0002-9149(00)01288-1.
- Higashi, Y. (2022) 'Roles of Oxidative Stress and Inflammation in Vascular Endothelial Dysfunction-Related Disease', *Antioxidants*. Available at: https://doi.org/10.3390/antiox11101958.
- Ighodaro, O.M. and Akinloye, O.A. (2018) 'First line defence antioxidants-superoxide dismutase (SOD), catalase (CAT) and glutathione peroxidase (GPX): Their fundamental role in the entire antioxidant defence grid', *Alexandria Journal of Medicine*, 54(4). Available at: https://doi.org/10.1016/j.ajme.2017.09.001.
- Katz, S.D. *et al.* (1992) 'Impaired endothelium-mediated vasodilation in the peripheral vasculature of patients with congestive heart failure', *Journal of the American College of Cardiology*, 19(5). Available at: https://doi.org/10.1016/0735-1097(92)90271-N.
- Khazaei, M., Moien-afshari, F. and Laher, I. (2008) 'Vascular endothelial function in health and diseases', *Pathophysiology*. Available at: https://doi.org/10.1016/j.pathophys.2008.02.002.
- Kij, A. *et al.* (2020) 'Development and validation of a rapid, specific and sensitive LC-MS/MS bioanalytical method for eicosanoid quantification - assessment of arachidonic acid metabolic pathway activity in hypertensive rats', *Biochimie*, 171–172. Available at: https://doi.org/10.1016/j.biochi.2020.03.010.
- Konior, A. *et al.* (2014) 'NADPH oxidases in vascular pathology', *Antioxidants and Redox Signaling*. Available at: https://doi.org/10.1089/ars.2013.5607.
- Kontidou, E. *et al.* (2023) 'Erythrocyte-Derived microRNAs: Emerging Players in Cardiovascular and Metabolic Disease', *Arteriosclerosis, Thrombosis, and Vascular Biology* [Preprint]. Available at: https://doi.org/10.1161/atvbaha.123.319027.
- Korzekwa, A. *et al.* (2007) 'Nitric oxide in bovine corpus luteum: Possible mechanisms of action in luteolysis', *Animal Science Journal*. Available at: https://doi.org/10.1111/j.1740-0929.2007.00430.x.
- Lassale, C. *et al.* (2018) 'Elements of the complete blood count associated with cardiovascular disease incidence: Findings from the EPIC-NL cohort study', *Scientific Reports*, 8(1). Available at: https://doi.org/10.1038/s41598-018-21661-x.
- Leung, S.W.S. and Vanhoutte, P.M. (2017) 'Endothelium-dependent hyperpolarization: age, gender and blood pressure, do they matter?', *Acta Physiologica*. Available at: https://doi.org/10.1111/apha.12628.
- Li, T. *et al.* (2020) 'Reversal of angiotensin-(1–12)-caused positive modulation on left ventricular contractile performance in heart failure: Assessment by pressure-

volume analysis', *International Journal of Cardiology*, 301. Available at: https://doi.org/10.1016/j.ijcard.2019.09.004.

- Lippi, G. *et al.* (2018) 'Red blood cell distribution width in heart failure: A narrative review.', *World journal of cardiology*, 10(2), pp. 6–14. Available at: https://doi.org/10.4330/wjc.v10.i2.6.
- Liu, Y. *et al.* (2011) 'H2O2 is the transferrable factor mediating flow-induced dilation in human coronary arterioles', *Circulation Research*, 108(5). Available at: https://doi.org/10.1161/CIRCRESAHA.110.237636.
- Ludmer, P.L. *et al.* (1986) 'Paradoxical Vasoconstriction Induced by Acetylcholine in Atherosclerotic Coronary Arteries', *New England Journal of Medicine*, 315(17). Available at: https://doi.org/10.1056/nejm198610233151702.
- Mahdi, A. *et al.* (2020) 'Red Blood Cell Peroxynitrite Causes Endothelial Dysfunction in Type 2 Diabetes Mellitus via Arginase', *Cells*, 9(7). Available at: https://doi.org/10.3390/cells9071712.
- Mahdi, A., Collado, A., *et al.* (2021a) 'Erythrocytes Induce Vascular Dysfunction in COVID-19', *SSRN Electronic Journal* [Preprint]. Available at: https://doi.org/10.2139/ssrn.3945298.
- Mahdi, A., Collado, A., *et al.* (2021b) 'Erythrocytes Induce Vascular Dysfunction in COVID-19', *SSRN Electronic Journal* [Preprint]. Available at: https://doi.org/10.2139/ssrn.3867953.
- Mahdi, A. *et al.* (2021) 'Novel perspectives on redox signaling in red blood cells and platelets in cardiovascular disease', *Free Radical Biology and Medicine*, 168. Available at: https://doi.org/10.1016/j.freeradbiomed.2021.03.020.
- Mahdi, A. *et al.* (2021) 'Sunitinib and its effect in the cardiovascular system', *Drug Discovery Today*. Available at: https://doi.org/10.1016/j.drudis.2021.05.003.
- Mahdi, A., Kövamees, O. and Pernow, J. (2020) 'Improvement in endothelial function in cardiovascular disease - Is arginase the target?', *International Journal of Cardiology*. Available at: https://doi.org/10.1016/j.ijcard.2019.11.004.
- Mak, S. and Newton, G.E. (2001) 'The oxidative stress hypothesis of congestive heart failure: Radical thoughts', *Chest*, 120(6). Available at: https://doi.org/10.1378/chest.120.6.2035.
- Malheiro, L.F. *et al.* (2021) 'Peripheral arterial tonometry as a method of measuring reactive hyperaemia correlates with organ dysfunction and prognosis in the critically ill patient: a prospective observational study', *Journal of Clinical Monitoring and Computing*, 35(5). Available at: https://doi.org/10.1007/s10877-020-00586-9.
- Marcinek, A. *et al.* (2023) 'Non-Invasive Assessment of Vascular Circulation Based on Flow Mediated Skin Fluorescence (FMSF)', *Biology*, 12(3). Available at: https://doi.org/10.3390/biology12030385.
- Maupoint, J. *et al.* (2016) 'Selective vascular endothelial protection reduces cardiac dysfunction in chronic heart failure', *Circulation: Heart Failure*, 9(4). Available at: https://doi.org/10.1161/CIRCHEARTFAILURE.115.002895.
- Mehta, P.K. and Griendling, K.K. (2007) 'Angiotensin II cell signaling: Physiological and pathological effects in the cardiovascular system', *American*

Journal of Physiology - Cell Physiology. Available at: https://doi.org/10.1152/ajpcell.00287.2006.

- Mende, U *et al.* (2001) 'Dilated cardiomyopathy in two transgenic mouse lines expressing activated G protein alpha(q): lack of correlation between phospholipase C activation and the phenotype.', *Journal of molecular and cellular cardiology*, 33(8), pp. 1477–91. Available at: https://doi.org/10.1006/jmcc.2001.1411.
- Mende, U. *et al.* (2001) 'Dilated cardiomyopathy in two transgenic mouse lines expressing activated G protein αq: Lack of correlation between phospholipase C activation and the phenotype', *Journal of Molecular and Cellular Cardiology*, 33(8). Available at: https://doi.org/10.1006/jmcc.2001.1411.
- Mohaissen, T. *et al.* (2022) 'Temporal relationship between systemic endothelial dysfunction and alterations in erythrocyte function in a murine model of chronic heart failure', *Cardiovascular research*, 118(12). Available at: https://doi.org/10.1093/cvr/cvab306.
- Montfort, W.R., Wales, J.A. and Weichsel, A. (2017) 'Structure and Activation of Soluble Guanylyl Cyclase, the Nitric Oxide Sensor', *Antioxidants and Redox Signaling*. Available at: https://doi.org/10.1089/ars.2016.6693.
- Nasri, H., Baradaran, A. and Rafieian-Kopaei, M. (2014) 'Oxidative stress and hypertension: Possibility of hypertension therapy with antioxidants', *Journal of Research in Medical Sciences*, 19(4).
- Natarajan, M. *et al.* (2016) 'Hemodynamic Flow-Induced Mechanotransduction Signaling Influences the Radiation Response of the Vascular Endothelium', *Radiation Research*, 186(2). Available at: https://doi.org/10.1667/RR14410.1.
- Neglia, D. *et al.* (2002) 'Prognostic role of myocardial blood flow impairment in idiopathic left ventricular dysfunction', *Circulation*, 105(2). Available at: https://doi.org/10.1161/hc0202.102119.
- Okunishi, H. *et al.* (1993) 'Marked Species-Difference in the Vascular Angiotensin II-Forming Pathways: Humans versus Rodents', *The Japanese Journal of Pharmacology*, 62(2). Available at: https://doi.org/10.1254/jjp.62.207.
- Ola, M.S. *et al.* (2017) 'Role of Tissue Renin-angiotensin System and the Chymase/angiotensin-(1-12) Axis in the Pathogenesis of Diabetic Retinopathy', *Current Medicinal Chemistry*, 24(28). Available at: https://doi.org/10.2174/0929867324666170407141955.
- Olkowicz, M., Chlopicki, S. and Smolenski, R.T. (2017) 'A primer to angiotensin peptide isolation, stability, and analysis by nano-liquid chromatography with mass detection', in *Methods in Molecular Biology*. Available at: https://doi.org/10.1007/978-1-4939-7030-8_14.
- Oyama, J.I. and Node, K. (2013) 'Endothelium-derived hyperpolarizing factor and hypertension', *Hypertension Research*. Available at: https://doi.org/10.1038/hr.2013.97.
- Pearson, J.D. (2000) 'Normal endothelial cell function', *Lupus*. Available at: https://doi.org/10.1191/096120300678828299.

- Pernow, J. *et al.* (2019) 'Red blood cell dysfunction: A new player in cardiovascular disease', *Cardiovascular Research*, 115(11). Available at: https://doi.org/10.1093/cvr/cvz156.
- Pernow, J. and Jung, C. (2013) 'Arginase as a potential target in the treatment of cardiovascular disease: Reversal of arginine steal?', *Cardiovascular Research*. Available at: https://doi.org/10.1093/cvr/cvt036.
- Proniewski, B. *et al.* (2018) 'Immuno-spin trapping-based detection of oxidative modifications in cardiomyocytes and coronary endothelium in the progression of heart failure in Tgaq*44 Mice', *Frontiers in Immunology*, 9(MAY). Available at: https://doi.org/10.3389/fimmu.2018.00938.
- Proniewski, B. *et al.* (2019) 'Multiorgan development of oxidative and nitrosative stress in LPS-induced endotoxemia in C57BL/6 mice: DHE-based in vivo approach', *Oxidative Medicine and Cellular Longevity*, 2019. Available at: https://doi.org/10.1155/2019/7838406.
- Proniewski, B., Miszalski-Jamka, T. and Jaźwiec, P. (2014) 'In vivo T2-mapping and segmentation of carotid artery plaque components using magnetic resonance imaging at 1.5T', in *Computing in Cardiology*.
- Prosser, H.C. *et al.* (2010) 'Regional vascular response to ProAngiotensin-12 (PA12) through the rat arterial system', *Peptides*, 31(8). Available at: https://doi.org/10.1016/j.peptides.2010.05.009.
- Przyborowski, K. *et al.* (2018) 'Vascular Nitric Oxide-Superoxide Balance and Thrombus Formation after Acute Exercise', *Medicine and Science in Sports and Exercise*, 50(7). Available at: https://doi.org/10.1249/MSS.0000000000001589.
- Rajendran, P. *et al.* (2013) 'The vascular endothelium and human diseases', *International Journal of Biological Sciences*. Available at: https://doi.org/10.7150/ijbs.7502.
- Reina-Couto, M. *et al.* (2021) 'Inflammation in Human Heart Failure: Major Mediators and Therapeutic Targets', *Frontiers in Physiology*. Available at: https://doi.org/10.3389/fphys.2021.746494.
- Ricciotti, E. and Fitzgerald, G.A. (2011) 'Prostaglandins and inflammation', *Arteriosclerosis, Thrombosis, and Vascular Biology*, 31(5). Available at: https://doi.org/10.1161/ATVBAHA.110.207449.
- Romuk, E. *et al.* (2019) 'Superoxide dismutase activity as a predictor of adverse outcomes in patients with nonischemic dilated cardiomyopathy', *Cell Stress and Chaperones*, 24(3). Available at: https://doi.org/10.1007/s12192-019-00991-3.
- Ruilope, L.M., Redón, J. and Schmieder, R. (2007) 'Cardiovascular risk reduction by reversing endothelial dysfunction: ARBs, ACE inhibitors, or both? Expectations from the ONTARGET Trial Programme', *Vascular Health and Risk Management*.
- Sallam, N.A. and Laher, I. (2020) 'Redox signaling and regional heterogeneity of endothelial dysfunction in db/db mice', *International Journal of Molecular Sciences*, 21(17). Available at: https://doi.org/10.3390/ijms21176147.
- Savarese, G. and Lund, L.H. (2017) 'Epidemiology Global Public Health Burden of Heart Failure', *CRF journal*, 3.

- Schächinger, V., Britten, M.B. and Zeiher, A.M. (2000) 'Prognostic impact of coronary vasodilator dysfunction on adverse long- term outcome of coronary heart disease', *Circulation*, 101(16). Available at: https://doi.org/10.1161/01.CIR.101.16.1899.
- Shah, A. *et al.* (2010) 'Endothelial Function and Arterial Compliance are not Impaired in Subjects With Heart Failure of Non-Ischemic Origin', *Journal of Cardiac Failure*, 16(2). Available at: https://doi.org/10.1016/j.cardfail.2009.10.019.
- Smyth, E.M. (2010) 'Thromboxane and the thromboxane receptor in cardiovascular disease', *Clinical Lipidology*. Available at: https://doi.org/10.2217/CLP.10.11.
- Sternak, M. *et al.* (2018) 'The deletion of endothelial sodium channel a (αENaC) impairs endothelium-dependent vasodilation and endothelial barrier integrity in endotoxemia in Vivo', *Frontiers in Pharmacology*, 9(APR). Available at: https://doi.org/10.3389/fphar.2018.00178.
- Streese, L. *et al.* (2019) 'Retinal Endothelial Function, Physical Fitness and Cardiovascular Risk: A Diagnostic Challenge', *Frontiers in Physiology*, 10. Available at: https://doi.org/10.3389/fphys.2019.00831.
- Sun, H.J. *et al.* (2020) 'Role of endothelial dysfunction in cardiovascular diseases: The link between inflammation and hydrogen sulfide', *Frontiers in Pharmacology*. Available at: https://doi.org/10.3389/fphar.2019.01568.
- Suryavanshi, S. V. and Kulkarni, Y.A. (2017) 'NF-κβ: A potential target in the management of vascular complications of diabetes', *Frontiers in Pharmacology*. Available at: https://doi.org/10.3389/fphar.2017.00798.
- Takai, S. and Jin, D. (2016) 'Improvement of cardiovascular remodelling by chymase inhibitor', *Clinical and Experimental Pharmacology and Physiology*, 43(4), pp. 387–393. Available at: https://doi.org/10.1111/1440-1681.12549.
- Teerlink, J.R. *et al.* (1993) 'Temporal evolution of endothelial dysfunction in a rat model of chronic heart failure', *Journal of the American College of Cardiology*, 22(2). Available at: https://doi.org/10.1016/0735-1097(93)90073-A.
- Toniolo, A. *et al.* (2013) 'Cyclooxygenase-1 and Prostacyclin Production by Endothelial Cells in the Presence of Mild Oxidative Stress', *PLoS ONE*, 8(2). Available at: https://doi.org/10.1371/journal.pone.0056683.
- Tousoulis, D., Antoniades, C. and Stefanadis, C. (2005) 'Evaluating endothelial function in humans: A guide to invasive and non-invasive techniques', *Heart*, 91(4). Available at: https://doi.org/10.1136/hrt.2003.032847.
- Tyrankiewicz, U. *et al.* (2013) 'Characterization of the cardiac response to a low and high dose of dobutamine in the mouse model of dilated cardiomyopathy by MRI in vivo', *Journal of Magnetic Resonance Imaging*, 37(3). Available at: https://doi.org/10.1002/jmri.23854.
- Tyrankiewicz, U. *et al.* (2018a) 'Activation pattern of ACE2/Ang-(1-7) and ACE/Ang II pathway in course of heart failure assessed by multiparametric MRI in vivo in Tg-q*44 mice', *Journal of Applied Physiology*, 124(1). Available at: https://doi.org/10.1152/japplphysiol.00571.2017.

- Tyrankiewicz, U. *et al.* (2018b) 'Activation pattern of ACE2/Ang-(1–7) and ACE/Ang II pathway in course of heart failure assessed by multiparametric MRI in vivo in Tgαq*44 mice', *Journal of Applied Physiology*, 124(1), pp. 52–65. Available at: https://doi.org/10.1152/japplphysiol.00571.2017.
- Tyrankiewicz, U. *et al.* (2019) 'Renin-Angiotensin-Aldosterone System in Heart Failure: Focus on Nonclassical Angiotensin Pathways as Novel Upstream Targets Regulating Aldosterone', in *Aldosterone-Mineralocorticoid Receptor - Cell Biology to Translational Medicine*. Available at: https://doi.org/10.5772/intechopen.87239.
- Tyrankiewicz, U. *et al.* (2021) 'Physical Activity and Inhibition of ACE Additively Modulate ACE/ACE-2 Balance in Heart Failure in Mice', *Frontiers in Pharmacology*, 12. Available at: https://doi.org/10.3389/fphar.2021.682432.
- Vanhoutte, P.M. (1989) 'Endothelium and control of vascular function state of the art lecture', *Hypertension*, 13(6). Available at: https://doi.org/10.1161/01.HYP.13.6.658.
- Varagic, J. *et al.* (2013) 'Predominance of AT1 blockade over mas-mediated angiotensin-(1-7) mechanisms in the regulation of blood pressure and renin-angiotensin system in mRen2.Lewis rats', *American Journal of Hypertension*, 26(5). Available at: https://doi.org/10.1093/ajh/hps090.
- Vercauteren, M. *et al.* (2006) 'Improvement of peripheral endothelial dysfunction by protein tyrosine phosphatase inhibitors in heart failure', *Circulation*, 114(23). Available at: https://doi.org/10.1161/CIRCULATIONAHA.106.630129.
- Villar, I.C. *et al.* (2006) 'Novel aspects of endothelium-dependent regulation of vascular tone', *Kidney International*. Available at: https://doi.org/10.1038/sj.ki.5001680.
- Wang, B. *et al.* (2021) 'Metabolism pathways of arachidonic acids: mechanisms and potential therapeutic targets', *Signal Transduction and Targeted Therapy*. Available at: https://doi.org/10.1038/s41392-020-00443-w.
- Widder, J. *et al.* (2004) 'Vascular endothelial dysfunction and superoxide anion production in heart failure are p38 MAP kinase-dependent', *Cardiovascular Research*, 63(1). Available at: https://doi.org/10.1016/j.cardiores.2004.03.008.
- Wilkinson, I.B. *et al.* (2002) 'Pulse-wave analysis: Clinical evaluation of a noninvasive, widely applicable method for assessing endothelial function', *Arteriosclerosis, Thrombosis, and Vascular Biology*, 22(1). Available at: https://doi.org/10.1161/hq0102.101770.
- Yang, J. *et al.* (2013) 'Arginase regulates red blood cell nitric oxide synthase and export of cardioprotective nitric oxide bioactivity', *Proceedings of the National Academy of Sciences of the United States of America*, 110(37). Available at: https://doi.org/10.1073/pnas.1307058110.
- Yang, J. *et al.* (2018) 'Red Blood Cells in Type 2 Diabetes Impair Cardiac Post-Ischemic Recovery Through an Arginase-Dependent Modulation of Nitric Oxide Synthase and Reactive Oxygen Species', *JACC: Basic to Translational Science*, 3(4). Available at: https://doi.org/10.1016/j.jacbts.2018.03.006.

- Yoon, H.E. *et al.* (2016) 'PS 07-30 AGE-ASSOCIATED CHANGES IN THE VASCULAR RENIN-ANGIOTENSIN-SYSTEM IN MICE', *Journal of Hypertension*, 34(Supplement 1). Available at: https://doi.org/10.1097/01.hjh.0000500693.13738.68.
- Zhou, Z., Yang, J. and Pernow, J. (2018) 'Erythrocytes and cardiovascular complications', *Aging*. Available at: https://doi.org/10.18632/aging.101688.
- Zuchi, C. *et al.* (2020) 'Role of endothelial dysfunction in heart failure', *Heart Failure Reviews*. Available at: https://doi.org/10.1007/s10741-019-09881-3.

10. List of PhD student's publications

A. Publications related to the doctoral thesis;

1. **Mohaissen T**, Proniewski B, Targosz-Korecka M, Bar A, Kij A, Bulat K, Wajda A, Blat A, Matyjaszczyk-Gwarda K, Grosicki M, Tworzydlo A, Sternak M, Wojnar-Lason K, Rodrigues-Diez R, Kubisiak A, Briones A, Marzec KM, Chlopicki S. Temporal relationship between systemic endothelial dysfunction and alterations in erythrocyte function in a murine model of chronic heart failure. Cardiovasc Res. 2021 Oct 7:cvab306. doi: 10.1093/cvr/cvab306.
2. **Mohaissen T**, Kij A, Wojnar-Lason K, Buczek E, Król O, Kutryb-Zajac B, Ana B. Garcia-Redondo, Ana M Briones, Stefan Chlopicki1 "Ang-(1-12)/Ang II/TXA2 pathway in endothelial dysfunction the murine model of heart failure" (*under review European Journal of Pharmacology, Manuscript Number EJP-64754*)

B. Publications not related to the doctoral thesis;

1. Szczesny-Malysiak E, **Mohaissen T**, Bulat K, Kaczmarska M, Wajda A, Marzec KM. Sex-dependent membranopathy in stored human red blood cells. Haematologica. 2021 Oct 1;106(10):2779-2782. doi: 10.3324/haematol.2021.278895
2. Alcicek FC, **Mohaissen T**, Bulat K, Dybas J, Szczesny-Malysiak E, Kaczmarska M, Franczyk-Zarow M, Kostogrys R, Marzec KM. Sex-Specific Differences of Adenosine Triphosphate Levels in Red Blood Cells Isolated from ApoE/LDLR Double-Deficient Mice. Front Physiol. 2022 Feb 18;13:839323. doi: 10.3389/fphys.2022.839323. PMID: 35250640; PMCID: PMC8895041.
3. Sternak M, Bar A, Adamski MG, **Mohaissen T**, Marczyk B, Kieronska A, Stojak M, Kus K, Tarjus A, Jaisser F, Chlopicki S. Front Pharmacol. 2018 Apr 10;9:178.

The Deletion of Endothelial Sodium Channel α (αENaC) Impairs Endothelium-Dependent Vasodilation and Endothelial Barrier Integrity in Endotoxemia in Vivo.doi: 10.3389/fphar.2018.00178. eCollection 2018.

4. Smeda M, Kieronska A, Adamski MG, Proniewski B, Sternak M, **Mohaissen T**, Przyborowski K, Derszniak K, Kaczor D, Stojak M, Buczek E, Jasztal A, Wietrzyk J, Chlopicki S.Nitric oxide deficiency and endothelial-mesenchymal transition of pulmonary endothelium in the progression of 4T1 metastatic breast cancer in mice. Breast Cancer Res. 2018 Aug 3;20(1): Front Pharmacol. 2018 Apr 10;9:178. doi: 10.3389/fphar.2018.00178. ECollection 2018.
5. Adamski MG, Sternak M, **Mohaissen T**, Kaczor D, Wierońska JM, Malinowska M, Czaban I, Byk K, Lyngsø KS, Przyborowski K, Hansen PBL, Wilczyński G, Chlopicki S.Vascular Cognitive Impairment Linked to Brain Endothelium Inflammation in Early Stages of Heart Failure in Mice. J Am Heart Assoc. 2018 Mar 26;7(7):e007694. doi: 10.1161/JAHA.117.007694.
6. Kaczara P, Przyborowski K, **Mohaissen** T, Chlopicki S. Distinct Pharmacological Properties of Gaseous CO and CO-Releasing Molecule in Human Platelets. Int J Mol Sci. 2021 Mar 30;22(7):3584. doi: 10.3390/ijms22073584.
7. Tott S, Grosicki M, Glowacz J, **Mohaissen T**, Wojnar-Lason K, Chlopicki S, Baranska M. Raman imaging-based phenotyping of murine primary endothelial cells to identify disease-associated biochemical alterations. Biochim Biophys Acta Mol Basis Dis. 2021 Sep 1;1867(9):166180. doi: 10.1016/j.bbadis.2021.166180. Epub 2021 May 25.
8. Dybas J, Bulat K, Blat A, **Mohaissen T**, Wajda A, Mardyla M, Kaczmarska M, Franczyk-Zarow M, Malek K, Chlopicki S, Marzec KM Age-related and atherosclerosis-related erythropathy in ApoE/LDLR-/- mice. Biochim Biophys Acta

Mol Basis Dis. 2020 Dec 1;1866(12):165972. doi: 10.1016/j.bbadis.2020.165972. Epub 2020 Sep 17.